

https://dspace.org/

Optimisation of a high-throughput screening assay for nitrile hydratase enzymes

Ben-David, Ateret

2022
https://hdl.handle.net/10539/34594

Downloaded from a DSpace repository. https://dspace.org/



Optimisation of a High-throughput Screening Assay for Nitrile Hydratase Enzymes

by

Ateret Ben-David

(587747)

Dissertation

Submitted in fulfilment of the requirements for the degree

Master of Science

in

Molecular and Cell Biology

in the Faculty of Science, University of the Witwatersrand, Johannesburg, South Africa

Supervisor: Professor Karl Rumbold

Co-supervisor: Professor Dean Brady

June 2022

DECLARATION

I, Ateret Ben-David (587747), am a student registered for the degree of Master's by Dissertation (MSc) in the academic year 2021.

I hereby declare the following:

· I am aware that plagiarism (the use of someone else's work without their permission and/or without acknowledging the original source) is wrong.

· I confirm that the research proposal submitted for assessment for the above degree is my own unaided work except where explicitly indicated otherwise and acknowledged.

· I have followed the required conventions in referencing the thoughts and ideas of others.

· I understand that the University of the Witwatersrand may take disciplinary action against me if there is a belief that this is not my own unaided work or that I have failed to acknowledge the source of the ideas or words in my writing.

Signature: 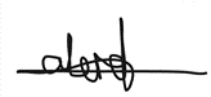 6 June 2022

ABSTRACT

Nitrile hydratases (NHase) are important enzymes that can transform nitriles, which are low-cost intermediates, into high-value industrial chemicals like acrylamide. To increase the use of NHase as a biocatalyst in industry, it needs to be engineered to work in harsher conditions. A high-throughput screening assay must be developed before indirect evolution can be conducted so that enzyme activity of the mutants can be determined. In this study, a coupled-enzyme assay was employed to convert the amide generated by the NHase to hydroxamic acid, which could then be colorimetrically identified. The NHase was successfully transformed and expressed prior to assay optimisation. Multiple steps were engaged in the optimisation process, including examining the influence of substrate and product inhibition on the NHase and amidase, as well as the effect of temperature, pH, and organic solvent on the assay. The optimal conditions were determined to be 100 mM acetonitrile and 1.0 µg/µl NHase which were incubated for 10 minutes. After which 0.4 units of amidase and 20 mM hydroxylamine were added to the well and incubated for a further 30 minutes. The optimal incubation temperature and pH were determined to be 35˚C and pH 8. The study resulted in a sensitive, high-throughput screening assay for NHase enzymes.

ACKNOWLEDGEMENTS

I would like to thank my supervisors Prof. Karl Rumbold and Prof. Dean Brady for their guidance and support along the journey.

I gratefully acknowledge that this project would not have been possible without the financial support from the National Research Fund (NRF).

The biggest thank you to Sasha Richardson and Dylan Moodley for their patience, guidance and most importantly their friendship.

Thank you to all my colleagues in Industrial Microbiology Laboratory (IMBL) and the Microbiology and Biotechnology department. Particularly thanks to Michael Tobin, who was always ready to help and made sure everything ran smoothly.

Thank you to Dr Botes and Dr Meyer, the postgraduate coordinators, who guided me and where always ready to answer my questions.

I would like to thank G-D for bringing me through this journey as without Him this would have not been possible.

Thank you to my husband, Ory, who encourages and supports me in being a better person every day. This master is in dedication to you.

To my beautiful, smart, kind kids, Noam, Eliyah and Yemima thank you for allowing me to do my Masters and for your patience throughout it. I love you all so much. I hope that my hard work encourages you to do hard things in life.

Thank you to my parents Daniel and Raelene Ben-David who have been there throughout everything for me, providing me with encouragement, helping with the kids and helping financially when needed.

To my dearest sister, Batya, thank you for everything.

This work is based on the research supported in part by the National Research Foundation of South Africa (Grant Numbers: 122062).



TABLE OF CONTENTS

DECLARATION ..... **ii**

ABSTRACT ..... **iii**

ACKNOWLEDGEMENTS ..... **iv**

LIST OF FIGURES ..... **viii**

LIST OF SCHEMES ..... **x**

LIST OF TABLES ..... **xi**

LIST OF ABBREVIATIONS ..... **xii**

Chapter 1: Introduction **1**

1.1 Literature review 1

1.1.1 The nitrile hydratase enzyme 1

1.1.2 Enzyme engineering 7

1.1.3 Screening and selection techniques 8

1.2 Rationale 10

1.3 Aim and objectives 12

1.3.1 Aim 12

1.3.2 Objectives 12

Chapter 2: Protein expression of Nitrile Hydratase from *R. rhodochrous* ATCC BAA-870 using a two-plasmid vector system **13**

2.1 Introduction 13

2.1.1 Recombinant protein expression and its effect on biocatalysis 13

2.1.2 Two-plasmid vector system used for recombination of the *R. rhodochrous* ATCC BAA-870 Nitrile Hydratase 13

2.1.3 The host system used for Nitrile Hydratase expression 15
2.2 Methods and materials: 17
2.2.1 Materials 17
2.2.2 Methods 20
2.3 Results and Discussion 24
2.3.1 Conformation of transformation 24
2.3.2 Comparison of the growth curves and growth rates for each plasmid as well as the co-transformed cells 24
2.3.2 Co-expression of the *R. rhodochrous* ATCC BAA-870 Nitrile Hydratase 28
2.3.3 Transformation efficiencies for co-transformed and individually transformed plasmids 31
Chapter 3: Optimising a high-throughput screening assay for the *R. rhodochrous* ATCC BAA-870 nitrile hydratase enzyme 34
3.1 Introduction 34
3.2 Materials and methods 36
3.2.1 Materials 36
3.2.2 Methods 37
3.3 Results and discussion 42
3.3.1 The effect of hydroxylamine on the assay 42
3.3.2 The optimal concentration of acetohydroxamic acid for maximum assay sensitivity. 47
3.3.3 Optimisation of the amidase activity within the assay 49
3.3.4 Optimisation of the NHase activity within the assay 57
3.3.5 Optimisation of the assay temperature 63
3.3.7 The effect of organic solvents on the assay 66
3.3.8 The effect of different nitrile substrates on the assay 69
3.3.9 Analysis of the kinetic parameters for NHase in this assay 71
Chapter 4: General discussion and conclusion 77

4.1 Future work and suggestions……81

REFERENCES.....82

LIST OF FIGURES

Figure 1.1: The active site of a Co-type nitrile hydratase from *Pseudonocardia thermophila*….3

Figure 1.2: A ribbon drawing of the tertiary structure of the Co-type nitrile hydratase from *P. thermophila*……4

Figure 2.1 Plasmid maps of pET-21a(+) with beta subunit insert and pRSFDuet-1 with alpha and chaperon inserts……..19

Figure 2.2: Growth curves representing the change in biomass of differentaily transformed T7 Express competent *E. coli* cells in LB media measured at OD_{600}……26

Figure 2.3 Growth rates of the transformants in T7 Express competent *E. coli*……..27

Figure 2.4: Co-Expression and individual expression of the nitrile hydratase alpha and beta subunits in T7 Express competent *E. coli*…….30

Figure 2.5: Transformation effeciencies of co-transformed T7 Express competent *E. coli* with varied plasmid ratios, as well as independently transformed cells……..32

Figure 2.6: Co-expression of T7 Express competent *E. coli* cells that were transformed using a 4:1 and a 1:1 ratio of pRSFDuet-1 to pET21a(+) plasmids……..33

Figure 3.1: The effect of hydroxylamine concentration on NHase activity……..44

Figure 3.2: The effect of hydroxylamine concentration on amidase activity……46

Figure 3.3: Standard curve to determine acetohydroxamic acid concentration……48

Figure 3.4: Amidase activity as a function of acetamide concentration…….51

Figure 3.5: Amidase activity as a function of acetonitrile concentration……..53

Figure 3.6: The effect of amidase concentration on the rate of change of absorbance in time…56

Figure 3.7: The effect of acetonitrile concentration on the activity of NHase……58

Figure 3.8: The effect of acetamide concentration on the activity of NHase……60

Figure 3.9: The effect of NHase concentration on the rate of change of absorbance in time….62

Figure 3.10: Determining the temperature optimum for the assay……64

Figure 3.11: Determining the pH optimum for the assay…….66

Figure 3.12: The effect of organic solvents on the assay……...……68

Figure 3.13: The effect of different nitrile substrates on the assay……70

Figure 3.14: The effect of reaction time on acetohydroxamic acid produced using different concentrations of acetonitrile……72

Figure 3.15: The Lineweaver-Burk plot for the NHase……74

Figure 3.16: The Eadie-Hofstee plot for the NHase…….74

Figure 3.17: The Hanes-Woolf plot for the NHase……75

LIST OF SCHEMES

Scheme 1.1: Reactions catalysed by nitrile enzymes……1

Scheme 3.1: NHase and amidase catalyse the conversion of nitrile to hydroxamic acid……36

Scheme 3.2: The effect of hydroxylamine on the assay. Amidase transfers the acyl group from the amide to hydroxylamine……..……42

Scheme 3.3: Hydroxamic acid is the final, measurable product in the assay……..…..47

Scheme 3.4: The amidase enzyme uses amides as substrates, and the nitrile substrate could be present during the process……49

Scheme 3.5: The amidase enzyme is the second enzyme in the coupled assay……54

Scheme 3.6: Nitriles are substrates of the NHase enzyme while amides are the reaction's products……...…….57

Scheme 3.7: NHase is coupled with a second enzyme in order to determine its activity…….61

LIST OF TABLES

Table 2.1: Summary of characteristics for the pRSFDuet-1 and pET21a(+) plasmids……15

Table 2.2: Summary of the characteristics of T7 Express competent *E. coli* and *E. coli* BL21(DE3) cells……...17

Table 2.3: The *E. coli* strains used as hosts in this study……..18

Table 2.4: shows the concentration of antibiotics employed in the LB broth medium and LB agar plates for each transformant…….20

Table 3.1 A summary of kinetic parameters for the NHase…….76

Table 4.1: Summery of ideal parameters for performing the assay ……..81

LIST OF ABBREVIATIONS

BRENDA	Braunschweig ENzyme Database
CFU	colony forming units
Co-NHase	non-corrin cobalt-type nitrile hydratase
CL	crude lysate
CP	crude protein
ER-PCR	error prone -PCR
E. coli	Escherichia Coli
ESS	enzyme substrate substrate complex
Fe-NHase	nonheme iron-type nitrile hydratase
FACS	fluorescence-activated cell sorting
HIV-1	HIV type 1 protease
H-NHase	high molecular mass nitrile hydratase
HPLC	high-performance liquid chromatography
HTS	high throughput screening
IB	inclusion bodies
IPTG	isopropyl β-D-1-thiogalactopyranoside
kDa	kilo Daltons
K_m	Michaelis-Menten constant
L-NHase	Low molecular mass nitrile hydratase
LB	Luria Bertani
min	minute
NHase	nitrile hydratase

NMR	nuclear magnetic resonance
OD	optical density
P. thermophila	Pseudonocardia thermophila
PDB	protein data base
R. rhodochrous	Rhodococcus rhodochrous
RBS	ribosome binding sight
RET	resonance energy transfer
rpm	rounds per minute
SI	substrate inhibition
PAGE	polyacrylamide electrophoresis
SDS	sodium dodecyl sulphate
T7 RNAP	T7 RNA polymerase
TLC	Thin-layer chromatography
TLP-ste	thermolysin-like protease
UV	ultra-violate
Vmax	maximum reaction rate

Chapter 1: Introduction

1.1 Literature review

Many plants and soil microorganisms use nitriles in their metabolic processes therefore there is a plethora of enzymes found in nature that are able to metabolise nitrile compounds efficiently (Martínková *et al.*, 2014; Yamada and Kobayashi, 1996). Nitrilase and nitrile hydratase (NHase), which both use nitrile as a substrate, are the two most important enzymes for converting nitrile. (Kobayashi *et al.*, 1989). The enzymes use two distinct routes for nitrile hydrolysis (Scheme 1.1). Nitrilase catalyses the conversion of nitriles to carboxylic acid in the first pathway, while NHase catalyses the conversion of nitriles to amides in the second pathway, which are then swiftly converted to carboxylic acid in the presence of a second enzyme amidase (Kobayashi *et al.*, 1993).

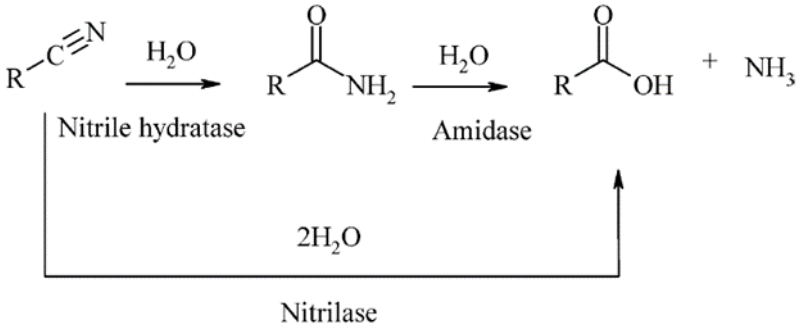

Scheme 1.1: Reactions catalysed by nitrile enzymes. Nitrile hydratase converts nitrile into amides which are consequently converted to carboxylic acids via amidase. Alternatively, nitrilase can convert nitriles to carboxylic acid directly.

1.1.1 The nitrile hydratase enzyme

The focus of this study was on NHase (EC 4.2.1.84) a metalloenzyme. NHase is composed of alpha and beta subunits that usually combine to form a $\alpha_2\beta_2$ heterotetramer (Sasaki *et al.*, 2002). The molecular masses of the alpha and beta subunits are 23 kDa and 26 kDa respectively. The amino acid sequences of the two subunits are not similar, although the alpha and beta subunits from different species are highly comparable. The beta subunit contains two highly conserved arginine residues which form a bond with the sulfur atoms in the cystine residues found in the alpha subunits. In this way a strong bond is formed ensuring the subunits are binding in a precise manner (Liu *et al.*, 2012). The active site of the nitrile hydrates has conserved cysteine residues, CXXCSC, that are involved with the binding of the metal ion in

the centre. NHase was first discovered in *Arthrobacter sp.* J1 which was later renamed *Rhodococcus rhodochrous* (Asano *et al.*, 1980). Although since then many other bacterial genera have been discovered to produce NHase, *R. rhodochrous* has remained the primary source of novel NHases.

1.1.1.1 Cobalt and iron-type NHases

NHase is a metalloenzyme that requires metal ions in its active site. In order to have catalytic activity, a nonheme iron (Fe-NHase) or non-corrin cobalt (Co-NHase) is required. The metal ion is responsible for the catalytic hydration of the enzyme as well as the structural folding of the enzyme (Gong *et al.*, 2017). The two types of NHases have a significant degree of sequence similarity, and their alpha subunits have the three conserved cysteine residues in the active area. Furthermore, they are structurally similar and share a common response mechanism (Gong *et al.*, 2017). The alpha subunit provides all the protein ligands for the metal ion which is found at the interface between the alpha and beta subunits in the central cavity. The metal ion is located in a claw-like setting to deprotonated peptide nitrogens, a cysteine thiolate, sulfur atoms in the cysteine residues and a water molecule (Gumataotao *et al.*, 2013; Hopmann, 2014). The cysteine residues are post translationally modified to cysteine sulfunic acid and cysteine sulfenic acid (Gumataotao *et al.*, 2013; Hopmann, 2014).

1.1.1.1.1 Amino acid sequence in catalytic site of the cobalt and iron- type NHase

NHases have a conserved sequence made up of 7 amino acids in their active site (Figure 1.1). However, the Fe-type and Co-type NHases differ by two amino acid residues at positions 109 and 114. The Fe-type NHase has a 'CSLCSCT' sequence in its active site, whereas the Co-type NHase has a 'CTLCSCY' sequence (Payne *et al.*, 1997). The S and T in the Fe-type NHase stand for αSer109 and αThr114, respectively, whereas the T and Y in the Co-NHase stand for αThr109 and αTyr114. The αThr109 in the Co-type NHase forms a hydrophobic interaction with the side chain of αVal36, however, in the Fe-type NHase the equivalent amino acid residue, αSer109, does not associate with αVal36 (Frederick *et al.*, 2006; Payne *et al.*, 1997). In addition, the αTyr114 residue in the Co-type NHase establishes a hydrogen bond with αLeu119 and αLeu121 via a water molecule (Frederick *et al.*, 2006; Payne *et al.*, 1997). On the other hand, in the Fe-type NHase, the equivalent residue at position 114, αThr114, establishes a hydrogen bond with αSer113 found in the cysteine cluster. The hydrogen bond between αThr114 and αSer113 causes the residues to move closer together, making the active

site more open compared to the Co-type NHase (Frederick *et al.*, 2006; Payne *et al.*, 1997). The difference in conformation of the active site could be the reason for different substrate preferences between the two NHases. Cobalt-type NHase prefer aliphatic nitriles whereas the Fe-type NHase are able to catalyse aromatic nitrile substrates.

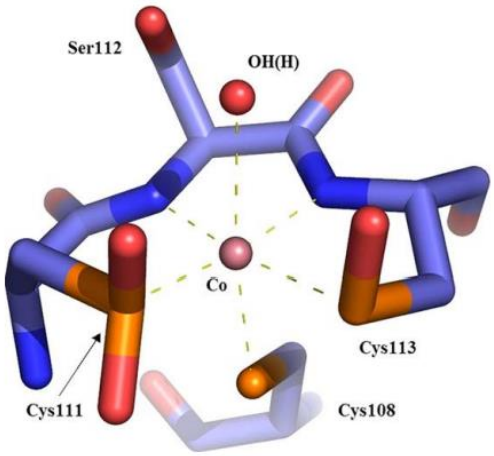

Figure 1.1: The active site of a Co-type nitrile hydratase from *Pseudonocardia thermophila.* The metal ion forms 6 bonds with two deprotonated peptide nitrogens, a cysteine thiolate, two sulfur atoms in cysteine residues at the active site, and a water molecule in a claw-like configuration. The figure is reprinted from Mitra and Holz (2007).

1.1.1.1.2 Crystal structure of the Co-type NHase

There are 39 X-ray crystal structures of NHases from bacterial species deposited in the PDB. Despite the number of NHases discovered in the *Rhodococcal* species, no Co-type NHase from this species has yet to be crystallized. The reason for this is that the Co-type NHase from *Rhodococcal* species may be a difficult protein target to crystallize. Below in Figure 1.2, is a ribbon drawing of the tertiary structure of the Co-type NHase from *P. thermophila* based on a crystal structure determined by Miyanaga (2001).

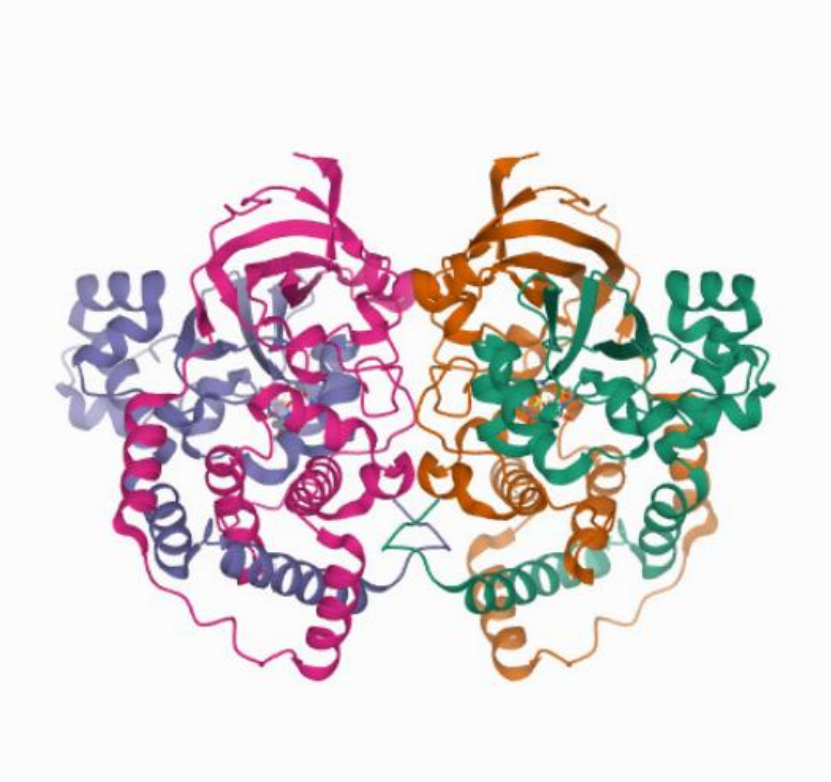

Figure 1.2: A ribbon drawing of the tertiary structure of the Co-type nitrile hydratase from *P. thermophila*. The NHase is a heterotetramer made up of $\alpha_2\beta_2$ subunits. The alpha subunits are in orange and pink, while the beta subunits are in purple and green. The pink and purple unit and the green and orange unit represent one heterodimer. The image was reprinted from the protein data bank (PDB) (Bank, n.d.) and was originally constructed by Miyanaga (2001).

1.1.1.1.3 Catalytic mechanism

Several catalytic mechanisms for NHase have been proposed based on synthetic and theoretical modelling studies, molecular dynamic simulations, substrate docking studies and X-ray crystal structures.

One method that was proposed suggested that the nitrile compound binds directly to the metal ion in the centre of the active site causing the water molecule to be displaced. In this way the metal ion acts as a Lewis acid, by facilitating a nucleophilic attack by the water molecule on the carbon of the nitrile (Desai and Zimmer, 2004)

1.1.1.2 Low and high molecular mass NHase

Within *R. rhodochrous* J1 two types of Co-NHase have been discovered, these being the high molecular mass nitrile hydratase (H-NHase) and a low molecular mass nitrile hydratase (L-NHase) (Kobayashi *et al.*, 1991). The L-NHase is a 130 kDa protein made up of two alpha-beta heterodimers, each with one cobalt ion. Conversely, the H-NHase is a 520 kDa protein containing nine to ten pairs of alpha-beta subunits. The two proteins share a 42.89% sequence similarity (Frederick *et al.*, 2020) and therefore the H-NHase is thought to have evolved through horizontal gene transfer and gene duplication. Although the amino acid residues, CTLCSC, that are located in the active site of all Co-NHases are conserved in both (Frederick *et al.*, 2020).

1.1.1.3 Evaluation of the substrate profile of the low and high molecular mass NHase

1.1.1.3.1 Substrate profile of H-NHase

The substrate profile of the H-NHase was performed by Nagasawa (1991) using 61 small nitrile compounds. The study showed that the H-NHase favoured short unbranched aliphatic nitriles, like acetonitrile and acrylonitrile. The catalytic activity decreased to less than 5% as the size of the chain increased and there was no activity against the branched and aromatic nitriles.

1.1.1.3.2 Substrate profile of L-NHase

Studies evaluating the substrate profile for L-NHase showed that this enzyme was able to catalyse short aliphatic nitrile compounds as well as longer chained compounds such as n-butyronitrile and methacrylonitrile. According to Wieser (1998), L-NHase may catalyse branching aliphatic nitriles as well as aromatic nitriles like benzonitrile. Furthermore, the enzyme has a high catalytic activity for substituents of benzonitrile (Wieser *et al.*, 1998). Since the L-NHase has a larger substrate profile than the H-NHase, it is more in demand to synthetic chemists. The L-NHase used in this study comes from *R. rhodochrous* ATCC BAA-870.

1.1.1.3.3 Substrate profile of the L-NHase from R. rhodochrous ATCC BAA-870

A recent study by Mashweu (2020) looked at the substrate profile of the L-NHase enzyme from *R. rhodochrous* ATCC BAA-870 a wide range of nitriles of varying sizes, degrees of branching and with different substituents. The results revealed that the L-NHases active site was accommodating and was able to catalyse aromatic compounds with large substituents adjacent to the nitrile group. However, substituents on either side of the nitrile group were sterically

hindered. In addition, branching aromatic compounds were not catalysed, which again indicates that steric hindrance around the cyano group is the primary barrier to substrate conversion (Mashweu *et al.*, 2020). This could be because the active site is located deep within the alpha subunit, and the channel leading to it is made up of bulky aromatic amino acids that can limit substrate access (Pravda *et al.*, 2014). Although electrophilicity has shown to affect the rate of the reaction, it cannot prevent the overall reaction (Mashweu *et al.*, 2020).

1.1.1.4 Application of NHase

1.1.1.4.1 Biotransformation in industry

Nitriles are simple to synthesis through several organic chemical pathways from inexpensive substrates, therefore, they have been recognised as important intermediates in the production of high-value industry compounds (Martínková *et al.*, 2014). The present chemical processes for converting nitriles to commercial chemicals, however, have a number of limitations. Adverse reaction circumstances include strong acidic or basic solutions, high temperatures, hazardous by-product production, and significant volumes of salt, to name a few (Kaul and Banerjee, 2008). Since enzymes are naturally evolved to perform under mild reaction conditions using them as biocatalysts is a more environmentally friendly and cost-effective way of producing industrial compounds. Furthermore, because enzymes are stereo- and regio-selective, utilizing them as a biocatalyst allows for the production of novel substrates that chemical processes cannot achieve (Banerjee *et al.*, 2003). The most successful application of NHase in industry is the manufacturing of acrylamide, which is one of the most important industrial chemicals, used in the production of coagulators, stock adhesives, paints, soil conditioners and recovering agents (Yamada and Kobayashi, 1996). In the late 1980s, Mitsubishi Rayon Company (Japan) generated 6,000 tons of acrylamide per year using a NHase from *Pseudomonas chlororaphis* B23 (Yamada and Kobayashi, 1996). Using a NHase from *R. rhodochrous J1*, the yield was increased to almost 30,000 tons per year (Kobayashi *et al.*, 1991). In addition whole-cell NHase is used as a catalyst in the pharmaceutical and food additives industry (Bhalla *et al.*, 2018). An interesting application of nicotinamide in industry is its use in treating arthritis as it aids in cartilage production (Bhalla *et al.*, 2018). Therefore, nitrile-converting enzymes have become crucial in the organic chemistry industry.

1.1.1.4.2 Bioremediation

Since nitriles are used as intermediate compounds and as organic solvents in industry, massive amounts of nitrile-containing chemical waste are produced. Nitriles contain a toxic

cyano group that has mutagenic and carcinogenic qualities that can have negative health consequences (Gong *et al.*, 2017). Therefore, a method to dispose of industrial levels of nitrile is in huge demand. Microorganisms utilise nitriles in their metabolic processes, making them ideal candidates for nitrile waste treatment. Bacterial mixed cultures comprising of NHases and nitrilaseshave been shown to breakdown 99% of hazardous nitrile compounds in both continuous and batch culture systems (Wyatt and Knowles, 1995).

1.1.2 Enzyme engineering

1.1.2.1 NHase as a target for enzyme engineering

Biocatalysts are valuable tools for the organic synthesis of industrial chemicals as they are superior to current chemical methods as they portray a number of key benefits, such as, high selectivity, high yield, mild reaction conditions, energy efficiency and the procedures are environmentally friendly (Riva and Fessner, 2014). However, although enzymes have high capabilities, they are evolved towards the needs of their natural role and host and may lack certain requirements that are needed for an enzyme to be an industrial catalyst. Even when the industrial process works well, the incentive to look for a better biocatalyst to improve the productivity remains. Therefore, enzyme engineering is being used to optimise the catalytic efficiency, specificity and substrate range of enzymes. Furthermore, there are efforts to improve the stability of the enzyme in order to resist harsh production conditions such as elevated temperatures, very acidic or basic pH values and high substrate/product concentration. This is necessary in order to maintain high work cycles and increase product yields so that the enzymes can be utilised in industry.

1.1.2.2 Methods used for enzyme engineering

Enzyme engineering methods can be categorized into rational design and indirect evolution.

1.1.2.2.1 Rational design

Rational design methods generally involve the comparison of the amino acid sequence or the tertiary structure of the protein with a homologous protein that has shown to have the desired function. Then using site-directed mutagenesis the promising amino acid residues are implemented into the protein of interest (Strompfová *et al.*, 2008). Making use of rational design TLP-ste, a thermolysin-like protease from *Bacillus stearothermophilus*, was engineered to be eight times more thermostable and functional at 100°C than the wild-type by substituting thermostability-related amino acids (Riva and Fessner, 2014).

However, the use of rational design is limited since it necessitates a considerable deal of knowledge about the protein sequence, structure, catalytic mechanism, structure-function mechanism, and structure-ligand link (Brenner and Lerner, 1992). Our current understanding of how to adjust protein structure in order to improve protein function is insufficient, therefore relying solely on this method could hinder the development of potential mutants.

1.1.2.2.2 Indirect evolution

Indirect evolution mimics the natural evolution process that occurs through random mutagenesis and sexual recombination. This technique, unlike rational design, requires limited previous understanding of the protein sequence and structure. The gene encoding the desired protein is randomly altered during indirect evolution, resulting in a huge library of mutants. After that, the mutant library must be screened or selected in order to find the mutant with the desired trait. The most commonly used methods to introduce random mutations include error-prone PCR (EP-PCR), chemical mutagens and UV radiation.

The improved activity level of each mutation in the library can be conceptualised as climbing a fitness landscape (Packer and Liu, 2015). The aim of protein engineering is to climb this landscape towards peak activity levels through taking mutational steps (Packer and Liu, 2015). Over several generations of protein engineering there should be an accumulation of beneficial mutations that ultimately result in an improved phenotype.

However, since indirect evolution generates large mutant libraries, the success of this technique relies on the availability of a high-throughput selection or screening method that is able to detect mutants with the desired feature. It is critical that the technique used to select or screen enzymes is sensitive and specific to the desired enzyme property. As a result, most screening and selection procedures try to identify the phenotype associated with the mutant gene. Consequently, the lack of high-throughput screening and selection methods available limits the search for desirable mutations.

1.1.3 Screening and selection techniques

The screening and selection step is the bottleneck in the overall process of directed evolution. There is continues research being done to improve screening and selection techniques for probing the vast protein sequence space.

Screening is the process of inspecting the phenotype of each individual library member in order to determine the variant with the desired biocatalytic activity (Packer and Liu, 2015). In

contrast selection bypasses the need to inspect individual phenotypes by linking the biocatalytic activity of interest to the ability of the organism to survive (Packer and Liu, 2015).

1.1.3.1 Selection techniques

If the enzyme is able to fulfil a metabolic function a selection method that separates active library members that contain the gene of interest can be developed (Packer and Liu, 2015). Although NHase performs a metabolic activity that aids in the organism survival, it requires amidase to convert amide products into carboxylic acid, which is the nitrogen compound used by the cell. As a result, both enzymes would need to be linked which could result in random mutations to the amidase, thus leading to optimisation of the amidase over the NHase. In addition, since the selection technique is based on survival, it would not be able to differentiate which enzyme has evolved.

1.1.3.2 Screening techniques

In screening techniques, the gene variants must be individually expressed on either a solid media or in multi-well liquid plate. The individual expression allows for spatial separation of the variants which in turn allows for the phenotype of the variants to be linked to the genotype.

1.1.3.2.1 Current screening techniques

Current screening techniques available to screen for NHase include, nuclear magnetic resonance (NMR), mass spectroscopy, gas chromatography and high-performance liquid chromatography (HPLC). These techniques are not high-throughput and would be tedious and inefficient at screening large mutant libraries of at least 10,000 mutants per round of evolution.

1.1.3.2.2 Current high-throughput screening techniques

Techniques such as fluorescence-activated cell sorting (FACS) has been employed to screen bulk populations of mutant cells. FACS identifies and isolates cells that contain a desired variant based on the presence of a fluorescent reporter molecule. Since this process does not require spatially separating out the variant it is a much faster, high-throughput screening process that can screen up to 10^8 library members in less than 24 hours (Santoro and Schultz, 2002). Resonance energy transfer (RET) is a technique that relies on the transfer of energy between two chromo- or fluorophores. The transfer of energy between the two fluorophores allows for the study of protein interactions and conformations. Coupled with FACS this technique has been used as a high-throughput screening method for enzyme engineering (Olsen

et al., 2000). Another technique called cell surface display uses anchoring motifs to display the protein of interest on the surface of the cell (Lee *et al.*, 2003). This technique can be useful for enzyme engineering of the substrate selectivity of an enzyme since the protein can react with the substrate on the surface of the cell. Coupling this technique with FACS it can be used for high-throughput screening of mutant enzymes.

The current high-throughput screening techniques discussed above require expensive equipment and reagents. Furthermore, the research required to get the technique to work for the NHase enzyme for all the different parameters that can be evolved (pH, temperature, substrate selectivity profile) would be tedious.

1.1.3.3 Microwell plates for high-throughput screening

Using a microwell plate, traditional enzyme activity experiments can be carried out by miniaturising the reaction components. The components can be added manually (so that it can be carried out in any laboratory), or the throughput can be exponentially enhanced using robotic systems that are available. Among the enzyme assays available, colorimetric or fluorometric assays are the most convenient (Packer and Liu, 2015). The colour can be measured spectroscopically for a quantitative assay, or the colour can be assed visually for a qualitative assay. Furthermore, because colorimetric assays may be performed continuously, information concerning enzyme kinetics can be easily derived.

1.1.3.3.1 Colorimetric assay for detection of nitrile hydratase by Banerjee

Banerjee (2003) developed a colorimetric assay which had a pH indicator dye (bromothymol blue) within it that changed colour based on the pH. Upon the release of hydrogen ions during the nitrilase catalytic reaction the colour changed from blue to green indicating nitrilase activity. Sahu (2019) then adapted this assay so that it could be used to detect NHase activity via the accumulation of amides. However, when this experiment was attempted (results not shown), it was discovered that the amides are not significantly acidic, and their accumulation did not result in a colour change. Furthermore, other components within the cell, such as ammonia, could be causing the colour shift, making this approach insufficiently specific.

1.2 Rationale

NHases are needed for the production of high-value industry compounds such as amides. Using NHases as a biocatalyst to manufacture industry compounds instead of chemical methods that need harsh conditions offers several advantages, including being more

environmentally friendly and cost effective. Enzymes are also stereo- and regio-selective, therefore using them as a biocatalyst allows for the creation of novel substrates that chemical processes cannot (Benerjee *et al.*, 2002). Furthermore, NHases are being used in bioremediation to remove toxic nitrile waste that is produced in industry (Gong *et al.*, 2017). Since microorganisms employ nitriles in their natural metabolic processes, using their nitrile hydrolysing enzymes for nitrile waste treatment is ideal.

However, despite their tremendous capabilities, enzymes have evolved to meet the needs of their natural role and may lack some characteristics required for an enzyme to function as an industrial catalyst. Even when the industrial process works well, the desire to find a superior biocatalyst to boost productivity continues. Therefore, enzyme engineering is being used to optimise the catalytic efficiency, specificity and substrate range of enzymes. Furthermore, attempts are being made to increase the enzyme's stability so that it can withstand tough manufacturing circumstances such as high temperatures, very basic or acidic pH values and substrate/product concentration. Enzyme stability is critical for maintaining intense work cycles and increasing product yield.

There are two main enzyme engineering methods. The first is the rational design method, which examines the protein's tertiary structure or homologous amino acid sequence to discover prospective amino acid residues that might be swapped to increase enzyme activity. However, a great amount of knowledge about the protein sequence and structure is required (Brenner and Lerner, 1992) and our current understanding of how to adjust protein structure in order to improve protein function is insufficient. As a result, relying only on this strategy could stifle the emergence of possible mutants. The second enzyme engineering method is indirect evolution. In this method mutations are added randomly to the DNA sequence and results in large libraries with mutant enzymes. Therefore, the success of indirect evolution relies on the availability of a high-throughput selection or screening method that is able to detect mutants with the desired feature.

Current screening and selection methods are inefficient, complicated and require expensive equipment that is not available in all laboratories. Therefore, in order to optimise the search for desirable mutations that could be utilised in industry, a screening method needed to be identified and optimised.

This project will result in a screening method for NHase enzymes, specifically the NHase from *R. rhodochrous* ATCC BAA-870, as well as improve the body of knowledge in the fields of biocatalysis and green chemistry.

The *R. rhodochrous* species has been the key source of new NHases and thus developing an assay based on the *R. rhodochrous* ATCC BAA-870 strain will allow strains with homologous sequences to be easily adapted to this assay.

1.3 Aim and objectives

1.3.1 Aim

Identify and optimise a high-throughput screening assay for detecting nitrile hydratase activity.

1.3.2 Objectives

1) Co-transform T7 Express competent *E. coli* cells with the pRSFDuet-1 plasmid carrying the alpha and chaperon subunits, as well as the pET21a(+) plasmid containing the beta subunit.

2) Successfully co-express the two subunits of the nitrile hydratase enzyme.

3) Identify and optimise a high-throughput screening technique to measure nitrile hydratase activity.

Chapter 2: Protein expression of Nitrile Hydratase from *R. rhodochrous* ATCC BAA-870 using a two-plasmid vector system

2.1 Introduction

Prior to developing a screening assay, expression of the Nitrile Hydratase (NHase) was carried out. One of the most crucial criteria for effective application of enzymes is that the expression and isolation of the required enzyme be repeatable.

2.1.1 Recombinant protein expression and its effect on biocatalysis

The development of recombinant protein expression has revolutionised biochemistry and the use of biocatalysts for industrial and therapeutic applications. The advent of recombinant protein expression has allowed proteins to be genetically engineered, synthesised and then purified quickly and in large amounts. Expression of specific proteins outside of the native cell allows for the protein's biochemistry to be studied independent of other host cell metabolic processes which could interfere with the enzyme characterisation.

Although in theory recombinant protein expression seems straightforward: inserting a gene of interest into a vector, transforming a host cell, induction followed by protein purification; in practice, there are several things that can go wrong, such as, poor growth of host, losing the plasmid, no expression of the protein, inclusion body (IB) formation and protein inactivity (Rosano and Ceccarelli, 2014). There are many factors that need to be taken into consideration to ensure the ultimate aim of large volumes of soluble, active recombinant protein can be achieved.

2.1.2 Two-plasmid vector system used for recombination of the *R. rhodochrous* ATCC BAA-870 Nitrile Hydratase

The plasmids were designed by Joni Frederick at the University of Cape Town (2006). First attempts were made by him to clone the subunits and the chaperone protein into one plasmid, specifically the pET28a(+) or the pET20b(+) plasmids. However, in both plasmids only the beta and chaperone subunits were cloned, with the chaperone subunit being overexpressed compared to the beta subunit. This indicated that the ribosome binding site (RBS) of the chaperone was being recognised by the *E. coli* while the RBS for the subunits needed further investigation. Upon investigation the alpha subunit's RBS was identified as a rare site which made it unrecognisable by the ribosomes of the *E. coli*. In order to increase the recognition of the transcript of the alpha subunit the RBS was mutated to a sequence identical to that of the

chaperone. However, this did not seem to increase the expression of the alpha subunit. Interestingly, upon investigation of enzyme activity, there was some conversion of benzonitrile to benzamide, indicating some activity was present despite the very low expression (Frederick *et al.*, 2006). Based on these findings Frederick investigated the use of a two-plasmid system. The use of a two-plasmid system ensures that the subunits are expressed independent of each other as transcription of each subunit is under the control of each plasmid's expression promoter. Since the two-plasmid method produced more equal expression of the subunits, it was decided to adopt the two-plasmid vector system for protein expression in this study. The beta subunit of the L-NHase from *R. rhodochrous* ATCC BAA-870 was cloned into a pET21a(+) plasmid while the alpha subunit as well as the chaperone protein was cloned into a pRSFDuet-1 plasmid.

Protein expression can be tricky when working with only one plasmid so adding a second plasmid can add a level of complexity. Many factors need to be taken into consideration when selecting plasmids for a two-plasmid expression system such as plasmid compatibility, copy number, selection markers and expressivity.

2.1.2.1 Plasmid compatibility of the pRSFDuet-1 and pET21a(+) plasmids

Plasmid compatibility as well as copy number lies within the replicon of the plasmid. The replicon is a genetic element that consists of the origin of replication as well as other *cis*-acting elements. For a multi-plasmid expression system to work the plasmids must not fall within the same incompatibility group which means that they must have different origins so that the plasmids are not competing for the same replication machinery within the cells. In this study the pET21a(+) plasmid was used, which possess the pMB1 replicon, a derivative of ColE1, and has low copy number with 20-60 copies per cell. The pRSFDuet-1 plasmid contains the RSF 1030 (NTP1) replicon and has a high-copy number. The difference in copy number can affect equal expression of the plasmids and will be discussed in more detail in Section 2.3.

2.1.2.2 Selection markers on the pRSFDuet-1 and pET21a(+) plasmids

To prevent the growth of plasmid-free cells, a plasmid must contain a resistance marker such as antibiotic resistance genes (Rosano and Ceccarelli, 2014). Since two plasmids are used in the expression host in order to ensure that both plasmids are maintained, each plasmid must have a different resistance marker (Brzoska and Firth, 2013; Sninsky *et al.*, 1981). The pRSFDuet-1 plasmid contains the genes for kanamycin resistance, whereas pET21a(+) contains the genes for ampicillin resistance.

2.1.2.3 pRSFDuet-1 and pET21a(+) plasmids both use the T7 promoter system

The T7 promoter system is popularly used for protein expression as it can result in over 50% of the *E. coli's* total cell protein accounting for the target protein (Baneyx, 1999; Graumann and Premstaller, 2006). The method operates by inserting the gene of interest near the promoter, which is recognized by T7 RNA polymerase (T7 RNAP). The gene encoding the T7 RNAP is under the control of the *LacUV5* promoter. In the absence of an inducer the *lac* repressor protein binds to the operator next to the *LacUV5* promoter and inhibits expression of the T7 RNAP. When lactose or a lactose analogue such as isopropyl β-D-1-thiogalactopyranoside (IPTG) is present it binds the *lac* repressor thus allowing for transcription of the T7 RNAP which is then available to bind at the T7 promoter and transcribe the gene of interest. The T7 expression system is used in both the pRSFDuet-1 and pET21a(+) plasmids, making subunit expression as straightforward as possible. Table 2.1 below summarises the main characteristics of the two expression plasmids.

Table 2.1: Summary of characteristics for the pRSFDuet-1 and pET21a(+) plasmids

	pRSFDuet-1	pET21a(+)
Subunit expression	Alpha subunit and chaperone protein	Beta subunit
Size	3829 bp	5443 bp
Insert size	618 bp and 444 bp	675 bp
Copy number	>100	20- 60
Promoter	T7lac	T7lac
Replicon	RSF 1030 (NTP1)	pBR322, derived from ColEI
Selection marker	Kanamycin	Ampicillin
Expressed protein size	22.7 kDa and 16.7 kDa	25.1 kDa

2.1.3 The host system used for Nitrile Hydratase expression

There is a wide variety of different hosts and vectors that can be used in recombinant protein expression. Deciding on which such options to use requires consideration and understanding of their elements as well as understanding what is required for the protein of interest. The *R. rhodochrous* ATCC BAA-870 NHase has previously been expressed in the *E. coli* BL21(DE3) cell line (Frederick *et al.*, 2006). The BL21(DE3) strain of *E. coli* is the most used expression

strain. BL21 cells are deficient in the Lon protease which is responsible for degrading foreign proteins (Gottesman, 1996). They are also deficient in the gene coding for the outer membrane protease OmpT, whose function is to degrade extracellular proteins (Grodberg and Dunn, 1988). Furthermore, it has the *hsd*SB mutation which prevents plasmid loss by preventing DNA methylation which signals for DNA cleavage by endogenous restriction endonucleases (Rosano and Ceccarelli, 2014). The DE3 indicates that this strain of *E. coli* BL21 has a λDE3 prophage inserted within its chromosome which carries the T7 RNA polymerase under the control of the *lac*UV5 promoter. However, previous expression of the *R. rhodochrous* ATCC BAA-870 NHase in *E. coli* BL21(DE3) cells showed that there was uneven expression of the beta subunit compared to the low expression of the alpha subunit. Expression of the NHase in *E. coli* BL21(DE3) cells was also initially attempted in this study (results not shown), however despite changing expression conditions there was still uneven expression of the subunits. Therefore, transformation of the plasmid into a T7 Express competent *E. coli* strain was done in order to see if the strain of *E. coli* that is used for expression could improve the outcome.

The T7 Express competent *E. coli* strain is an enhanced BL21(DE3) derivative, with the main difference being that the gene carrying the T7 RNA polymerase is inserted into the lac operon on the *E. coli* chromosome and is expressed under the control of the *lac* promoter (New England Biolabs). This provides more control for the induction of the T7 RNA polymerase and consequently more control of transcription of genes downstream of the T7 promotor located on the plasmid. The tighter the control of these genes the less 'leakiness' or basal expression occurs in the absence of an inducer. In addition, the T7 Express competent *E. coli* strain has a higher transformation efficiency than the BL21(DE3) strain even with the use of toxic clones (Anton *et al.*, 2016). A summary of difference between the two strains is seen in Table 2.2 below.

Table 2.2: Summary of the characteristics of T7 Express competent *E. coli* and *E. coli* BL21(DE3) cells

Strain	T7 Express competent *E. coli*	BL21(DE3)
B strain	Yes	Yes
Transformation efficiency	0.6-1 x 10^9 cfu/µg pUC19	1–5 x 10^7 cfu/µg pUC19 DNA
T7 RNA polymerase location	In the lac operon- no λ prophage	λ prophage carrying the T7 RNA polymerase gene
Protease deficiencies	Lon and OmpT	Lon and OmpT
Resistant to phage T1 (*fhuA2*)	Yes	Yes
Animal product	Yes	Yes
Restrict methylated DNA (McrA-, McrBC-, EcoBr-m-, Mrr-)	No	Yes
Genotype	fhuA2 lacZ::T7 gene1 [lon] ompT gal sulA11 R(mcr-73::miniTn10--Tet^S)2 [dcm] R(zgb-210::Tn10--Tet^S) endA1 Δ(mcrC-mrr)114::IS10	fhuA2 [lon] ompT gal (λ DE3) [dcm]ΔhsdS λ DE3 = λ sBamHIo ΔEcoRI-B int::(lacI::PlacUV5::T7 gene 1) i21 Δnin5

2.2 Methods and materials:

2.2.1 Materials

2.2.1.1 Chemicals and reagents

The chemicals were acquired from Sigma-Aldrich (SA) and Merck Chemicals. All chemicals were of analytical grade.

2.2.1.1 *E. coli* strains

Two *E. coli* strains were used in this study and are listed below in Table 2.3. The T7 Express competent *E. coli* strain was used for protein expression while the DH5α strain was used for storage of the plasmids.

Table 2.3: The E. coli strains used as hosts in this study

Strain	Feature	Supplier
T7 Express competent *E. coli*	Expression strain	Novagen
DH5α	Cloning strain	Novagen

2.2.1.2 Recombinant expression systems

Based on the protocol developed by Frederick (2006) a two-construct expression system was used and the plasmids were ordered from GenScript (USA). The same plasmids were used in this study. The gene sequence of the alpha subunit as well as the chaperone protein were inserted as a single construct into the pRSFDuet-1 plasmid in the second multiple cloning site (MCS) between the *Nde*1 and *Pac*1 restrictions sites. The gene sequence of the beta subunit was inserted into the pET-21a(+) plasmid within the MCS between the *Nde*1 and *Xho*1 restriction sites. At the carboxy-terminal (C-terminal) the native stop codon of the beta subunit was removed in order to incorporate the His-tag from the vector for easy purification. With the intention of optimising expression, the native ribosome binding sites (RBS) of the alpha and beta subunits were removed to allow the RBS of the plasmids to be the only site where ribosome binding could occur. Since the genetic sequence of the chaperone protein is within the alpha subunit its RBS could not be altered.

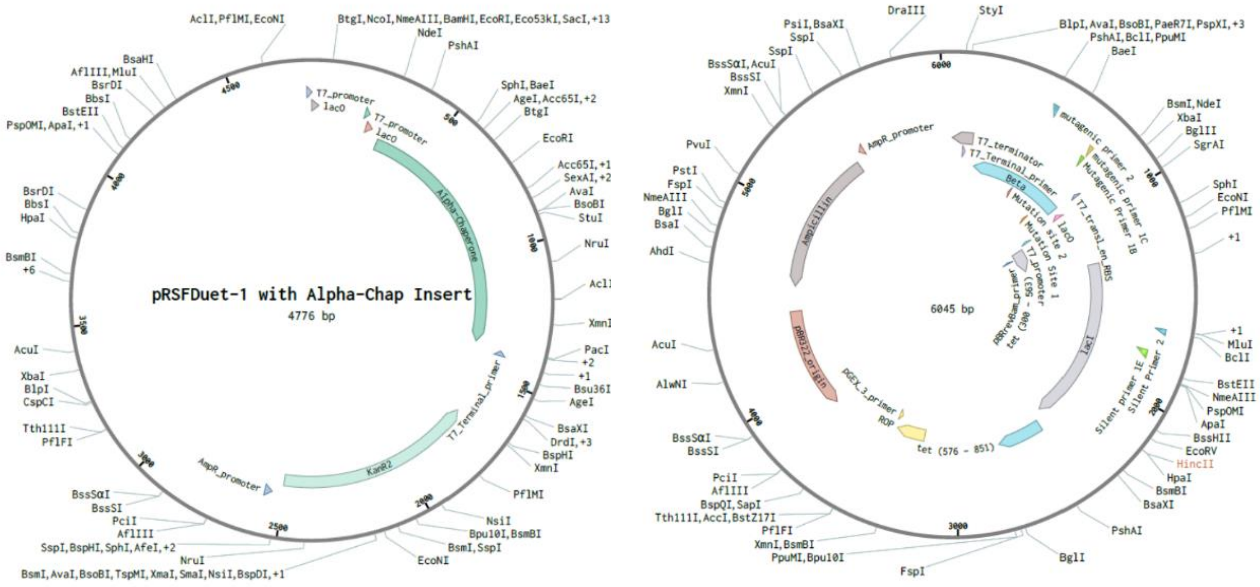

Figure 2.1 Plasmid maps of pET-21a(+) with beta subunit insert and pRSFDuet-1 with alpha and chaperon inserts. The maps was originally constructed by Schmid (2020) using Benching.

3.2.1.3 Media

The Luria Bertani (LB) medium was produced using 5% NaCl, 5% yeast extract and 10% tryptone. The LB agar was produced using the same ingredients at the LB medium except 1% agar was added. All media and agar were sterilised by autoclaving at 120℃, 1 atm for 20 min.

The LB medium was stored at room temperature while the LB agar plates were stored at -4 ˚C. To avoid contamination and antibiotic degradation, the medium and plates were only stored for two weeks.

3.2.1.4 Antibiotics

Kanamycin and ampicillin were used to maintain the plasmid within the transformed cells. The cells transformed with just pRSFDuet-1 had a final concentration of 25 mg/ml of kanamycin in the LB broth or agar while the cells transformed with the pET21a(+) plasmid had a final concentration of 50 mg/ml of ampicillin (Table 2.4). When the plasmids were co- transformed both ampicillin and kanamycin was used.

Table 2.4: shows the concentration of antibiotics employed in the LB broth medium and LB agar plates for each transformant.

Transformant	Antibiotics	Final concentration
αβc	Kanamycin and Ampicillin	25 mg/ml and 50 mg/ml
α	Kanamycin	25 mg/ml
β	Ampicillin	50 mg/ml

2.2.2 Methods

2.2.2.1 Transformation of pRSFDuet-1 and pET21a(+) plasmids

2.2.2.1.1 Competent cell preparation

Super-competent T7 Express competent *E. coli* cells were used for the transformation. Competent cells were prepared by taking a single colony from a fresh streak plate to inoculate a 5 ml starter culture of LB broth. The cells were allowed to grow overnight at 37˚C while shaking. A 1 in 100 dilution of the starter culture was then used to inoculate 50 ml of fresh LB broth. The culture was allowed to grow at 37˚C while shaking until an optical density measured at 600 nm (OD_{600}) of ~ 0.5 using the S-20 Spectrophotometer (Boeco, Germany) was reached. From here on all glassware, buffers and disposables were chilled before use. The cells were placed on ice for 20 minutes before being centrifuged at 4˚C at 5000 rpm for 10 minutes. The pellet was then resuspended in 10 ml of ice cold 0.1 M $MgCl_2$ and was incubated on ice for 30 minutes. The cells were then collected via centrifugation again at 4˚C at 4000 rpm for 10 minutes. The pellet was then resuspended in 1 ml ice cold 0.1 M $CaCl_2$ supplemented with 15% glycerol and was incubated on ice for 10 minutes. Subsequently, 50 µl of cells were aliquoted into cryogenic vials (Sigma-Aldrich) and stored at -80˚C.

2.2.2.1.2 Transformation of T7 Express competent E. coli by heat shock

The super-competent cells were thawed on ice and transferred from cryogenic vials to Eppendorf tubes (Eppendorf, Hamburg, Germany). Transformation was performed by adding 100 ng of each plasmid to the tubes and allowing the cells and plasmids to incubate together on ice for 40 minutes. This incubation period allows for the plasmids to come into close contact with the porous cell walls. The tubes were then placed in a Dri-Block DB-2D (Techne, United Kingdom) at 45˚C for 1 minute. Immediately thereafter the cells were placed back on ice for 2 minutes in order to close the pores in the membrane and retain the plasmids. After which 1 ml

of LB broth with no antibiotics was placed in the tubes and the tubes were incubated at 37˚C for 1 hour with shaking. The time spent without antibiotics allowed the transformed cells to start producing antibiotic resistant genes. Lastly, the cells were plated at various dilutions and grown over night at 37˚C. The number of colony forming units (CFU) were counted on the following day and the transformation efficiencies were calculated

2.2.2.1.3 Confirmation of transformations using sequencing

Selected colonies that were grown on LB agar plates with antibiotics (which is already an indication that transformation was successful) were grown over night in LB broth medium with antibiotics at 37˚C while shaking at 200 rpm. The Zyppy^{TM} plasmid miniprep kit (Zymo Research, USA) was used to extract the plasmids from the cells. The extracted plasmids were then subjected to sequencing. Inqaba Biotech (Pretoria, South Africa) was employed to sequence selected colonies that contained both plasmids to ensure the presence of both the plasmid and the insert within the transformed cells.

2.2.2.2 Glycerol stocks of the transformed cells

A colony for each type of transformed cell (cell containing either the pRSFDuet-1 or the pET21a(+) plasmid or a cell containing both plasmids) was grown in LB broth medium with the relevant antibiotic at 37˚C while shaking at 200 rpm until an $OD_{(600)} = 0.5$ was reached. An aliquot of 500 µl of broth was transferred into a Cryotubes (Lasec SA, Johannesburg, Gauteng, South Africa) followed by the addition of 500 µl of 50% glycerol solution. The tubes were quickly agitated by hands to ensure mixing of the broth with the glycerol. The aliquots were stored at -80˚C until needed.

2.2.2.3 Expression of the subunits and chaperone proteins

2.2.2.3.1 Plate culture of the transformed cells

Glycerol stocks of the transformed cells were streaked onto LB agar plates containing the relevant antibiotics (50 mg/ml ampicillin and 25 mg/ml kanamycin) using sterile techniques. The plates were incubated at 37˚C overnight. The cultures were then maintained at 4˚C but only colonies from freshly streaked cultures (streaked bi-weekly) were used to prevent contamination, mutation or loss of plasmid.

2.2.2.3.2 Growth of starter culture

A colony of transformed cells from a freshly streaked plate was inoculated into 5 ml LB broth medium with the relevant antibiotic. The starter culture was either grown over night or in the morning on the same day that induction was to take place in order to limit the loss of either plasmid due to depletion of antibiotics or toxicity from metabolic biproducts. The broth was incubated at 37˚C while shaking at 200 rpm until the broth was opaque.

2.2.2.3.3 Expansion of starter culture

From the starter culture 2 ml was added to a further 200 ml LB broth medium with antibiotics so that a 1:100 ratio was achieved. A 1 L baffled Erlenmeyer flask was used so that there was good aeration of the shake culture. The broth was incubated at 37˚C while shaking at 200 rpm until an $OD_{(600)}$ = 0.3-0.5 was achieved at which point the culture was induced.

2.2.2.3.4 Induction of the culture

Once an $OD_{(600)}$ = 0.3-0.5 was achieved the culture was then induced by addition of 800 µl of IPTG to give a final concentration of 0.4 mM. Thirty minutes prior to induction 200 µl of cobalt chloride was added so that there was a final concentration of 0.1 mM. The culture was placed in a 16˚C incubator for 20 hours with shaking at 200 rpm. The cells were harvested by centrifugation for 10 minutes at 8000 x *g* at 4˚C. The supernatant containing the broth was discarded and the pellet was washed using 0.5 mM Tris- HCl buffer (pH 7.2) after which the cells were stored at -20˚C overnight. Freezing of the pellet overnight helped with sheering of the cell walls during sonication.

2.2.2.4 Cell disruption via sonication

The frozen pellet was weighed and was resuspended in lysis buffer (0.5 mM Tris- HCl buffer, pH 7.2) using a ratio of 10 ml lysis buffer to 1 g of pellet to get the appropriate amount of lysis buffer for sonication. Sonication was done using Soniprep Ultrasonic Instrument (Matthews Studio Equipment, California, USA) at a power outage of 17 Watts. The resuspended pellet was placed in ice and was exposed to discontinuous blasts of ultrasound (10 cycles of 30 seconds on and 30 seconds off) so that there was a total of 5 minutes of ultrasound exposure. Sonication was done on ice and was cycled so that the heat produced by the sonication process would not denature the proteins that were released.

2.2.2.5 Harvesting of the crude protein extract

A sample of the crude lysate, which contained both the soluble and insoluble proteins, was taken for future analysis of the subunit solubility. The crude lysate was then centrifuged for 20 minutes at 20 000 x *g* at 4˚C. The supernatant which contained the cell-free crude protein extract was appropriately stored for downstream NHase assays and/or purification. The pellet was stored at -20˚C for future analysis of the insoluble protein fractions.

2.2.2.6 Storage of the crude protein extract

The supernatant that contained only the soluble fractions of protein, also referred to as the crude protein extract, was stored at 4˚C on ice. Freezing of the protein was discouraged as the freeze-thawing process could affect the activity of the enzyme. The crude protein was stored at a high concentration as higher concentrations of protein prevent aggregation. Prior to each use the crude protein lysate was centrifuged to remove any protein aggregates (seen as white particles) and the concentration of protein was redetermined.

2.2.2.7 Determination of protein concentration

The Qubit 2.0 Fluorometer (Invitrogen by Life Technologies, USA) was used to quantify the protein concentration. The protocol involved using 199 µl of the Qubit protein buffer and the addition of 1 µl of Qubit protein reagent into Qubit tubes. The tubes were vortexed to homogenise the solution and 2 µl of the solution was removed. Thereafter, 2 µl of a diluted protein sample in distilled water was added to the solution, so that the total volume in the tubes was 200 µl. After homogenising the tubes by vortex they were incubated at room temperature for 15 minutes. The tubes were then placed inside the fluorometer, and the concentration was given based on a standard curve.

2.2.2.8 Visualisation of protein on sodium dodecyl sulphate-polyacrylamide electrophoresis (SDS-PAGE) gel

Electrophoresis was carried out using the Laemmli method (Laemmli, 1970). A 12% polyacrylamide gel was prepared using 40% acrylamide/bisacrylamide, 1.5 M Tris-HCl (pH 8.8), 10% SDS, 10% ammonium persulfate (APS) and tetramethylethylenediamine (TEMED). The protein samples were mixed with a 2x sample buffer (0.5 mM Tris-HCl (pH 6.8), 10% SDS, 1% bromophenol blue, 50% glycerol and 5% 2-mercaptoethanol), and boiled for 5 minutes at 95˚C using a Dri-Block DB-2D (Techne, United Kingdom) so that the protein was linearised. The protein samples were then loaded into the wells and 1x running buffer (3% Tris

Base, 14% glycine and 1% SDS) was poured into the chambers. An Unstained Protein Ladder (Thermo Fisher Scientific, USA) with a molecular weight range between 10 and 200 kDa was used. The gels were stacked at 80 V and once the protein samples were aligned the gels were run at 120 V. The polyacrylamide gels were stained with 0.1% solution of Coomassie Blue R-250 (40% methanol, 10% glacial acetic acid) overnight with shaking. The gels were then de-stained (20% methanol, 10% glacial acetic acid) until the gels were clear.

2.2.2.9 Growth curves

The starter culture and expansion culture were done using the same protocol described in Sections 2.2.2.3.2 and 2.2.2.3.3. However, once the expansion culture was initiated, 500 µl of the culture was extracted every 30 minutes and the absorbance was measured using S-20 Spectrophotometer (Boeco, Germany). The absorbance values were recorded and were used to construct growth curves.

2.2.2.10 Statistical Analysis

Duplicate experiments were done, and the data was analysed using the Student t-test in excel. The differences were considered significant for * $p < 0.05$ or ** $p < 0.01$

2.3 Results and Discussion

2.3.1 Conformation of transformation

Transformation conformation was achieved by submitting the plasmids to Inqaba Biotech for sequencing. BioEdit Sequence Alignment Editor was used to align the sequences returned from Inqaba with the gene sequences of each subunit and chaperon protein. There was perfect alignment indicating that the plasmids with the correctly orientated gene inserts where successfully transformed into the host cells.

2.3.2 Comparison of the growth curves and growth rates for each plasmid as well as the co-transformed cells

2.3.2.1 Growth curves

Growth curves were constructed in order to better understand the transformed cells growth patterns as well as how the growth changes once expression is induced. Understanding the transformed cells' growth patterns and how expression affects them is a crucial initial step in determining the ideal conditions for protein expression.

The growth curves were created by measuring the optical density of a culture at 30-minute intervals while it was incubated at 37°C. The induction of the co-transformed cells was initiated at the beginning of the exponential phase which was achieved at 120 minutes after incubation. This is in line with a previous study that was done using the same plasmids, excepts they were transformed into *E. coli* BL21(DE3) cells (Soobben, 2020). The expression was induced by the addition of 0.4 mM IPTG and 0.1 mM $CoCl_3$. The overexpression of protein within recombinant host cells causes a metabolic load due to energy and resources being directed towards protein production. This is illustrated by the blue curve in Figure 2.2 which has slower growth over time compared to the co-transformed cells that were not induced (orange curve). Although the induced recombinant cells grew slower at 37°C, the rate of growth was still steady at this temperature, which could have resulted in the cells entering the death phase before there was sufficient time for protein expression. In addition, had the cells entered the death phase, the number of cells available to express the protein would have dropped dramatically, and the dying cells would have lysed, releasing the protein into the external environment. As a result, lower temperatures, such as 16°C, were chosen as a good expression temperature over 37°C since a lower temperature slows down the cell growth rate.

The two plasmids were individually cloned into T7 Express competent *E. coli* in order to determine the plasmid burden that each one has on the growth of the cell. Although the pRSFDuet-1 plasmid, which contains the alpha and chaperone subunits, appears to grow faster at first (purple curve) than the pET21a(+) plasmid (yellow curve), they eventually achieve the same biomass.

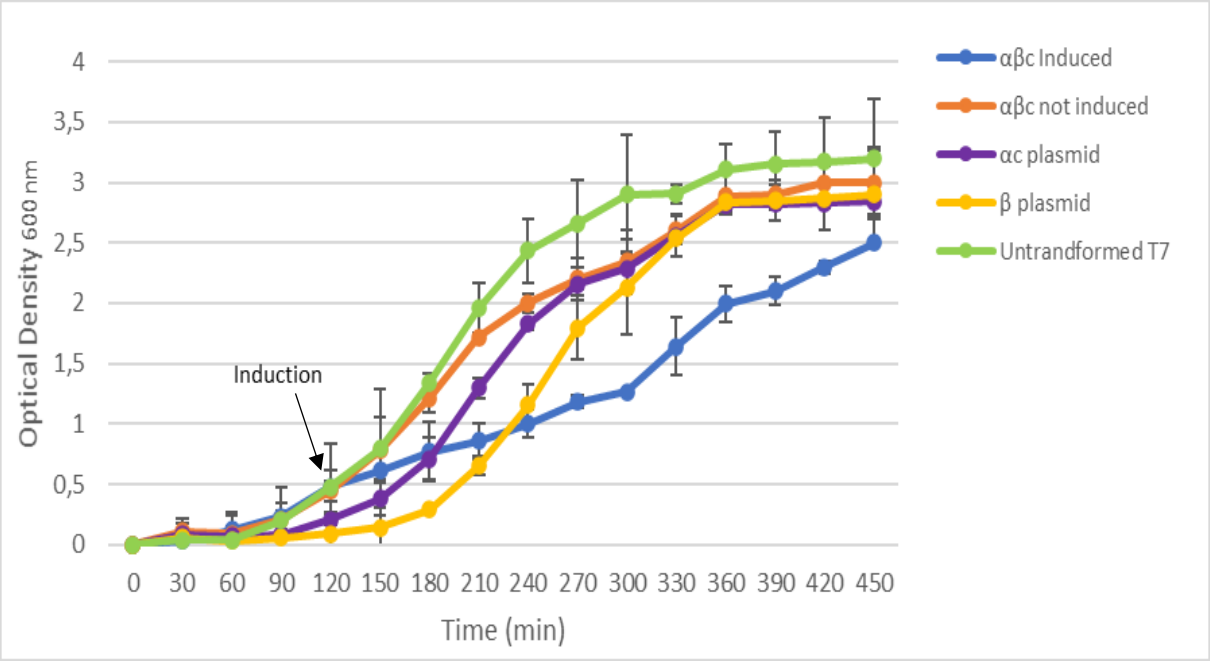

Figure 2.2: Growth curves representing the change in biomass of differentaily transformed T7 Express competent *E. coli* cells in LB media measured at OD_{600}. A starter culture of the transformed cells where grown to an OD of 0.1 prior to being added to 200 ml of fresh broth in order to ensure equal starting biomass. 500 µl of culture was removed in 30-minute intervals in order to measrure the OD at 600 nm. Induction of the co-transformed cells took place at 120 minutes using 0.4 mM IPTG. The green curve represents untransformed cell; the orange curve represents co-transformed cells that were not induced; the purple curve represents cells transformed with both the alpha and chaperone subunits; the yellow curve represents cells transformed with the beta subunit; the blue curve represents co-transformed cells that were induced with addition of 0.4 mM IPTG at 120 minutes. The standard deviation between duplicate measurements is indicated by the error bars.

2.3.2.2 Growth rates

Growth rates were used as a metric to better understand the metabolic and replication burden that each plasmid has on T7 Express competent *E. coli* cells. The growth rates were determined using just the exponential phase from the growth curves in Figure 2.2. In Figure 2.3 the green bar graph depicts untransformed T7 Express competent *E. coli* cells, which has the maximum growth rate, as expected. When comparing the growth rates of uninduced co-transformed cells (orange bar) to induced co-transformed cells (blue graph), a significant difference is observed. This again indicates that there is a metabolic burden associated with protein expression.

The pRSFDuet-1 plasmid which contains the alpha and chaperone subunits is the smaller of the two plasmids yet has a higher copy number. The pET21a(+) plasmid which contains the beta subunit is a larger plasmid but has a low copy number. Due to replication and maintenance of the additional plasmid DNA, both the copy number and the size of the plasmid have an impact on the level of plasmid burden. Although the pRSFDuet-1 plasmid appears to attain higher biomasses earlier than the pET21a(+) plasmid in Figure 2.2, their growth rates are similar as seen in Figure 2.3. Although the copy number and size of the plasmids are different neither one significantly affects the growth rate of the cell.

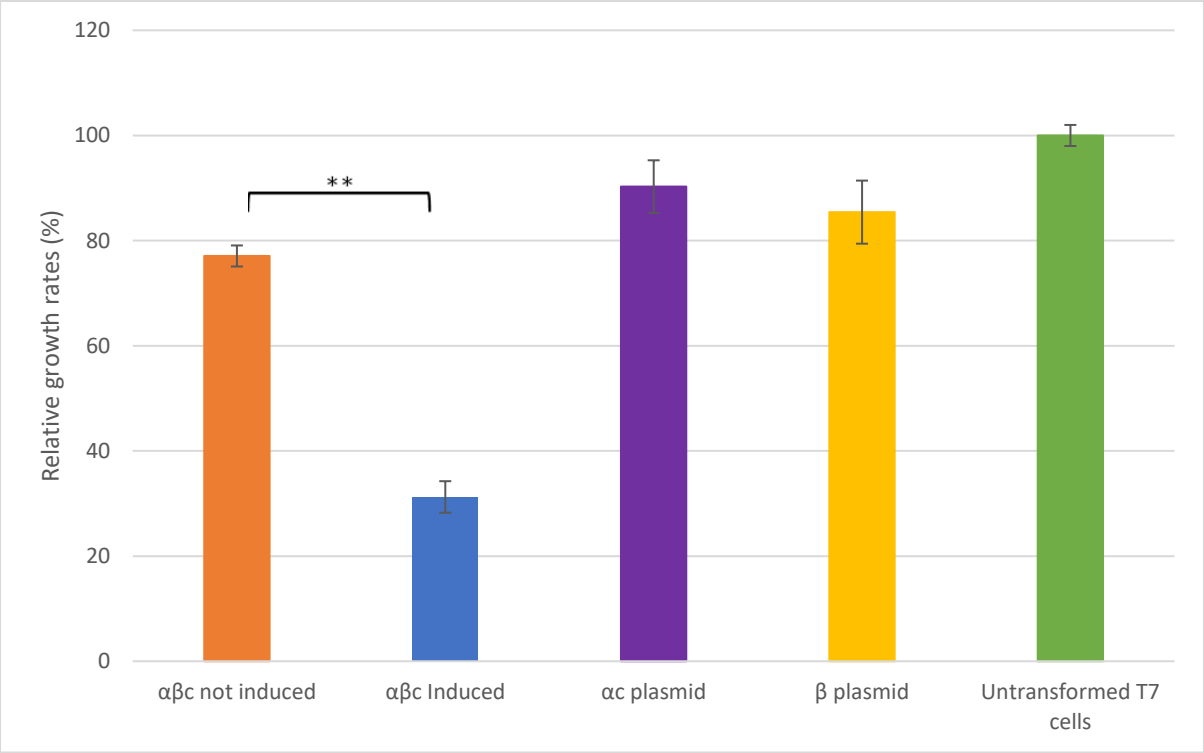

Figure 2.3 Growth rates of the transformants in T7 Express competent *E. coli*. The growth rates of the transformants were calculated using only the exponential phase from the growth curves. The growth rates are expressed as relative activity (%) taking the growth rate of the untransformed T7 Express competent *E. coli* cells at 100%. ** indicates significant difference of $p < 0.01$. The standard deviation between duplicate measurements is indicated by the error bars. The two plasmids used in this study have similar growth rates and have minimal burden on the host.

2.3.2 Co-expression of the *R. rhodochrous* ATCC BAA-870 Nitrile Hydratase

The appropriate expression parameters were established based on the growth patterns of the recombinant cells as well as previous studies and litriture. There are a number of expression paramaters that influnce the quantity and quality of the expressed recombonint protein. This includes IPTG concentration, temperature, time and optical density of the culture at time of induction.

Aside from expressing the protein successfully, the expression parameters must be optimised for high levels of protein activity. If the expression paramaters are not correct it can lead to protein instability and aggregation which will compromise the proteins activity. When recombinant proteins are expressed in *E. coli* host cells the spatio-temporal control of its expression is lost. The host's microenvironment may differ from the protein's initial source in terms of pH, osmolarity, cofactors, and folding processes. Furthermore, high levels of expression result in a large concentration of hydrophobic regions within polypeptides, which may form contacts and cause incorrect folding and aggregation. Build up of these insoluble protein aggregates are called inclusion bodies (IBs). Altering the various parameters that influence the degree of expression, such as temperature, IPTG concentration, and time, can slow down the expression rate, reducing molecular crowding of the cell, which leads to unfavourable protein folding conditions.

Since the induced recombinant cells showed a steady increasing growth pattern at 37°C, a lower temperature was chosen, which would reduce the growth rate and provide sufficient time for protein expression before the cells entered the death phase. In addition, previous expression trials showed that the best expression temperature for the nitrile hydratase protien was at 16˚C for 20 hours (Schmid, 2020). This is in line with our knowledge of protein expression and literature. Slower protein synthesis gives the freshly synthesized peptide strand more time to fold appropriately. Furthermore, low temperature reduces aggregation by removing temperature-dependent hydrophobic interactive forces (Vera *et al.*, 2007).

The expression of the NHase enzyme was conducted at 16˚C for 20 hours using 0.4 mM IPTG and 0.1 mM cobalt chloride. The cultures were then centrifuged to remove the broth and 50 mM Tris-HCl lysis buffer was added. The cells were lyssed via sonication.

The protein subunits were run on an SDS-PAGE gel, which separates proteins by size, to see if the proteins of interest were successfully expressed. In order to determine the level of aggregation, crude lysate (CL), which contains both the soluble and insoluble fractions, and

crude protein (CP), which only contains the soluble fraction after seperation by centrifugation, were run on the gel in parallel. Lanes 3 and 4, which reflect the CL and CP of the alpha subunit expression, respectively, reveal a good deal of alpha protein expression (Figure 2.4). Since the bands in lanes 3 and 4 are equally dense, the alpha protein is soluble, as evidenced by the bulk of the protein found in the supernatant. This implies that the alpha protein is primarily stable and folding properly.

On the other hand, the band in lane 5 that represents the CL of the beta subunit is slightly larger than the band in lane 6 that represents the CP of the beta subunit. This implies that at the current expression parameters, the beta subunit is slightly insoluble indicating instability and aggregation. Frederick (2006) and Schmid (2020) did co-expresssian studies of the same plasmids and found similar results. It is possible that the beta subunit is aggregating because it is not expressed with the chaperone protein, which has been shown to help in protein folding (Frederick et al., 2006; Hartl and Hayer-Hartl, 2002). However, because of the modest aggregation, there were still sufficent soluble beta subunits in the supernatant available to form $\alpha_2\beta_2$ hetrodimers.

Looking at lanes 1 and 2, which represent the CL and CP of co-expressed cells, it can be seen that the beta subunit is expressed at a higher concentration than the alpha subunit. When the level of expression of the alpha subunit during co-expression is compared to the level of expression when it is expressed independently, it is clear that the alpha subunit is expressed at lower levels during co-expression. Previous study by Frederick (2006) and Schmid (2020) validated these findings. It is particularly intriguing because the alpha subunit was cloned into the pRSFDuet-1 plasmid, which has a high copy number and hence should contain a large amount of alpha protein. However, although it is reasonable to assume that a high copy number will result in a high protein yield, a high plasmid number can cause metabolic stress, which can lead to plasmid instability.

It is possible that when two genes are co-expressed, twice as many polypeptides are produced, resulting in protein instability. However, the width of the alpha subunit bands in lanes 1 and 2 are the same, indicating that its solubility is unaffected, suggesting that the reduced expression of the alpha subunit during co-expression is unrelated to increased polypeptide instability. In addition, protein toxicity of the alpha subunit towards the T7 Express competent *E. coli* host must be considered. Protein toxicity occurs when recombinant protein performs an unneeded and harmful function in the host cell. However, because both the alpha and beta subunits of

the protein were successfully synthesized in equal amounts when individually expressed, the protein poses no risk to *E. coli*, making it a suitable host.

Although, the co-expression of the subunits affects the expression levels of the alpha subunit, co-expression of the two subunit proteins in the same cell has various advantages over expression in two different systems with post-expression reconstitution of protein partners. The proper folding of each subunit is due to subunit interactions *in vivo*. The importance of protein subunit interaction during co-expression has showed increased amounts of properly folded proteins and decreased proteolytic degradation proteins (Sørensen and Mortensen, 2005).

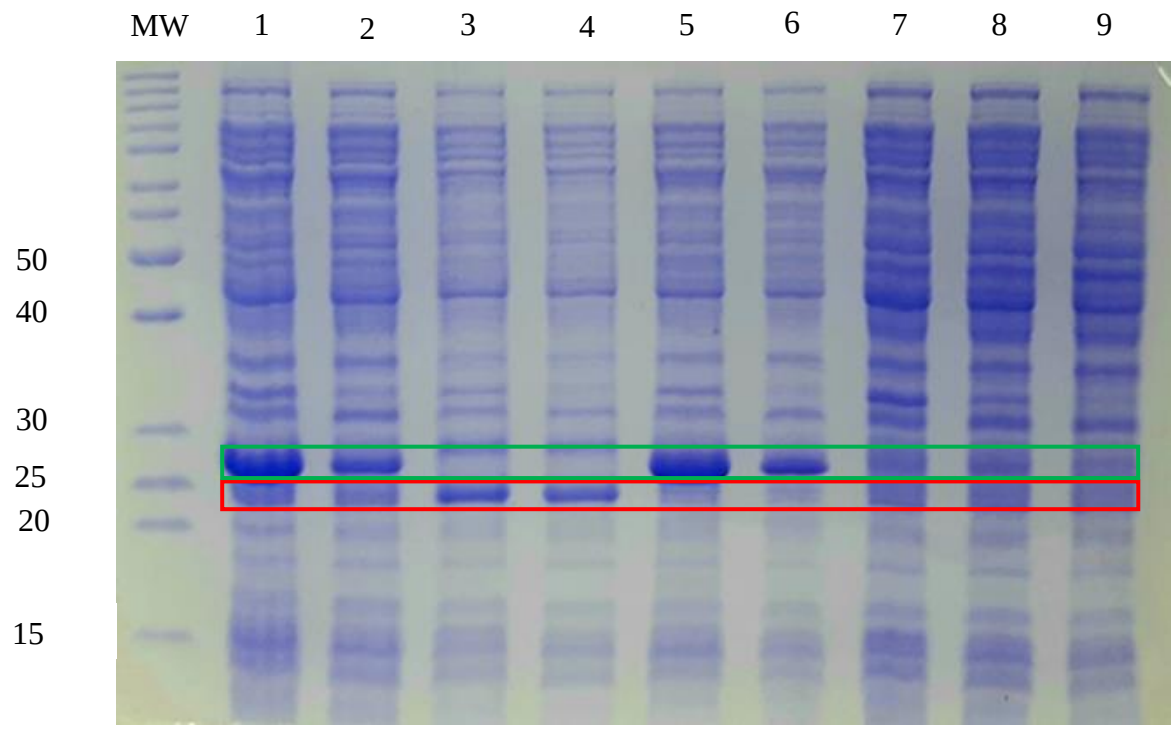

Figure 2.4: Co-Expression and individual expression of the nitrile hydratase alpha and beta subunits in T7 Express competent *E. coli* cells. Cultures containing T7 Express competent *E. coli* transformed with either the pRSFDuet-1 or the pET21a(+) plasmids or co-transformed with both plasmids were grown until an OD_{600} = 0.3. The expression of the subunits was induced by the addition of 0.4 mM IPTG and 0.1 mM $CoCl_2$, for 20 hours at 16˚C. The solution after sonication is called the crude lysate (CL) which contains both soluble and insoluble proteins. The crude protein (CP) contains only the soluble protein once the lysate is centrifuged. Lane 1 and 2: CL and CP of co-transformed cells; Lane 3 and 4: CL and CP of

alpha and chaperone subunits; lane 5 and 6: CL and CP of beta subunit; Lane 7 and 8: CL and CP of co-transformed cells that were not induced and Lane 9: untransformed T7 Express competent *E. coli* cells. The green box indicates the beta subunit which is 27 kDa and the red box indicates the 23 kDa alpha subunit

2.3.3 Transformation efficiencies for co-transformed and individually transformed plasmids

Based on a suggestion by Frederick (2006) in order to try increase the expression of the alpha subunit during co-expression a 4:1 ratio of pRSFDuet-1 to pET21a(+) plasmid was transformed into super-competent cells using heat-shock. The transformation efficiencies were calculated as seen in Figure 2.5. The transformation efficiency of the 4:1 ratio of pRSFDuet-1 to pET21a(+) plasmid was significantly lower than the 1:1 ratio, which was expected as an increase in plasmid concentration can hinder the movement of plasmid into the pores of the cell. However, only a single colony was needed to determine whether an increased ratio of the alpha subunit would even out the co-expression of the subunits. The SDS-PAGE analysis of the expression (Figure 2.6) showed that a 4:1 ratio did not increase alpha subunit concentration during co-expression. This result was in contrast to the result obtained by Frederick (2006) who showed that the 4:1 ratio increased the alpha subunit expression.

Figure 2.5 shows that the transformation efficiencies of the individually transformed plasmids are significantly different. The pRSFDuet-1 plasmid that contains the alpha subunit is a smaller plasmid compared to the pET21a(+) plasmid and thus has an advantage of moving through the pores during heat-shock more easily.

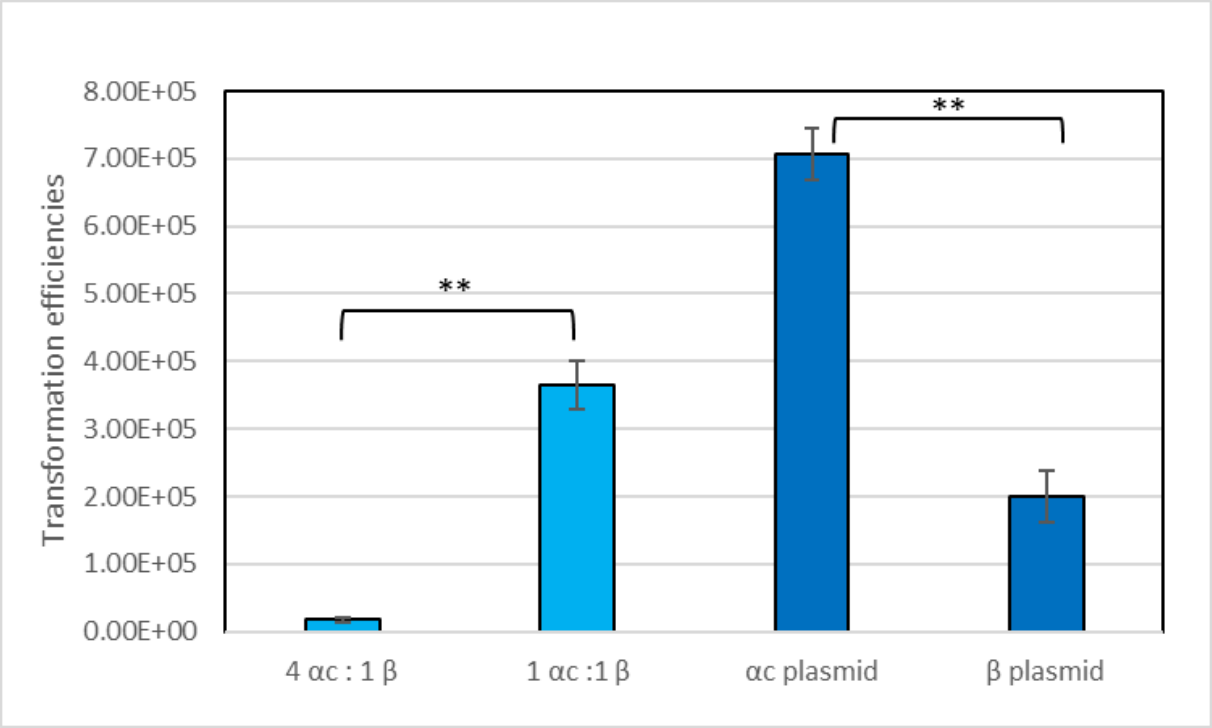

Figure 2.5: Transformation effeciencies of co-transformed T7 Express competent *E. coli* cells with varied plasmid ratios, as well as independently transformed cells. Heat-shock transformations were done using a 1:1 and a 4:1 ratio of pRSFDuet-1 plasmid carrying the alpha and chaperone subunits to pET21a(+) plasmid containing the beta subunit. Each plasmid was individually transformed into T7 Express competent *E. coli*, yielding transformation effcieincies for each plasmid. The standard deviation between duplicate measurements is indicated by the error bars.** indicates significant difference of $p < 0.01$.

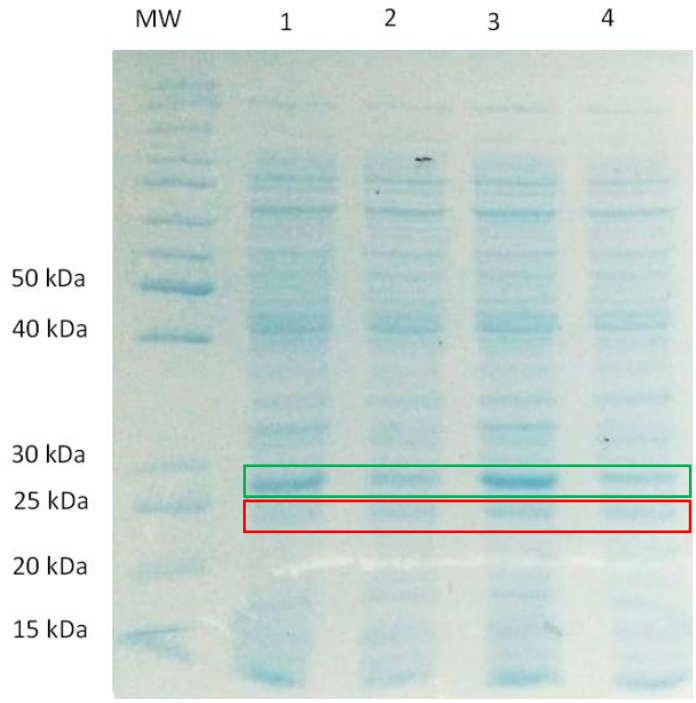

Figure 2.6: Co-expression of T7 Express competent *E. coli* cells that were transformed using a 4:1 and a 1:1 ratio of pRSFDuet-1 to pET21a(+) plasmids. The expression of the subunits were induced by the addition of 0.4 mM IPTG and 0.1 mM $CoCl_2$, for 20 hours at 16˚C. The solution after sonication is called the crude lysate (CL) which contains both soluble and insoluble proteins. The crude protein (CP) contains only the soluble protein once the lysate is centrifuged. Lane 1 and 2: CL and CP of 4:1 ratio of co- transformed cells; Lane 3 and 4: CL and CP of 1:1 ratio of co-transformed cells. The green box indicates the beta subunit which is 27 kDa and the red box indicates the 23 kDa alpha subunit

Chapter 3: Optimising a high-throughput screening assay for the *R. rhodochrous* ATCC BAA-870 nitrile hydratase enzyme

3.1 Introduction

Developing a sensitive enzyme assay that is suitable for high-throughput screening (HTS) requires identification of relevant substrate forms, buffers, characterisation of co-factors, measurement of kinetic parameters and choice of a detection technology for the final assay (Robinson, 2015). In addition, the cost of reagents, the amount of enzyme required, and the simplicity of implementation within the laboratory must all be addressed while establishing the enzyme assay (Onyeogaziri and Papaneophytou, 2019).

HTS assays need to be able to test millions of samples, often over the course of numerous enzyme preparations and weeks of assay repetition. Therefore, HTS assays need to be designed to be highly repeatable. HTS assays must meet stringent requirements that are more demanding than those required by typical bench-top activity assays. The chemical elements of the high-throughput enzymatic assay, such as the buffer and substrates, must remain stable over a long period, and must not deteriorate or be impacted by the equipment and automated machinery used.

To ensure high repeatability, reliability and quality, it is of utmost importance to obtain a thorough grasp of the enzymology and biochemistry of the chosen enzyme within the context of the specific assay. Enzyme activity is strongly influenced by a number of factors such as the concentration of substrate, product and enzyme, temperature, pH and ion strength (Bisswanger, 2014). Thus, in order to ensure that the assay is highly accurate, sensitive and reproducible these parameters must be optimised, and the protocol developed must be rigorously maintained. Enzymes have their highest activity under optimal conditions and deviations from those decrease their activity. The higher the divergence, the higher the impact on activity. Since each enzyme is unique, few general rules apply, and scientific research for each enzyme is required for an assay specific application.

Current techniques used to detect amide production include high-performance liquid chromatography (HPLC), thin-layer chromatography (TLC), nuclear magnetic resonance **(**NMR) spectroscopy and mass spectroscopy (Hertzberg and Pope, 2000). These techniques are cumbersome, time consuming, relatively difficult and cannot perform at high-throughput levels (Hertzberg and Pope, 2000). In this study a coupled enzyme assay was used because the products of nitrile hydrolysis by a nitril hydratase (NHase) are amides which are difficult to

detect with regular techniques. By coupling the NHase with an amidase enzyme the amide produced by the NHase becomes a substrate for the amidase, which results in production of a more easily detectable compound, hydroxamic acid, that could then be determined with a colorimetric reaction (Wyk and Caroline, 2008). The colour can be visualised easily by eye for qualitative assessment, or the absorbance can be measured quantitatively by a spectrometer. Colorimetric assays can be miniaturised easily which means that multi-well plates and a microplate reader can be combined to create high-throughput abilities. With automated equipment thousands to millions of samples can be tested rapidly.

A prominent coupled enzyme assay used in the past for other NHase's is the phenol-hypochlorite method, developed by Fawcett and Scott (Fawcett and Scott, 1960). This method relies on forming a coloured complex between the phenol-hypochlorite and ammonia group that is released when the amidase catalyses the amide to its respective carboxylic acid (Cameron *et al.*, 2005; Okamoto and Eltis, 2007). However, this assay is not ideal for a high-throughput screening technique for the random mutagenesis of the NHase enzyme because crude protein is used in the assay which means that the ammonia produced endogenously by the microbial cells will be present in the samples. Therefore, this assay can result in false positives.

To ensure accuracy and given that the optimal screening strategy is to evaluate the product produced by the enzyme directly (Aharoni *et al.*, 2005) another assay method had to be identified and optimised. The hydroxamic acid assay is usually used to test an amidases acyl transfer ability by measuring the production of hydroxamic acid that results due to the acyl group transfer from the amide to a hydroxylamine (Bhatia *et al.*, 2016; Fournand *et al.*, 1998). By adding an additional incubation step, the NHase activity can be measured indirectly (Scheme 3.1). This assay is more accurate than the phenol-hypochlorite method since the final product is dependent on an amide which would only be present if the NHase was successful. The amidase used in this assay was purchased from Sigma-Aldrich and originates from the species *R. rhodochrous* ATCC BAA-870.

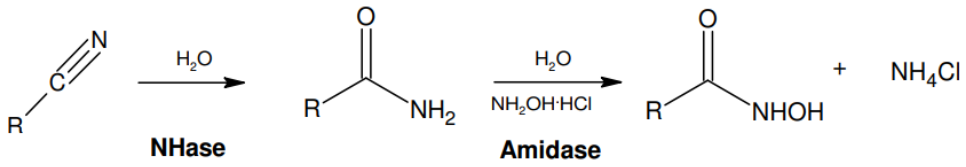

Scheme 3.1: NHase and amidase catalyse the conversion of nitrile to hydroxamic acid.

There are various challenges in successfully accomplishing a coupled enzyme assay, as two reactions are addressed one after the other in the same reaction medium. The general issues encountered are differences in the optimal conditions for both enzymes such as pH or temperature change (Mouafo Tamnou *et al.*, 2021). In addition, the enzyme kinetics of coupled enzyme assays are more complicated and open to inaccuracies. Thus, understanding the enzymes kinetics of each enzyme in the coupled assay is essential to ensuring that a sensitive and accurate assay is developed.

An enzyme-coupled assay for the high-throughput screening of the NHase from *R. rhodochrous* ATCC BAA-870 is presented here. In particular, the parameters that effect enzyme activity and the accuracies of the enzyme kinetics were investigated in detail, to: (1) ensure compatibility of the assays, (2) optimise the concentration of substrate for each enzyme to increase the assays sensitivity, (3) identify the concentration and incubation time for each enzyme to optimally detect the reaction kinetics, (4) define the necessary pH and temperature conditions and (5) examine the effects of various organic solvents and nitrile substates on enzymatic activity.

3.2 Materials and methods

3.2.1 Materials

Chemicals were purchased from Sigma-Aldrich (SA) and Merck Chemicals. All chemicals were of analytical grade.

Care was taken in the preparation of the iron (III) and hydroxamic acid solutions to prevent extensive hydrolysis which could affect the absorption values (Knight and Sylva, 1974; Monzyk and Crumbliss, 1979).

The preparation of the nitrile substrates was done on the day of experimentation and were kept in the dark as nitriles are sensitive molecules.

3.2.2 Methods

The physiological conditions that exist within the organism that produces the enzyme, or literature relating to homologous enzymes, can be used as a guide for setting up the initial assay, offering starting conditions for initial test parameters such as buffer, salt concentrations, pH and temperature.

The assay was developed so that the total volume of the NHase incubation step remained at 100 µl while the volume of the amidase incubation step was performed with a further 100 µl volume to result in at 200 µl total volume. Afterwards, 50 µl of acidic ferric chloride solution (0.1 M $FeCl_3$ in 0.1 M hydrochloric acid) was added, and the total acetohydroxamic acid concentration was measured at a volume of 250 µl. This ensured that all concentrations were determined using the same volume as according to Beer's law the length of the pathway can affect absorbance values.

The optimisation of the assay was performed sequentially, so that the results from the previous experiment were used for optimising the next step.

3.2.2.1 Investigation into the effect of hydroxylamine on the assay

Hydroxylamine is added to the wells and acts as a nucleophile by accepting the acyl group from the amide. Any chemical in the reaction can influence the activity of the enzyme and therefore needs to be investigated.

3.2.2.1.1 Determining the effect of hydroxylamine on NHase activity in biocatalytic reactions

The uncoupled assay involved two incubation steps. The first was with the NHase and the second with the amidase. In the first incubation step, 50 µl of increasing concentrations of hydroxylamine, ranging from 0-100 mM (prepared in 50 mM Tris-HCl pH 7.2), were added to the wells of a 96 well plate. This was followed by the addition of 50 µl of 50 mM acetonitrile (dissolved in 50 mM Tris-HCl, pH 7.2) and lastly 1 µg/µl of crude NHase enzyme (prepared in 50 mM Tris-HCl, pH 7.2) was added to the wells which started the reaction. Additional, 50 mM Tris-HCl, pH 7.2, was added to the wells, so that the total volume of the first reaction was 150 µl. The reaction took place at 37˚C and ran for 30 minutes. The second incubation step involved the addition of 50 µl of 1 unit amidase enzyme (Sigma-Aldrich) (prepared in 50 mM Tris-HCl, pH 7.2), which brought the total assay volume up to 200 µl. The reaction was then allowed to react for a further 30 minutes before being terminated by the addition of 50 µl of an acidic ferric chloride solution (0.1 M $FeCl_3$ in 0.1 M hydrochloric acid). The reddish/brownish

colour that formed was measured by the Victor Nivo Multimode Microplate Reader (PerkinElmer, USA) at 510 nm.

3.2.2.1.2 Determining the effect of hydroxylamine on amidase activity in biocatalytic reactions

Since specifically the amidase reaction was being investigated here only one incubation step was needed. 50 µl hydroxylamine was added to the wells in increasing concentrations ranging from 0–100 mM (prepared in 50 mM Tris-HCl, pH 7.2). This was followed by the addition of 50 µl of 50 mM acetamide (Sigma- Aldrich) (prepared in 50 mM Tris-HCl, pH 7.2). Lastly, 50 µl of 1 unit amidase enzyme (prepared in 50 mM Tris-HCl, pH 7.2) was added which started the reaction. The 50 mM Tris-HCl, pH 7.2 was added to the wells so that the total volume of the reaction was 200 µl. The reaction was incubated at 37˚C for 30 minutes before it was terminated through addition of acidic ferric chloride solution (0.1 M $FeCl_3$ in 0.1 M hydrochloric acid). The coloured compound was then measured spectroscopically at 510 nm.

3.2.2.2 Determining the optimal concentration of the final product, acetohydroxamic acid, in order to maximise the assay's sensitivity

The ideal concentration of acetohydroxamic acid produces a sensitive signal while the required reactant concentrations are kept to a minimum. To determine the optimal concentration a standard curve was constructed. Increasing concentrations of acetohydroxamic acid (Sigma-Aldrich) ranging from 0 to 50 mM were used. The acetohydroxamic acid was prepared in 50 mM Tris-HCl, pH 7.2 and 200 µl of the solution was added to the wells. An acidic ferric chloride solution (50 µl of 0.1 M $FeCl_3$ in 0.1 M hydrochloric acid) was added to the well. The absorbance of the formed coloured complex was measured by the Victor Nivo Multimode microplate reader (PerkinElmer, USA) at 510 nm.

3.2.2.3 Optimisation of the amidase activity within the assay

3.2.2.3.1 Determining the optimal acetamide concentration on amidase activity

Only one incubation step was required because specifically the amidase enzyme was investigated. The acetamide (Sigma- Aldrich) was prepared in 50 mM Tris-HCl, pH 7.2 and 50 µl of increasing concentrations ranging from 0-100 mM were added to the well. In addition, 50 µl of 20 mM hydroxylamine and 50 µl of 50 mM Tris-HCL, pH 7.2, was added to the wells. Lastly, 50 µl of 1 unit amidase was added to the wells to start the reaction. The total volume of the reaction in the well was 200 µl. The reaction was incubated for 30 minutes at 37˚C. The

reaction was then terminated by the addition of 50 µl of 0.1 M $FeCl_3$ in 0.1 M hydrochloric acid and the absorbance was measured at 510 nm.

3.2.2.3.2 Determining the effect of acetonitrile concentration on the amidase activity

Since acetonitrile from the first incubation step could be left in the wells during the second, the effect of acetonitrile on the amidase enzyme was investigated. 50 µl of increasing concentrations of acetonitrile ranging from 0 to 100 mM (prepared in 50 mM Tris-HCl, pH 7.2) were added to each well. In addition, the wells contained 50 µl of 100 mM acetamide and 50 µl of 20 mM hydroxylamine which were both prepared in Tris-HCl, pH 7.2. The reaction was initiated with 50 µl of 1 unit amidase (prepared in 50 mM Tris-HCl, pH 7.2). The 96 well plate was incubated for 30 minutes at 37˚C before the reaction was terminated with 50 µl of 0.1 M $FeCl_3$ in 0.1 M hydrochloric acid. The absorbance was measured at 510 nm.

3.2.2.3.3 Determining the optimised concentration of amidase for optimal timely product conversion

The optimal amidase concentration was determined by using a 0.2 to 1 unit range of amidase. 50 µl of amidase was added to the wells already containing 50 µl of 100 mM acetamide and 50 µl of 20 mM hydroxylamine. The amidase enzyme and the two substrates were prepared in 50 mM Tris-HCl, pH 7.2. In order to maintain a consistent volume (200 µl) in which the amidase reaction takes place, 50 µl of 50 mM Tris-HCl was also added to the well. The reaction was incubated at 37˚C and was stopped at 10-minute intervals by adding 50 µl of 0.1 M $FeCl_3$ in 0.1 M hydrochloric acid. The absorption was measured at 510 nm.

3.2.2.4 Optimisation of the NHase activity within the assay

3.2.2.4.1 Determining the optimal acetonitrile concentration on the NHase activity

The uncoupled assay involved two incubation steps, the first with NHase and second with amidase. In the first incubation step, 50 µl of acetonitrile concentrations ranging from 0 to 100 mM were mixed with 1 µg/µl of crude NHase enzyme. The first incubation reaction was maintained at 100 µl by adding Tris-HCl (50 mM, pH 7.2). The reaction was incubated at 37˚C for 30 minutes. The NHase reaction was inhibited by the addition of 50 µl of 20 mM hydroxylamine. The amidase incubation step began after 50 µl (0.4 units) of amidase was added. All the enzymes and substrates were prepared using 50 mM Tris-HCl, pH 7.2. The reaction was incubated at 37˚C for another 30 minutes before being terminated by addition of

50 µl of 0.1 M $FeCl_3$ in 0.1 M hydrochloric acid. The brownish/red colour was measured at 510 nm.

3.2.2.4.2 Determining the effect of acetamide concentration on NHase activity

Acetamide is the product of NHase and thus the effect of product inhibition needed to be investigated. In order to evaluate this, varying concentrations of acetamide needed to be present during the NHase incubation step. The wells contained 50 µl of 100 mM acetonitrile, and 40 µl of increasing acetamide concentrations ranging from 0 to 100 mM, and 1 µg/µl of crude Nhase enzyme. In order to maintain a volume of 100 µl during the NHase incubation step extra Tris-HCl (50 mM, pH 7.2) was added to make up the missing volume, depending on the volume of crude NHase solution that was used. The reaction was incubated at 37˚C for 30 minutes. This was followed by the addition of 50 µl of 20 mM hydroxylamine and 50 µl of 0.4 units of enzyme. All the enzymes and substrates were prepared using 50 mM Tris-HCl, pH 7.2. This second reaction was then incubated for a further 30 minutes at 37˚C. The reaction was terminated by the addition of 50 µl of 0.1 M $FeCl_3$ in 0.1 M hydrochloric acid. The brownish/red colour was measured at 510 nm.

3.2.2.4.3 Determining the optimised concentration of NHase for optimal product conversion

To determine the optimal concentration of NHase and reaction time, increasing concentrations of crude NHase, ranging from 0.2 to 1 µg/µl, were used. The wells contained 50 µl of 100 mM acetonitrile and relevant volumes of 50 mM Tris-HCl (pH 7.2). The volume of added buffer depended on the volume of NHase enzyme so the reaction volume of 100 µl, was maintained in the first reaction. The reaction was incubated at 37˚C and was stopped at 10-minute intervals by adding 50 µl of 20 mM hydroxylamine. Directly after the addition of hydroxylamine 50 µl (0.4 units) of amidase was added and the reaction was incubated for a further 30 minutes at 37˚C. All the enzymes and substrates were prepared using 50 mM Tris-HCl, pH 7.2. The reaction was terminated by adding 50 µl of 0.1 M $FeCl_3$ in 0.1 M hydrochloric acid. The absorbance was measured at 510 nm.

3.2.2.5 Determination of the optimal temperature for the assay

To determine the optimal temperature for this assay both incubation steps were conducted at temperatures ranging from 20˚C to 70˚C. The first incubation step was conducted using 50 µl of 100 mM acetonitrile, 1 µg/µl of crude NHase and 50 mM Tris-HCl pH 7.2 to reach a final volume of 100 µl. The reaction was incubated at temperatures detailed above for 10 minutes.

The second incubation step included the addition of 50 µl of 20 mM hydroxylamine and 50 µl (0.4 units) of amidase. The reaction was incubated for 30 minutes, at the same temperature as the first reaction. All enzymes and substrates were prepared using 50 mM Tris-HCl, pH 7.2. The reaction was terminated by adding 50 µl of 0.1 M $FeCl_3$ in 0.1 M hydrochloric acid. The absorbance was measured at 510 nm.

3.2.2.6 Determination of the optimum pH for the assay

The effect of pH on the assay was investigated by using various buffers at a range of different pH values: pH 3.0, 4.0, 5.0 and 6.0 (50 mM citrate buffer); pH 7.0 and 8.0 (50 mM Tris-HCl buffer) and pH 9.0 and 10 (50 mM Glycine-NaOH buffer). In the first reaction 50 µl of 100 mM acetonitrile and 1 µg/µl of crude NHase were incubated in the buffers detailed above. The reaction was incubated at 35˚C (adjustment of temperature based on the previous results) for 10 minutes. The second incubation step included the addition of 50 µl of 20 mM hydroxylamine and 50 µl of 0.4 units of amidase.The reaction was incubated at 35˚C for 30 minutes. The enzymes and substrates were prepred using the buffers at the different pH values outlined above. The reaction was terminated by adding 50 µl of 0.1 M $FeCl_3$ in 0.1 M hydrochloric acid. The absorbance was measured at 510 nm.

3.2.2.7 Investigating the effect of organic solvents on the assay

The following organic solvents were tested for their effect on NHase activity: dimethyl sulfoxide (DMSO), methanol, acetone, ethanol, isopropanol, hexane and ethyl acetate. A concentration of 2 M acetonitrile was prepared in each of these organic solvents so that only 5 µl of the solution would be required to provide a final concentration of 100 mM acetonitrile in a 100 µl reaction volume. Thus, only 5% organic solvent was used in the reaction. In the first incubation step, 5 µl of 2 M acetonitrile prepared in each organic solvent, 1 µg/µl of crude NHase and 50 mM Tris-HCl buffer, pH 8, was used (pH had been adjusted after the previous optimisation step). The reaction took place at 35˚C for 10 minutes. This was followed by the addition of 50 µl of 20 mM hydroxylamine and 50 µl of 0.4 units of amidase (both prepared using 50 mM Tris-HCl buffer, pH 8). The second incubation step took place at 35˚C for 30 minutes. The reaction was terminated by the addition of 50 µl of 0.1 M $FeCl_3$ in 0.1 M hydrochloric acid. Absorbance was measured at 510 nm.

3.2.2.8 Investigating the effect of different nitrile substrates on the assay

The following nitrile substrates were investigated: Acetonitrile, acrylonitrile, butyronitrile, benzonitrile, 2-hydroxybenzonitrile, 4-chlorobutyronitrile and trimethylacetonitrile. In the first incubation step, 5 µl of 2 M nitrile substrate prepared in DMSO, 1 µg/µl of crude NHase and 50 mM Tris-HCl buffer, pH 8, was used. The reaction took place at 35˚C for 10 minutes. This was followed by the addition of 50 µl of 20 mM hydroxylamine and 50 µl of 0.4 units of amidase (both were prepared using 50 mM Tris-HCl buffer, pH 8). The assay was then incubated at 35˚C for 30 minutes. The reaction was terminated by the addition of 50 µl of 0.1 M $FeCl_3$ in 0.1 M hydrochloric acid. The absorbance was measured at 510 nm.

3.2.2.9 Analysis of the kinetic parameters of the NHase

First the absorbance for different substrate concentrations ranging from 0 to 100 mM was determined in a time-course enzyme reaction. The reaction mixture contained 50 µl of 0 to 100 mM acetonitrile, 1 µg/µl of NHase enzyme and 50 mM Tris-HCl buffer, pH8 bringing the total reaction volume up to 100 µl. The reaction was incubated at 35˚C and the reaction was stopped (as described above in previous assays) every 2 minutes for 10 minutes. Using the equation derived from the standard curve, the absorbance readings were used to give the concentration of acetohydroxamic acid produced at each time point for the different substrate concentrations. A graph of acetohydroxamic acid concentration against time was then plotted for each substrate concentration. The gradient of each of these graphs reflects the velocity of the reaction. Consequently, the velocity of each graph was plotted against the substrate concentration (Michaelis-Menten curve). Lastly, kinetic parameters were calculated using Lineweaver-Burk, Hanes-Woolf and Eadie-Hofstee equations. All the graphs and equations were generated and analysed using Microsoft Excel.

3.3 Results and discussion

3.3.1 The effect of hydroxylamine on the assay

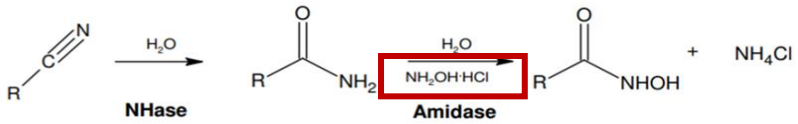

Scheme 3.2: The effect of hydroxylamine on the assay. Amidase transfers the acyl group from the amide to hydroxylamine.

The chemical components of the assay must be studied to discover their influence on enzyme activity (Bisswanger, 2014). In this assay, hydroxylamine, an additional substrate for amidase, was introduced to the wells. As a result, the first step in ensuring the compatibility of the assay was to ensure that the observed effect was exclusively due to the relationship between hydroxylamine and the amide. This was tested by uncoupling the assay so that hydroxylamine can be present in the NHase reaction prior to the addition of amidase.

3.3.1.1 The effect of hydroxylamine on NHase activity

To evaluate the effect of hydroxylamine concentration on NHase activity, increasing concentrations of hydroxylamine were added to the reaction mixture during the initial incubation of the NHase with the nitrile substrate. No colour was obtained when iron was added right after the NHase reaction (results not shown), but a coloured complex formed when amidase was introduced after the NHase reaction. This indicated that the observed effect was specifically due to the relationship between hydroxylamine and the amide.

NHase activity however was inhibited by the presence of hydroxylamine in the reaction mixture. NHase activity was determined relative to the reaction when 10 mM hydroxylamine was present. The relative activity decreased with increasing hydroxylamine concentration (Figure 3.1a). These results are in agreement with previous findings from Van Wyk (2008). At concentrations greater than 20 mM, very low NHase activity was detected and above 40 mM, the hydroxylamine caused precipitation of the enzyme. Since precipitation affects the absorbance readings, a concentration higher than 30 mM could not be used. The precipitation could be observed visually (Figure 3.1b). The decrease of NHase activity through hydroxylamine indicated that the assay needed to remain uncoupled since the addition of hydroxylamine at the same time as the NHase reaction would inhibit its true activity.

Introducing hydroxylamine after the NHase reaction and before amidase created a 'stopping point' in the assay through its inhibition of NHase. This is important in terms of the assay's enzyme kinetics. According to Michaelis–Menten, for the initial enzyme activity to be measured by the rate of product formation, the initial enzyme reaction needs to be rate-limiting. However, before a steady-state of product formation occurs, a lag phase takes place during which the intermediates are accumulating (Robinson, 2015). During this time, the rate of product formation is not a true reflection of the enzymes activity since the intermediate substrate concentration is limiting (Robinson, 2015). Therefore, uncoupling the two enzymes and inhibiting NHase ensures that the lag phase has passed before the amidase begins to

hydrolyse the amides that have collected. Furthermore, the 'stopping point' allows for optimisation of reaction time for each enzyme which will be discussed in more detail in the following sections.

A

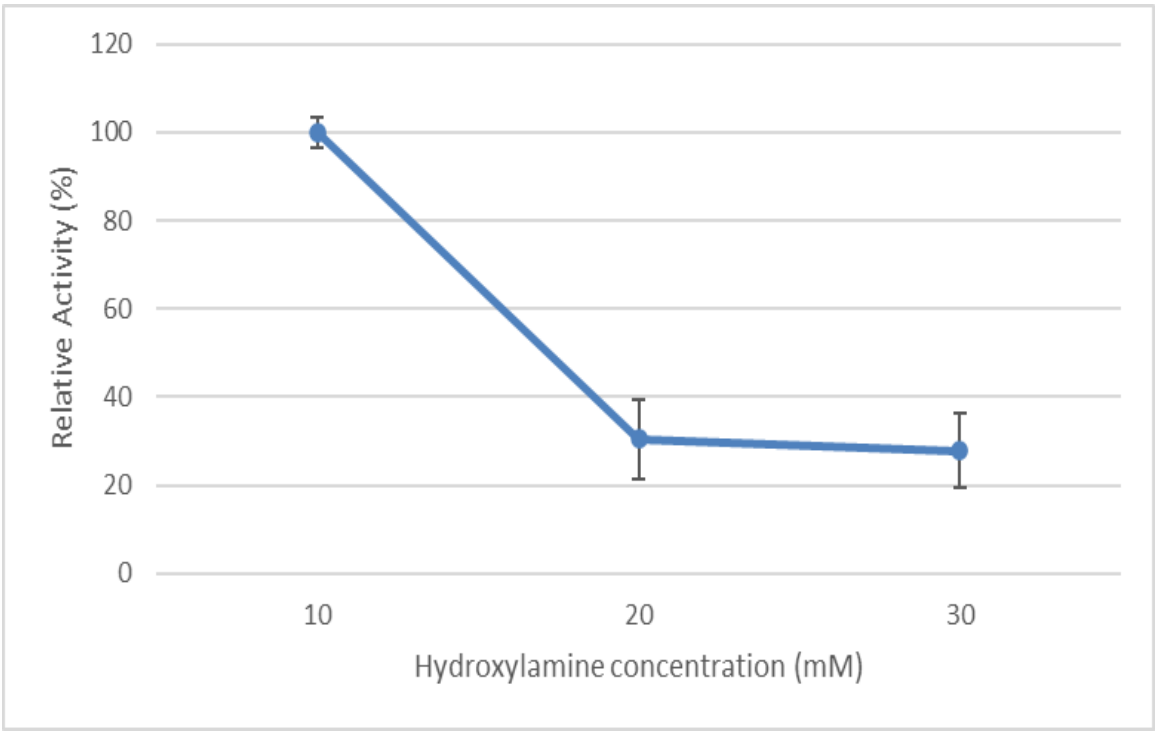

B

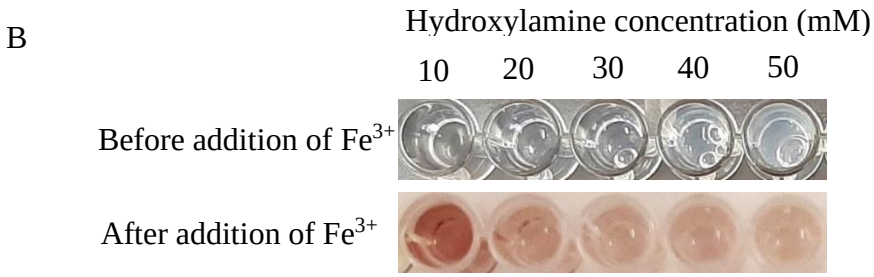

Figure 3.1: The effect of hydroxylamine concentration on NHase activity. Increasing concentrations of hydroxylamine were added to the wells during the NHase incubation step. 1.0 µg/µl of NHase protein and 50 mM of acetonitrile prepared in 50 mM Tris-HCl (pH 7.2) was used. The plate was incubated at 37˚C for 30 minutes after which the amidase step was initiated. The absorbance was measured at 510 nm. (A) The relative activity (%) for reactions containing increasing concentrations of hydroxylamine was determined relative to the maximum activity at 10 mM. The standard deviation between duplicate measurements is indicated by the error bars. (B) Visual representation of the observed effect of increasing hydroxylamine concentration on NHase activity.

3.3.1.2 The effect of hydroxylamine on amidase activity

Increasing concentrations of hydroxylamine were added to wells containing 50 mM acetamide (Sigma-Aldrich). The reaction started with the addition of 1.0-unit amidase enzyme and the assay was run at 37˚C at pH 7.2 for 30 minutes. The results in Figure 3.2a show that at lower concentrations of hydroxylamine, the amidase has its highest activity and with increasing concentration the amidase starts to be inhibited. This contrasts with previous reports that suggest that amidase remains active at higher concentrations of hydroxylamine and its activity is optimal at 500 mM (Vejvoda *et al.*, 2011; Van Wyk , 2008).

The discrepancy could be related to the fact that the amidases came from different species and therefore are affected differently by hydroxylamine. However, the discrepancy can also occur due to the different temperatures used in the assay. Hydroxylamines are unstable crystalline compounds and higher temperatures could cause them to decompose (Knight and Sylva, 1974; Monzyk and Crumbliss, 1979). This assay was conducted at 37˚C as suggested by Sigma-Aldrich, while Vejvoda (2011) conducted the assay at 28˚C. The higher temperature used in this assay could have resulted in less stable hydroxylamine which was emphasised at higher concentrations. Nonetheless, the optimum hydroxylamine concentration for amidase (20 mM) at 37˚C effectively limits NHase activity (Figure 3.1a) and consequently the assay was conducted using 20 mM of hydroxylamine.

A

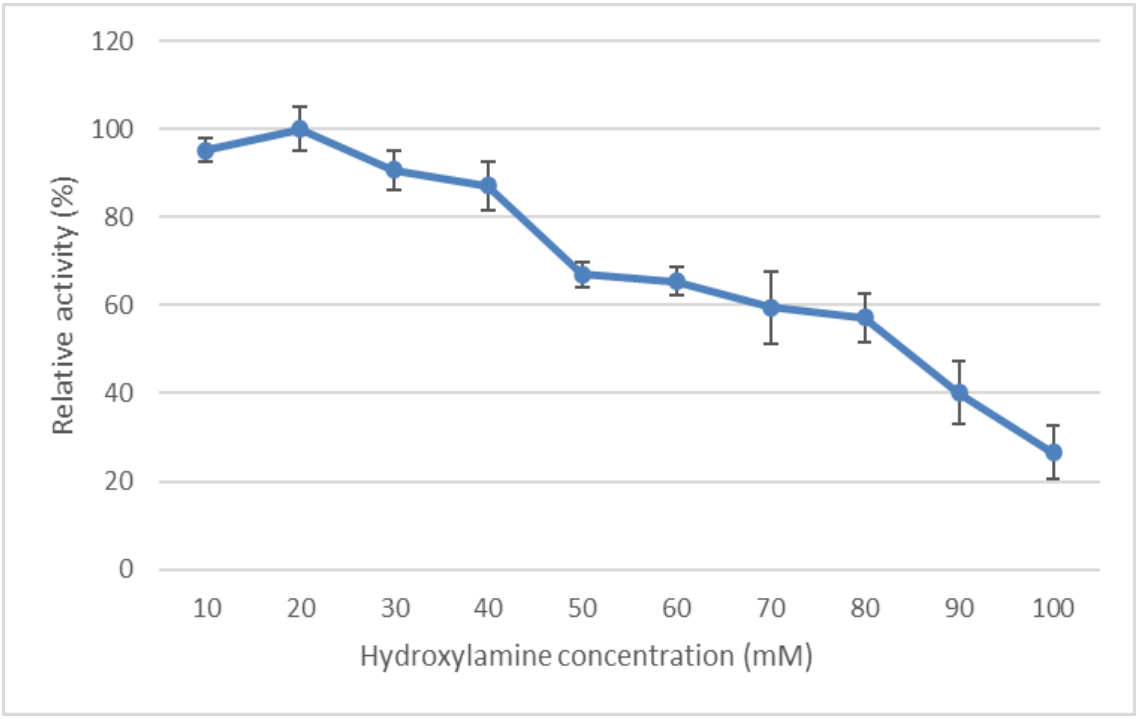

B

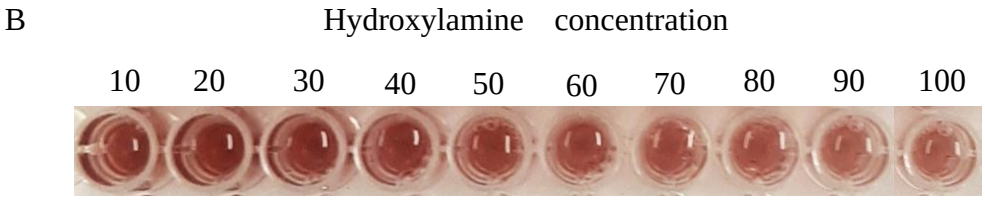

Figure 3.2: The effect of hydroxylamine concentration on amidase activity. Increasing concentration of hydroxylamine ranging from 0-100 mM, 50 mM of acetamide and 1-unit amidase were added to the wells. The plate was incubated for 30 minutes at 37˚C prior to being terminated with 50 µl of 0.1 M $FeCl_3$ in 0.1 M hydrochloric acid. The absorbance was measured at 510 nm. (A) The relative activity (%) for reactions containing increasing concentrations of hydroxylamine was determined relative to the optimal activity at 20 mM. The standard deviation between duplicate measurements is indicated by the error bars. (B) Visual representation of the observed effect of increasing hydroxylamine concentration on amidase activity.

3.3.2 The optimal concentration of acetohydroxamic acid for maximum assay sensitivity.

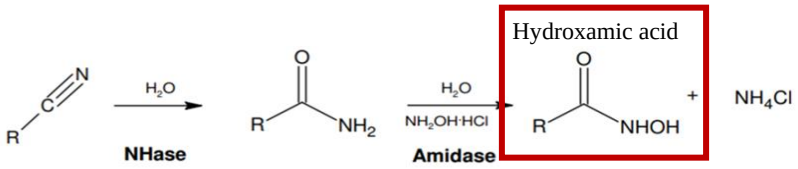

Scheme 3.3: Hydroxamic acid is the final, measurable product in the assay.

A standard curve is used in quantitative assays to accurately determine the concentration of the sample from the generated absorbance (Robinson, 2015). The standard curve used in this study was constructed by using ranging acetohydroxamic acid concentrations.

In order to maximise the sensitivity of the assay a standard curve of acetohydroxamic acid, the measurable product, was constructed. The standard curve was used to give an indication of the minimum concentration of acetohydroxamic acid that was needed to give a reasonable absorbance value that is sensitive enough to detect modest levels of enzyme activity. Once the minimum concentration of acetohydroxamic acid required to achieve a reasonable absorbance value was determined, it was used as a starting point for all subsequent parameter optimisations. Therefore, all subsequent parameter optimisations were targeted towards the generation of a sensitive assay. Developing a sensitive assay is critical for detecting even modest changes in NHase enzyme activity and prevents overlooking possible mutants in the mutant library (Zeng *et al.*, 2020). In addition, this optimisation was also instrumental in saving on enzyme and reagents because using excess amounts to obtain the minimum concentration of acetohydroxamic acid could be avoided.

The standard curve of acetohydroxamic acid (Figure 3.3a) is linear, showing an increase in absorbance as the concentration of acetohydroxamic acid increases. It is not ideal to use absorbance values above 1 because certain measuring equipment cannot accurately measure absorbance above this value (Acker and Auld, 2014). Still, the standard curve was constructed using absorbance values reaching 3. The Victor Nova plate reader that was utilised provides extremely accurate absorbance readings up to 3, as evidenced by the graph's linearity. Nonetheless, after the standard curve was created, it was obvious which acetohydroxamic acid concentration should be used to keep the absorbance measurement below 1. The best absorbance value to work with is 0.5 as it is a good compromise between limiting the optical noise in a spectrophotometer and having a strong enough signal to measure (Bisswanger, 2014).

Most assays are designed to work in the low nanomolar to high micromolar concentration range, to detect concentrations in a physiological cell (Hertzberg and Pope, 2000). However, this did not present a problem in this study, since the amount of substrate and time of the assay were controlled and could be optimised to ensure that a reasonable concentration and absorbance was achieved.

A

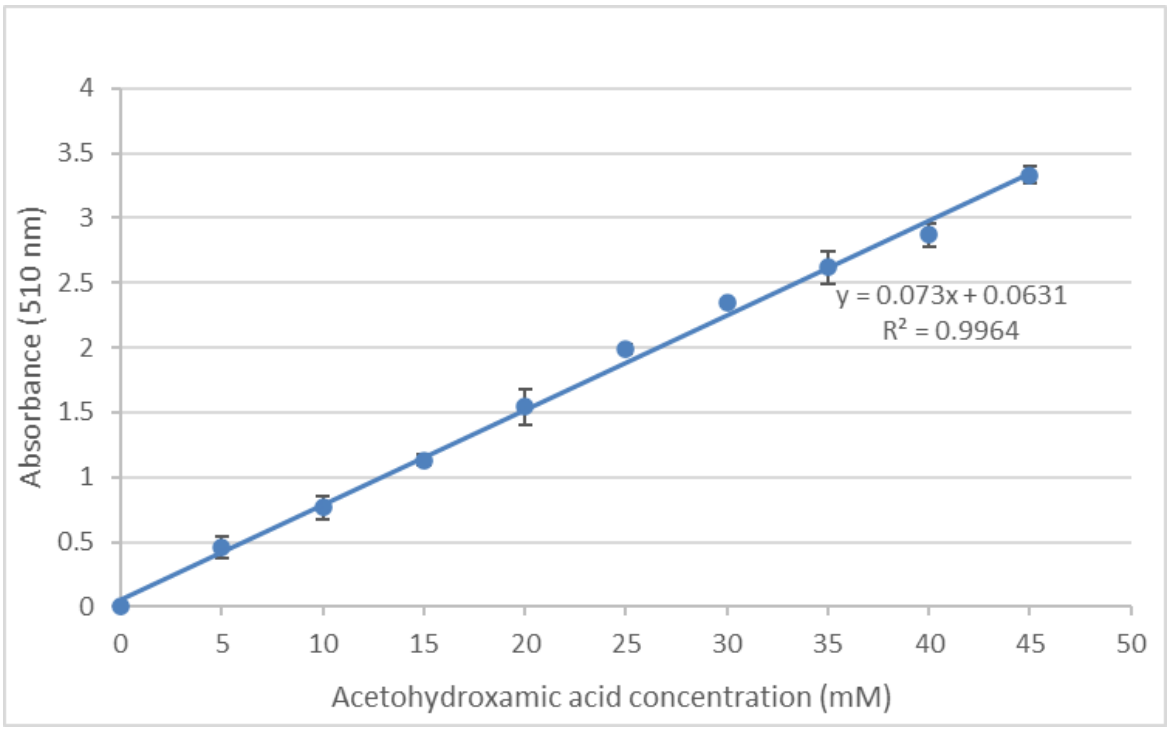

B

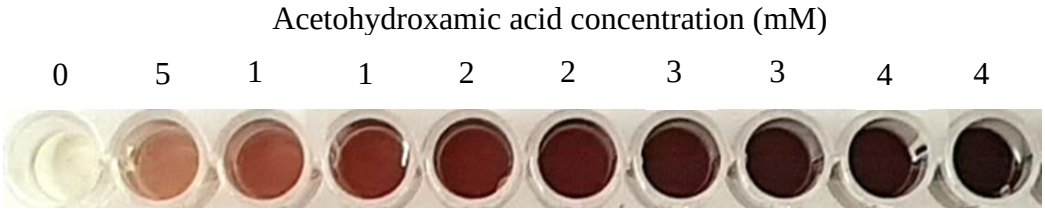

Figure 3.3: Standard curve to determine acetohydroxamic acid concentration. The standard curve was produced by using 200 µl of increasing concentrations of acetohydroxamic acid and 50 µl of 0.1 M $FeCl_3$ in 0.1 M hydrochloric acid. The absorbance was measured at 510 nm. (A) Standard curve of acetohydroxamic aid concentration. The standard deviation between duplicate measurements is indicated by the error bars. $R^2 = 0.9964$ showing a strong fit. (B) Visual representation of the observed effect of increasing acetohydroxamic acid concentrations.

3.3.3 Optimisation of the amidase activity within the assay

3.3.3.1 The effect of substrate concentration on amidase activity

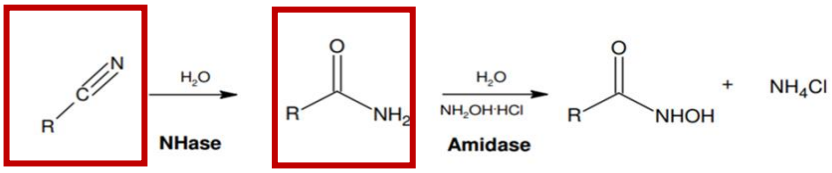

Scheme 3.4: The amidase enzyme uses amides as substrates, and the nitrile substrate could be present during the process.

The amidase reaction was optimised first because in a coupled enzyme assay, the second enzyme reaction must be the non-limiting one since the assay must be able to convert all of the intermediate chemical into the end product in order to assess the activity of the first enzyme (Easterby, 1973). In this case, to quantify the NHase enzyme activity, amidase must be able to fully convert the intermediate amide into the quantifiable acetohydroxamic acid. The optimisation of the amidase enzyme concentration which influences product production is discussed next but first the influence of substrate concentration on amidase activity was examined.

Modulation of the substrate concentration was chosen since it affects the primary rate and yield of enzymatic hydrolysis (Aslanzadeh *et al.*, 2014; Sun and Cheng, 2002). Although 5 mM of acetohydroxamic acid is sufficient to yield a sensitive absorbance, it is better to have an increased amount of substrate. With more substrate, there's an increased chance of enzyme and substrate colliding and forming a substrate-enzyme complex within a given period (Robinson, 2015; Roughton and Booth, 1946). This leads to a higher likelihood of detecting low activity, thus it raises the sensitivity of the assay.

However, enzyme inhibition can occur above a certain amount of substrate concentration. Substrate inhibition (SI) is a common occurrence that affects 25% of enzymes (Yoshino and Murakami, 2015). SI results in a divergence from Michaelis-Menten kinetics, such that the velocity of the curve climbs as the substrate availability increases, but then peaks before decreasing to either zero (complete inhibition) or a non-zero asymptote (partial inhibition) (Kokkonen *et al.*, 2021; Reed *et al.*, 2010; Wu, 2011; Yoshino and Murakami, 2015). Substrate inhibition is a physiological phenomenon that for example regulates many metabolic pathways as part of a negative feedback loop (Reed *et al.*, 2010).

The most used model of substrate inhibition was proposed by the Haldane-Andrews equation (Meriç *et al.*, 2002). A second substrate molecule can bind to the enzyme at the active site, resulting in the formation of an enzyme substrate-substrate complex (ESS), so that the product cannot be released, or the second substrate binds at a non-catalytic inhibitory site (Armstrong, 1930; Yoshino and Murakami, 2015). The binding of a second substrate molecule forms an inhibitory complex that slows down or stalls the reaction. Thus, investigating the effect of concentration on enzyme activity is crucial when optimising an assy. Moreover, due to increased substrate concentration in the reaction high viscosity might produce diffusional constraints, which can contribute to the substrate inhibitory effect (Miranda *et al.*, 1991).

3.3.3.1.1 The effect of acetamide concentration on amidase activity

Since amidase's substrate is acetamide, the effect of acetamide concentration on amidase was explored, to optimise the assay's sensitivity. Increasing concentrations of acetamide were added to the wells with 1 unit of amidase, 20 mM hydroxylamine and Tris-HCL (pH 7.2). The reaction was allowed to run for 30 minutes at 37˚C. Figure 3.4 indicates a rapid increase in amidase activity up to 20 mM of acetamide, before the activity begins to plateau. The binding of the substrates to the enzyme in a hyperbolic function is in accordance with the Michaelis–Menten equation (Bisswanger, 2014; Michaelis *et al.*, 2011). The observed result is due to the saturation of the enzyme, and regardless of how much more substrate is added the enzyme activity will not increase further, as all the enzymes are already bound and reacting (Easterby, 1973; Robinson, 2015). At the point of plateau the enzyme is at V_{max}. There is no decline in amidase activity even at a high concentration of 100 mM acetamide, indicating that there is no substrate inhibition at these concentrations.

In this experiment, the equation derived from the standard curve (Figure 3.3a) was used to calculate the amount of acetohydroxamic acid that was produced when 100 mM of acetamide was used. The result, extrapolated from the absorbance value, indicated an acetohydroxamic acid concentration of 9 mM. Therefore, when 100 mM of acetamide was used with 1.0 unit of amidase enzyme, only a tenth of the acetamide is converted to acetohydroxamic acid in 30 minutes. Since higher acetamide concentrations did not cause a decline in activity, even when the concentration reaches 100 mM, the use of a high concentration is suggested since it improves the probability of conversion and thus the sensitivity of the assay.

The original goal was to optimise the assay so that the absorbance would not exceed 0.5, however, since this is only the beginning of the optimisation process and subsequent steps

downstream could negatively affect the absorbance, a higher absorbance was taken as the optimised concentration for now.

A

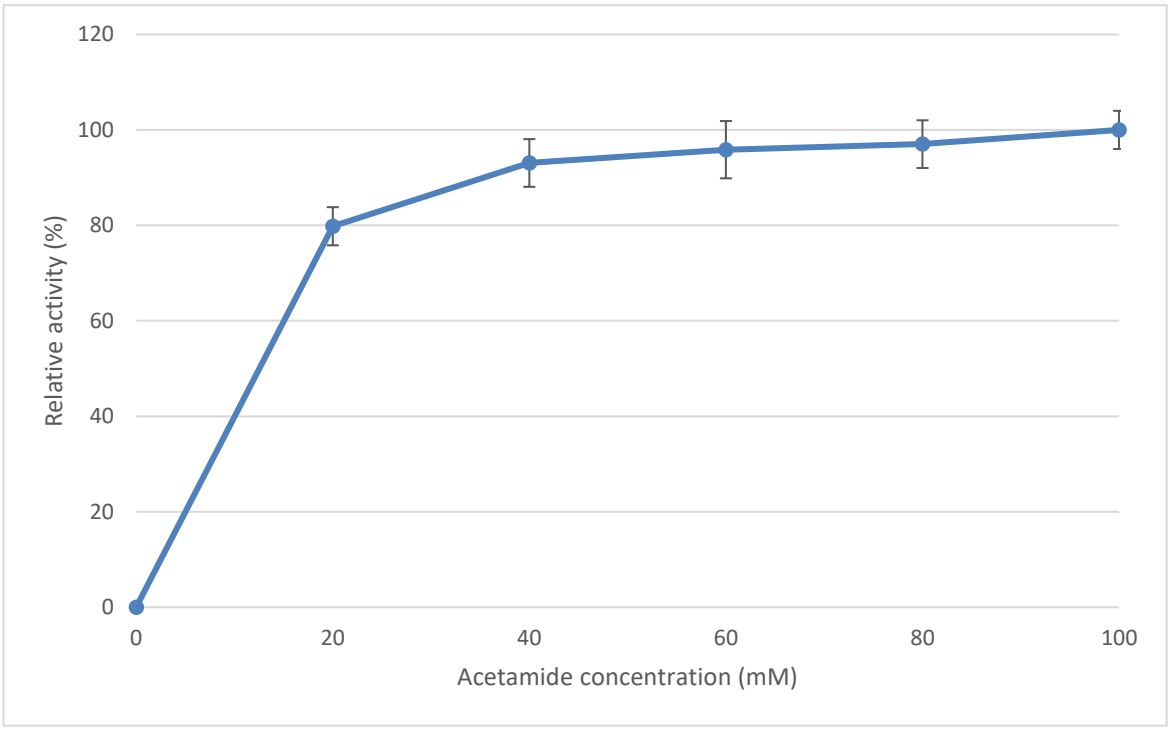

B

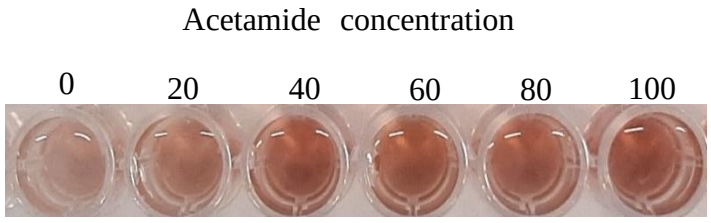

Figure 3.4: Amidase activity as a function of acetamide concentration. Increasing concentrations of acetamide ranging from 0-100 mM were added to wells containing 1-unit amidase and 20 mM hydroxylamine. The plate was incubated for 30 minutes at 37˚C prior to being terminated with 50 µl of 0.1 M $FeCl_3$ in 0.1 M hydrochloric acid. The absorbance was measured at 510 nm. (A) The relative activity (%) for reaction mixtures containing increasing concentrations of acetamide was calculated relative to the optimal activity at 100 mM. The standard deviation between duplicate measurements is indicated by the error bars. (B) A visual representation of the observed effect of increasing acetamide concentration on amidase activity.

3.3.3.1.2 The effect of acetonitrile concentration on amidase activity

Even though nitrile is not a direct substrate of the amidase enzyme, there could be residual nitrile left in the well that was not catalysed by the NHase in the previous step, therefore the effect of acetonitrile concentration on amidase activity was investigated. Increasing concentrations of acetonitrile were added with 1.0 unit of amidase enzyme and 100 mM acetamide at a pH of 7.2 The assay was allowed to run for 30 minutes at 37˚C. The results (Figure 3.5) show that even at a concentration of 100 mM, acetonitrile has a negligible effect on the amidase activity. This suggests that the concentration of acetonitrile can theoretically be increased to 100 mM, which would further increase the assay's sensitivity. However, in order to find the optimal acetonitrile concentration for the assay, the effect of acetonitrile concentration on NHase was assessed (section 3.3.4).

A

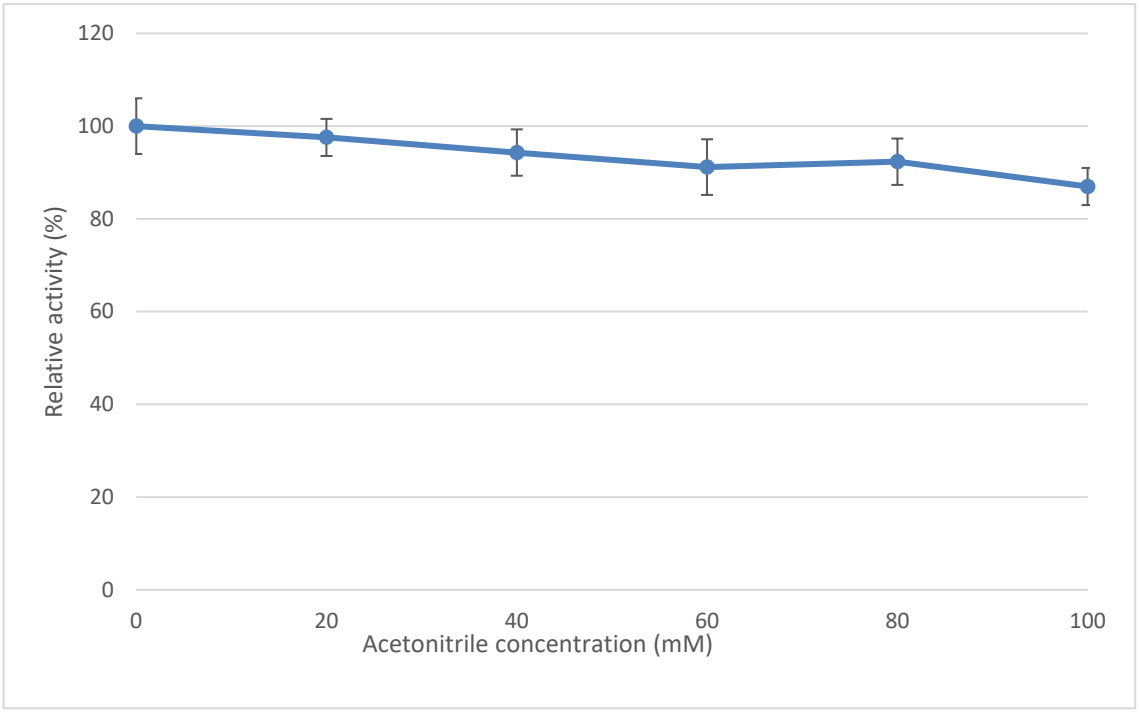

B

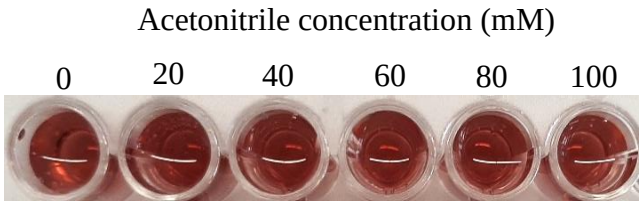

Figure 3.5: Amidase activity as a function of acetonitrile concentration. Increasing concentrations of acetonitrile ranging from 0-100 mM were incubated during the amidase reaction. In addition, the well contained 100 mM acetamide, 1-unit amidase and 20 mM hydroxylamine. The plate was incubated for 30 minutes at 37˚C prior to being terminated with 50 µl of 0.1 M $FeCl_3$ in 0.1 M hydrochloric acid. The absorbance was measured at 510 nm. (A) The relative activity (%) for reactions containing increasing concentrations of acetonitrile was calculated relative to the optimal activity of a blank without acetonitrile. The standard deviation between duplicate measurements is indicated by the error bars. (B) A visual representation of the observed effect of increasing acetonitrile concentration on amidase activity.

3.3.3.2 Optimisation of amidase concentration to achieve optimal timely product conversion

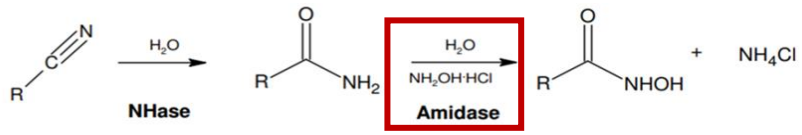

Scheme 3.5: The amidase enzyme is the second enzyme in the coupled assay.

To evaluate the effect of increasing enzyme concentration on the rate of the reaction, the substrate must be present in excess and less than 10% of the substrate should be depleted during the assay, so its concentration remains essentially unchanged, such that the reaction rate is independent of the substrate concentration (Blackmond *et al.*, 2006; Roskoski, 2007). In this way the amount of product generated over a certain length of time will only be influenced by the amount of enzyme present. When the rate of the reaction is independent of the substrate concentration, the kinetics are called *zero-order* (Blackmond *et al.*, 2006). Thus, after determining that high concentrations (up to 100 mM) of acetonitrile and acetamide have no inhibitory effect on amidase enzyme activity, the next step was to optimise amidase concentration and the rate of the reaction.

It is important to note here in order to eliminate any confusion, that during *optimisation* of amidase concentration the *zero-order* kinetics are adhered too. However, for the coupled enzyme assay to be quantitative, the coupled reactions must adhere to *first-order* kinetics (Cleland, 1979; Easterby, 1973). First-order kinetics is when the rate of the reaction is dependent on substrate concentration. That is, the amidase reaction rate must be dependent on the concentration of acetamide available, which is directly dependent on the activity of the NHase.

In a coupled enzyme assay, the second enzyme must be the non-limiting reaction since the assay must be able to convert all the intermediate compounds into the final product in order to assess the activity of the first enzyme. To ensure that amidase's reaction is non-limiting, the concentration of the enzyme must be optimised and should be in excess. The overall rate can then be used as a measure for the NHase activity, since free amidase will always be available to catalyse the acetamide, and the concentration of acetamide will be only determined by the rate of the NHase.

However, the amidase used in this assay was purchased from Sigma- Aldrich and is expensive, at approximately R12,000 for 1000 units. To put it in context, this assay is being developed for high-throughput screening of large mutant libraries, with a minimum of 10,000 mutants screened per cycle of evolution. If excess amounts of amidase are employed the assay becomes prohibitively expensive. Furthermore, because the assay is being miniaturized to be used in 96 well plates, excess levels of enzyme may be problematic to employ because the wells may not contain enough buffer volume to prevent the enzyme from precipitating.

Since employing excessive amounts of amidase is not feasible for this assay, the rate of the reaction, which has an inverse relationship with the concentration of amidase, must be optimised (Uhr, 1990). A high concentration of amidase will result in a quicker reaction, while a small concentration of amidase will result in a longer reaction time. By uncoupling the two reactions, it was possible to ensure the minimal necessary reaction time for the NHase step and therefore limit the amount of acetamide it can produce. While the amidase step has a longer reaction time, which allows for complete catalysis of the generated acetamide.

To test the different concentrations of amidase over time, varying concentrations of amidase were added into wells containing 100 mM acetamide and Tris-HCl (pH 7.2). The reaction was stopped at 10-minute intervals. Figure 3.6 shows that 0.2 units of enzyme generates an almost linear graph, however, the linearity of the graphs decrease when more enzyme units are used. The change in linearity is most profoundly seen at 10 minutes when 1.0 unit of enzyme was used (light blue graph). The absorbance value at 10 minutes for the 1.0-unit enzyme concentration is 0.7 when correlated with the standard curve above (Figure 3.3a) it indicates that approximately 10 mM of acetohydroxamic acid was produced. The starting concentration of acetamide was 100 mM, and after 10 minutes of hydrolysis using 1.0 unit of enzyme, 10% of the substrate had been hydrolysed. When more than 10% of the substrate has been hydrolysed the rate of the enzyme reaction slows down, indicated by the change in linearity of the graph.

The measured velocity of an enzyme reaction should be a linear function of the enzyme concentration. Therefore, when optimising the assay, it was important to work within the linear range. Based on the graphs in Figure 3.6 there were two potential options for this assay. The first was to use 1 unit of enzyme and limit the time to 10 minutes or use 0.2-0.4 units of enzyme and extend the time to 30 minutes. Since amidase is expensive, in order to keep the cost low,

yet at the same time ensure that the assay can remain quantitative, 0.4 units of amidase was chosen as an absorbance close to 0.7 could be reached with this concentration in 30 minutes.

A

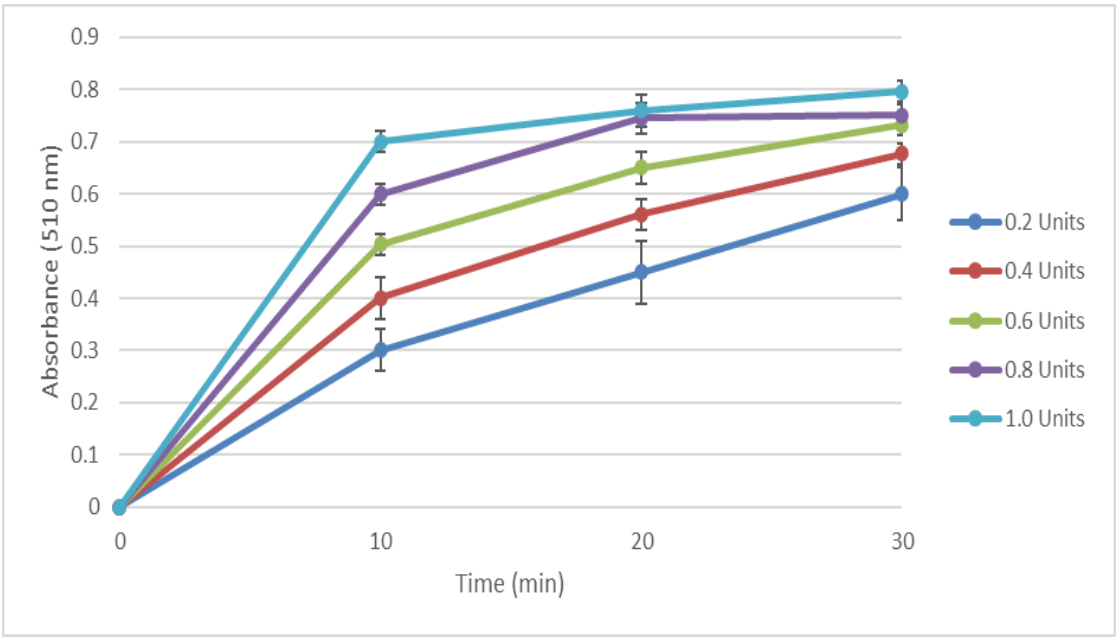

B

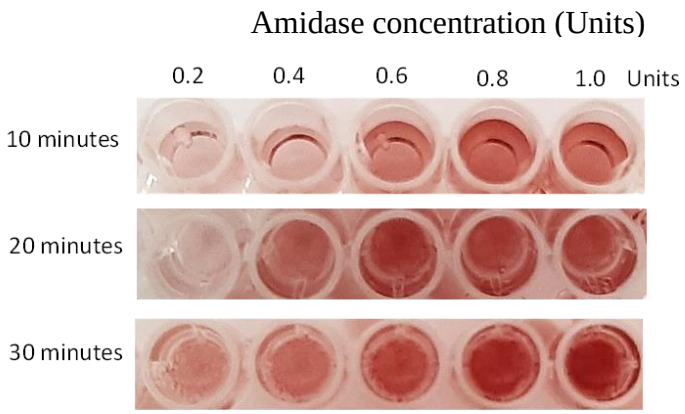

Figure 3.6: The effect of amidase concentration on the rate of change of absorbance in time. Increasing concentrations of amidase ranging from 0.2-1.0 unit were added to wells containing 100 mM acetamide and 20 mM hydroxylamine. The reaction was terminated at 10-minute intervals using 50 µl of 0.1 M $FeCl_3$ in 0.1 M hydrochloric acid. The absorbance was measured at 510 nm. (A) The rate of change of absorbance for increasing amidase concentrations. The standard deviation between duplicate measurements is indicated by the error bars. (B) A visual representation of the observed effect of increasing amidase concentration on product output over time.

3.3.4 Optimisation of the NHase activity within the assay

3.3.4.1 The effect of substrate and product concentration on NHase activity

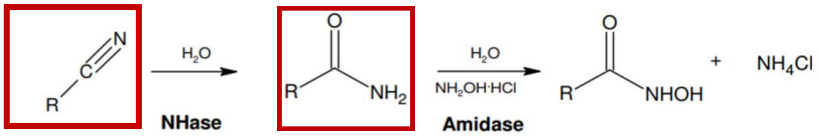

Scheme 3.6: Nitriles are substrates of the NHase enzyme while amides are the reaction's products.

NHase optimisation was performed after the amidase optimisation, since NHase must be the rate-limiting step so that any change in final product formation relates to the NHase activity.

The assay signal strength is directly correlated to the concentration of substrate. Increasing the substrate concentration should increase the assay's turnover until the substrate saturates the enzyme. This saturation point frequently yields the highest signal-to-background ratio possible for an assay (Eilertsen and Schnell, 2018; Uhr, 1990). However, after a certain point, substrate concentration can lead to substrate inhibition which would slow down or cease enzyme activity.

A product of an enzyme could be an inhibitor of the enzyme reaction. This naturally occurs in cells that use negative feedback loops in metabolic pathways to regulate their metabolism (Schmidt *et al.*, 1983). Product inhibition is especially prominent for enzymes that catalyse energetically unfavourable reactions (Fernandes *et al.*, 2022). In some circumstances, an accumulating product's inhibition significantly retards the rate of catalysis so that true initial velocities cannot be established using conventional assay methods (Alam *et al.*, 2017; Andrić *et al.*, 2010; Schmidt *et al.*, 1983). The structural similarities between substrates and inhibitors cause the majority of inhibitory interactions (Alam *et al.*, 2017; Fernandes *et al.*, 2022).

Continuous removal of the inhibitory product may mitigate the inhibitory effect (Fernandes *et al.*, 2022), however since this assay is uncoupled, the amidase is not catalysing the product (acetamide) until it has accumulated. Therefore, it is important to investigate these parameters so that the NHase enzyme activity that is measured is a true reflection of the enzyme itself and not a result of other factors.

3.3.4.1.1 The effect of acetonitrile concentration on NHase activity

In this study, the influence of substrate concentration on the kinetics of the NHase reaction was investigated by using increasing concentrations of acetonitrile (0 to 100 mM) at 37˚C in Tris-HCL (pH 7.2) for 30 minutes. The reaction was stopped through the addition of hydroxylamine, followed by the addition of amidase and a further 30 minutes of incubation. The results are shown in Figure 3.7. As expected, the rate of product formation increased with increasing amounts of acetonitrile. There was no substrate inhibition observed in this assay that was conducted until a concentration of 100 mM of acetonitrile. The substrate concentration was not increased above 100 mM, since the best range of absorbance for the assay to be measured in is between 0.5 and 1.0 and based on the standard curve (Figure 3.3a) this falls close to 10 mM of acetohydroxamic acid. Since the enzyme activity rate decreases after 10% of the substrate has been hydrolysed (Roskoski, 2007), which would affect the linear range, 100 mM of substrate is the optimal concentration for a sensitive absorbance reading.

A

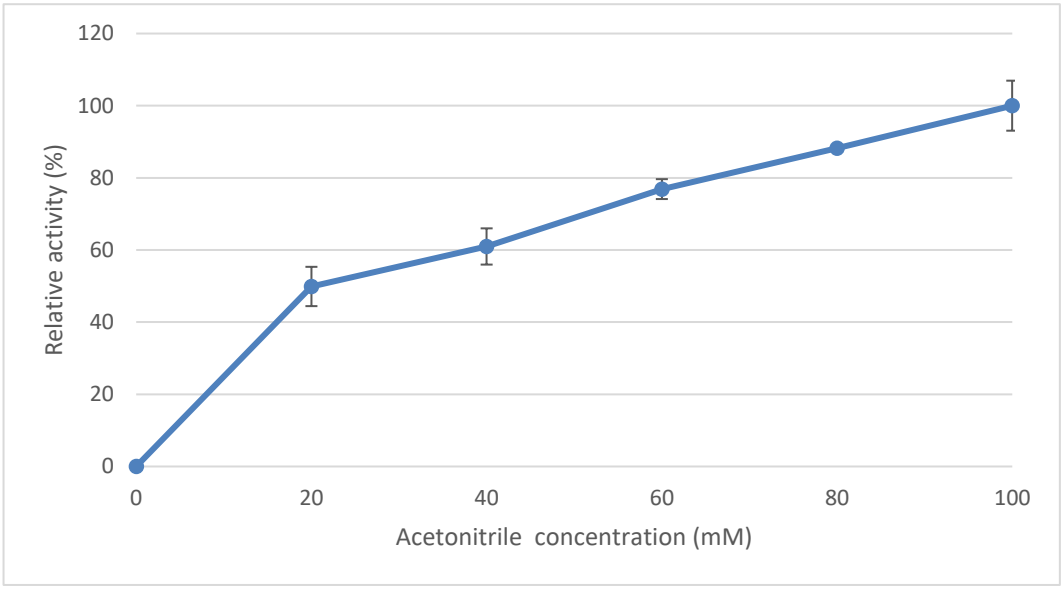

B

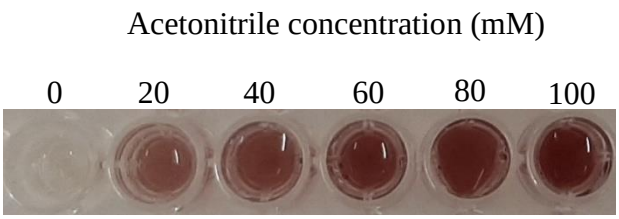

Figure 3.7: The effect of acetonitrile concentration on the activity of NHase. Increasing concentrations of acetonitrile ranging from 0-100 mM were incubated with 1 µg/µl of NHase for 30 minutes at 37˚C. Followed by the amidase incubation step. The absorbance was

measured at 510 nm. (A) The relative activity (%) for reaction mixtures containing increasing concentrations of acetonitrile was calculated relative to the optimal activity at 100 mM. The standard deviation between duplicate measurements is indicated by the error bars. (B) A visual representation of the observed effect of increasing acetonitrile concentration on NHase activity.

3.3.4.1.2 The effect of acetamide concentration on NHase activity

For the purpose of optimising the NHase reaction, it was necessary to determine the extent of product inhibition on the NHase. Increasing concentrations of acetamide (0- 100 mM) were added to wells during the NHase reaction. Testing this parameter proved challenging since the additional acetamide could directly react with the amidase enzyme, regardless of how much acetamide was produced due to hydrolysis of the acetonitrile by the NHase. Therefore, it was difficult to determine whether the resultant absorbance readings were due to the added acetamide or the acetamide produced. However, upon analysing Figure 3.8 it was interesting to see that there was an increase in relative activity up until 60 mM followed by a decrease in relative activity. The increase in relative activity can be attributed to the increase in added acetamide but the decrease was unexpected since Figure 3.4 showed that an increase in acetamide caused an increase in the absorbance continuously up to 100 mM. Thus, the decrease in relative activity indicates that NHase inhibition begins from 60 mM of acetamide. Nevertheless, the relative difference in activity between 60 mM and 100 mM is not significant, and considering the way the assay has been optimised, the amount of generated acetamide cannot surpass 60 mM.

Based on all the results obtained so far, 100 mM of acetonitrile concentration was selected for the assay, as it increased the assays sensitivity and resulted in no (or negligible) inhibitory effects on both coupling enzymes.

A

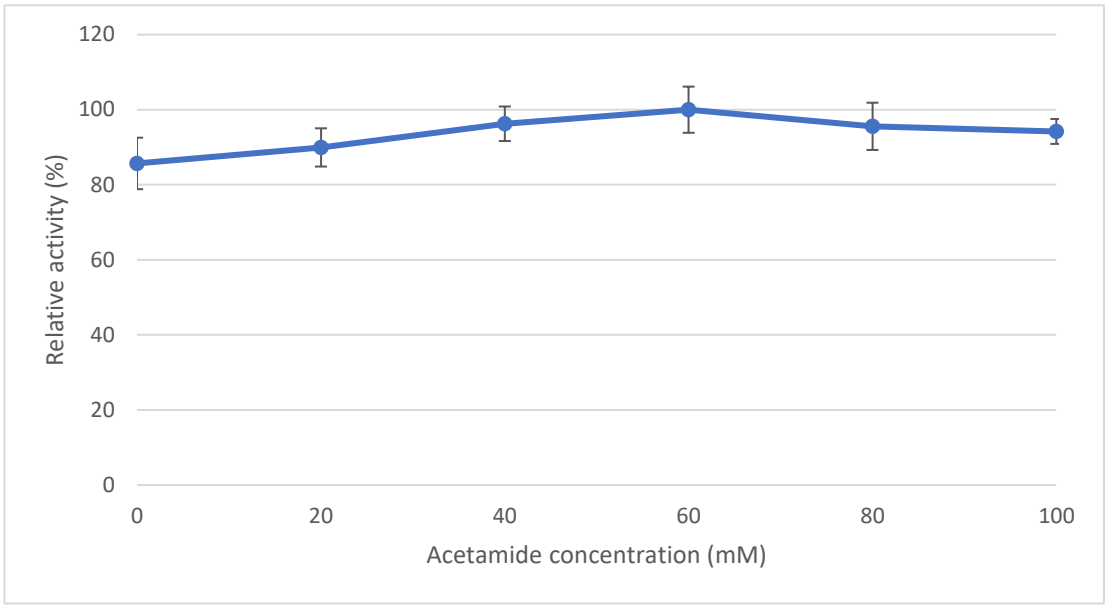

B

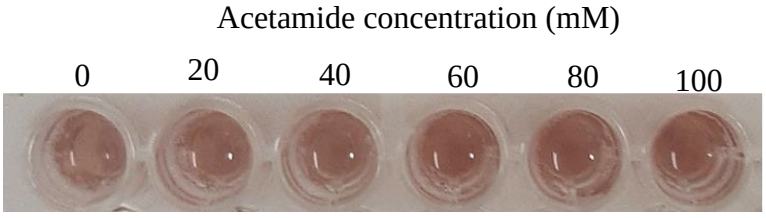

Figure 3.8: The effect of acetamide concentration on the activity of NHase. Increasing concentrations of acetamide were added to wells containing 1µg/µl NHase and 100 mM acetonitrile. The reaction was incubated for 30 minutes at 37˚C and was followed by the amidase incubation step. The absorbance was measured at 510 nm. (A) The relative activity (%) for reactions containing increasing concentrations of acetamide was calculated in relation to the optimal activity at 60 mM. The standard deviation between duplicate measurements is indicated by the error bars. (B) A visual representation of the observed effect of increasing acetamide concentration on NHase activity.

3.3.4.2 Optimisation of NHase concentration in order to achieve optimal, timely product conversion

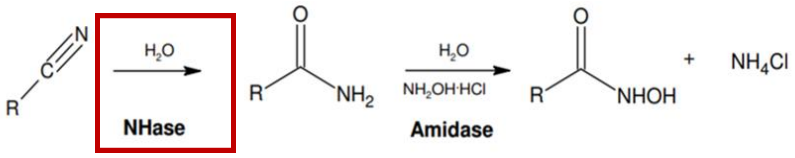

Scheme 3.7: NHase is coupled with a second enzyme in order to determine its activity.

The NHase concentration was assessed by adding increasing amounts of NHase ranging from 0.2- 1 µg/µl to wells containing 100 mM acetonitrile and 50 mM Tris-HCl (pH 7.2). Higher concentrations of enzyme were assessed, however, above 1 µg/µl of NHase the enzyme precipitated (results not shown). The miniaturisation of this assay (the NHase reaction took place in 100 µl) prevented high concentrations of enzyme from being used as there was not enough buffer to prevent detrimental effects on the protein.

Unlike the other components in the assay, the amount of enzyme used should be as small as possible; only catalytic amounts are required, a criterion that takes into account that enzymes are typically tedious to produce and expensive substances. The Michaelis–Menten equation is constructed, on the premise of modest, even insignificant enzyme levels (Bisswanger, 2017). Thus, the lower limit for enzyme concentration should be investigated to determine the amount that it sufficient to observe the reaction.

The reaction velocity is directly proportional to the enzyme concentration and exhibits a linear dependence, unlike substrate concentration that exhibits a hyperbolic relationship with reaction velocity. Therefore, working in the linear range is crucial. Based on the results in Figure 3.9, which shows that after 10 minutes the graph deviates from linearity, the time of the NHase reaction was limited to 10 minutes. Furthermore, 1 µg/µl of NHase concentration was determined as the optimal amount for the assay as it resulted in an absorbance of 0.3 after 10 minutes and the goal was to obtain an absorbance of 0.5 (the most accurate absorbance value to measure activity).

A

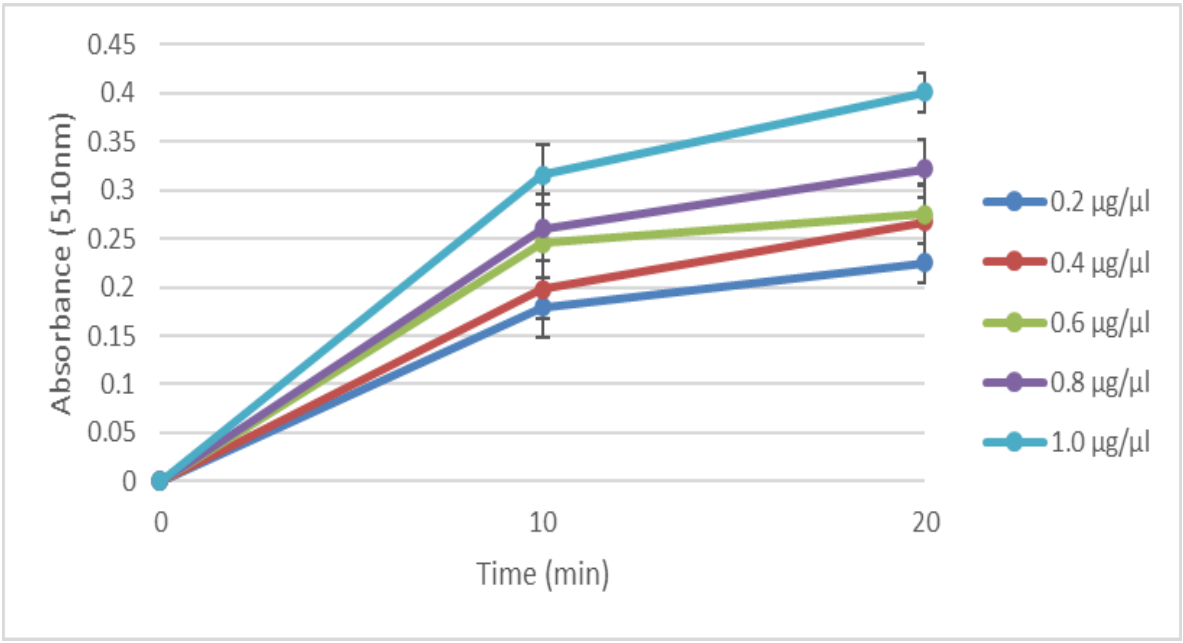

B

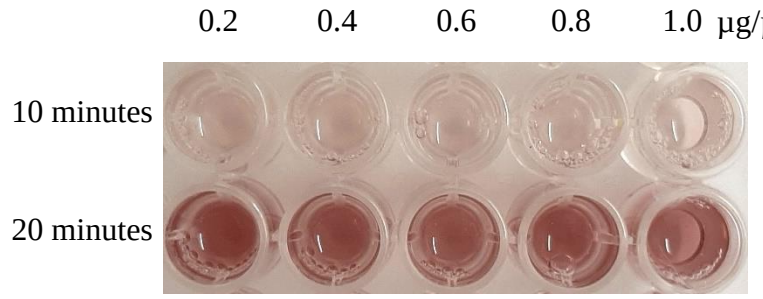

Figure 3.9: The effect of NHase concentration on the rate of change of absorbance in time. Increasing concentrations of NHase ranging from 0.2-1.0 µg/µl were added to wells containing 100 mM acetamide. The reaction was terminated every 10-minutes by the addition of 20 mM hydroxylamine and 1.0-unit amidase. The reaction was terminated with the addition of 50 µl of 0.1 M $FeCl_3$ in 0.1 M hydrochloric acid and the absorbance was measured at 510 nm. (A) The rate of change of absorbance for increasing NHase concentrations. The standard deviation between duplicate measurements is indicated by the error bars. (B) A visual representation of the observed effect of increasing NHase concentration on product output over time.

3.3.5 Optimisation of the assay temperature

Enzyme activity is influenced by temperature (Robinson, 2015). The empirical rule states that the velocity of any chemical reaction, including enzymatic reactions, rises two to three-fold per 10˚C increments (Bisswanger, 2014). However, at a certain temperature the enzyme will begin to denature due to the thermo-sensitivity of its native three-dimensional structure. As the structure of the enzyme destabilises the reaction velocity decreases. Both degree of temperature and extent of time spent at a certain temperature influence enzymatic activity. If the enzyme is tested right away at a modest denaturation temperature, its activity will be much higher than if it is stored at the same temperature for a longer time before the assay is performed (Bisswanger, 2014). It is critical to consider preparation time to avoid differential amounts of denaturation during preparation, which could result in unreliable assay results.

The effect of varying temperature on the relative activity of the assay was examined by incubating it at 20˚C, 30˚C, 40˚C, 50˚C, 60˚C, and 70˚C under standard assay conditions. Figure 3.10 shows the results. There are two peaks, the maximum relative activity is at 30˚C followed by a second peak at 50˚C. The double peak could be due to each enzyme in the coupled reaction preferring different temperatures. At 20˚C and 40˚C the relative activity was 85%, however after 50˚C there was a sharp decrease in the relative activity. This indicates that the assay in its entirety is best performed at lower temperatures. Furthermore, because the amidase reaction must be optimized to be non-limiting, the optimal temperature for amidase, which is 37˚C, must be considered. In addition, previous studies of homologous L-NHase suggest that the optimal temperature ranges from 20˚C to 40˚C (Cheng *et al.*, 2020; Lan *et al.*, 2017; Nagasawa *et al.*, 1991b; Yamada and Kobayashi, 1996b; Zhou *et al.*, 2010). Based on the above reasons 35˚C was decided on as the optimal temperature for the assay.

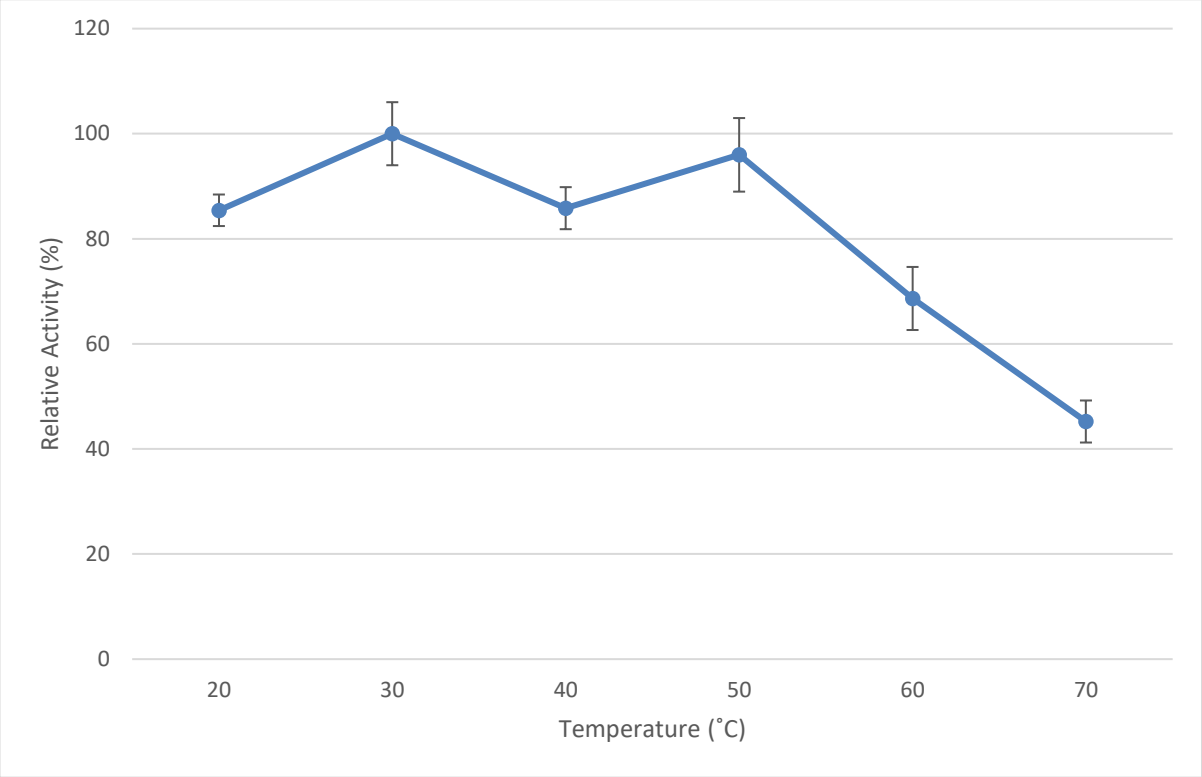

Figure 3.10: Determining the temperature optimum for the assay. The entire assay, which includes the NHase reaction as well as the amidase reaction, was carried out at various temperatures to determine the optimal temperature for the assay. Relative activity (%) was expressed as a percentage of the highest activity which was measured at 30˚C. The standard deviation between duplicate measurements is indicated by the error bars.

3.3.6 Optimisation of the assay pH

The pH of the reaction significantly impacts the activity of many enzymes. To determine the pH optimum, the selective pH range where the enzyme performs best, a pH versus activity curve should be constructed. The curve is usually bell-shaped, increasing from zero in the strong acidic region to a maximum value, and then falling back to zero in the strong alkaline zone. Enzymes are composed of different amino acid residues that have specific charges which dictate the three-dimensional protein structure of the enzyme. The amino acid residue charges are affected by the pH of the enzyme's surroundings, and thus can affect the enzyme structure and its catalytic ability. Additionally, the state of protonation of the functional amino acid groups in the catalytic site is also affected by the pH.

The HIV type 1 (HIV-1) protease is a notable example of how critical residues determine the enzyme's pH activity optimum. The pH range of the HIV-1 protease, an aspartyl protease, is

substantially wider than that of its eukaryotic counterparts. This is attributed to the absence of critical serine residues that establish hydrogen bonds with carboxyl oxygens of key aspartyl acid residues in the active site of the eukaryotic aspartyl protease (Ido *et al.*, 1991).

The effect of pH on the assay was investigated by using various buffers at a range of different pH values: pH 3.0, 4.0, 5.0 and 6.0 (50 mM citrate buffer); pH 7.0 and 8.0 (50 mM Tris-HCl buffer) and pH 9.0 and 10 (50 mM Glycine-NaOH buffer) (Figure 3.11). The curve generated does not depict the usual bell-shape but rather has two peaks which was expected since each enzyme in the coupled assay has a specific pH optimum. The two peaks are at pH 6.0 and pH 8.0. The amidase from *Pseudomonas aeruginosa* was purchased from Sigma-Aldrich and the pH optimum was previously determined as pH 7.2 but has also been reported as pH 7.5 in other studies (Kita *et al.*, 2000). The NHase from *R. rhodochrous* ATCC BAA-870 has not been characterised previously, however looking at other L-NHases from homologous species the pH optimum ranges from pH 7.0-9.0 (A *et al.*, 1998; Kashiwagi *et al.*, 2004; Prasad *et al.*, 2009).

Since both the amidase and NHase have pH optimums close to pH 8.0 it was chosen as the optimal pH for the assay. Furthermore, pH 6.0 has a more orange colour (Figure 3.11b) than the usual pink colour that has been seen in the assay.

A

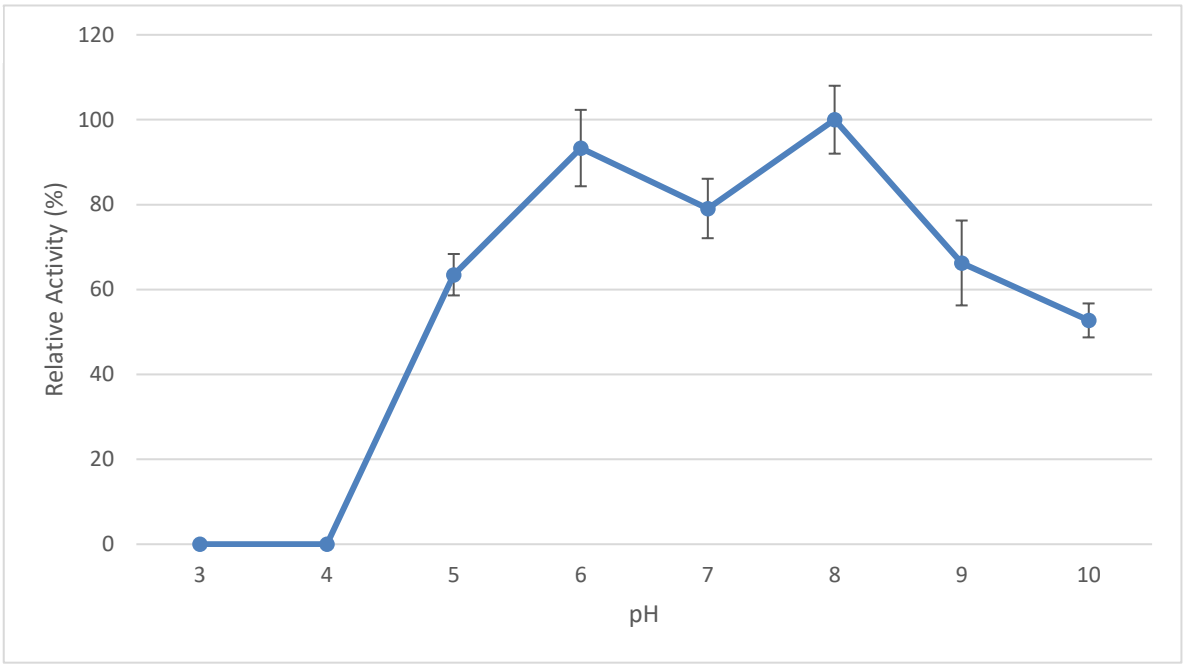

B

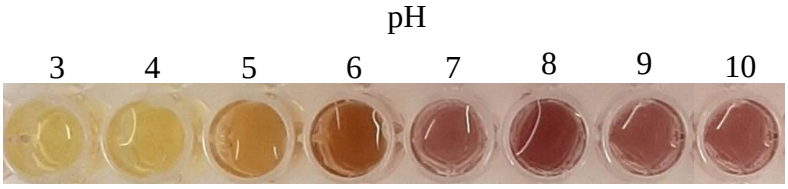

Figure 3.11: Determining the pH optimum for the assay. The entire assay, which includes the NHase reaction as well as the amidase reaction, was carried out at various pH values to determine the optimal pH range for the assay. (A) Relative activity (%) was expressed as a percentage of the highest activity which was measured at pH 8.0. The standard deviation between duplicate measurements is indicated by the error bars. (B) A visual representation of the observed effect of increasing pH of the assay.

3.3.7 The effect of organic solvents on the assay

Many nitrile substrates are insoluble in water and need to be dissolved in an organic solvent. Many organic solvents are low molecular weight molecules that can impair the enzyme even at low concentrations. The concentration of the organic solvent in the assay should be as low as possible. Since many nitriles are dissolved in organic solvents, research has been done on the effect of water-organic solvent biphasic systems on NHases. However, most of the research has been performed on the native cells compared to the cell-free NHase enzyme. NHases from *Rhodococcus ruber* (Chen *et al.*, 2018; van Pelt *et al.*, 2009), *Rhodococcus sp. M8* and *Brevibacterium* sp. CH2 (Lee *et al.*, 2019) all show good tolerance to organic solvents.

Solvent tolerance of the NHase enzyme in native cells has been attributed to the enzyme's unique multimeric nature (Martínková *et al.*, 2009) and a unique chaperon system that includes GroES2 chaperon protein, that helps the host prevent aggregation and facilitates effective folding of both newly synthesised protein as well as denatured aggregates (Shahar *et al.*, 2011; Takihara *et al.*, 2014a, 2014b).

There are significant variances in the reported tolerance of organic solvent use in assays containing isolated NHase enzyme systems. For example, the tolerance of *R. rhodochrous J1* enzyme to *n*-propanol and isopropanol was prominent (Nagasawa *et al.*, 1993). However, for *Rhodococcus equi* the NHase optimal activity was 90% in hydrocarbon solvents such as isooctane but has limited activity in methanol and ethanol (Prepechalová *et al.*, 2001).

In order to determine the consequence of organic solvents on NHase from *R. rhodochrous* ATCC BAA-870, seven organic solvents were chosen to be evaluated. The water-miscible organic solvents used in this study were methanol, acetone, ethanol and propanol, and the enzymatic activity relative to Tris-HCl (assigned 100%) were found to be 58%, 0%, 53% and 31% respectively (Figure 3.12). The water-miscible organic solvents resulted in relatively low NHase activity with acetone resulting in zero activity. The enzyme activity is thought to be lost due to the replacement of water molecules with hydrophilic organic solvents, which are essential to the catalytic ability of the enzyme (Gorman and Dordick, 1992). These findings point to the importance of keeping water molecules in the NHase enzyme's hydration shell.

The NHase activity was also tested using immiscible organic solvents which resulted in a two-phase system. Ethyl acetate and hexane were used to dissolve acetonitrile and their respective relative activities were 50% and 89% (Figure 3.12). Comparing these results to homologous NHases, the low activity when using ethyl acetate is unusual as previous studies have reported an increase in activity when compared to a buffer (Chiyanzu, 2008). The loss of enzyme activity when using ethyl acetate may be explained by the possible role of interfacial surface tension effects that ethyl acetate exerts on the enzyme (Halling-Sørensen *et al.*, 1998; Owusu and Cowan, 1989). However, 89% activity for hexane, which is the second highest relative activity, is on par with what has been reported for other NHases (Chiyanzu, 2008). The use of immiscible organic solvents has its advantages because it cannot displace the water molecules around the enzyme thereby maintaining enzyme activity. Furthermore, the two-phase system can be used to prevent substrate inhibition because the enzyme and the substrate are separated in the different phases (Cavicchioli *et al.*, 2011).

Lastly, the effect of dimethyl sulfoxide (DMSO) which is a popular organic solvent that is miscible with water and organic solvents and can dissolve polar and non-polar compounds was investigated. The relative activity for DMSO was 76% (Figure 3.12a) which is higher on the activity spectrum than most of the other organic solvents tested. Since DMSO has a relatively high activity and it is able to dissolve polar and non-polar compounds it was chosen as the organic solvent of choice for this assay when assessing various nitrile substrates.

A

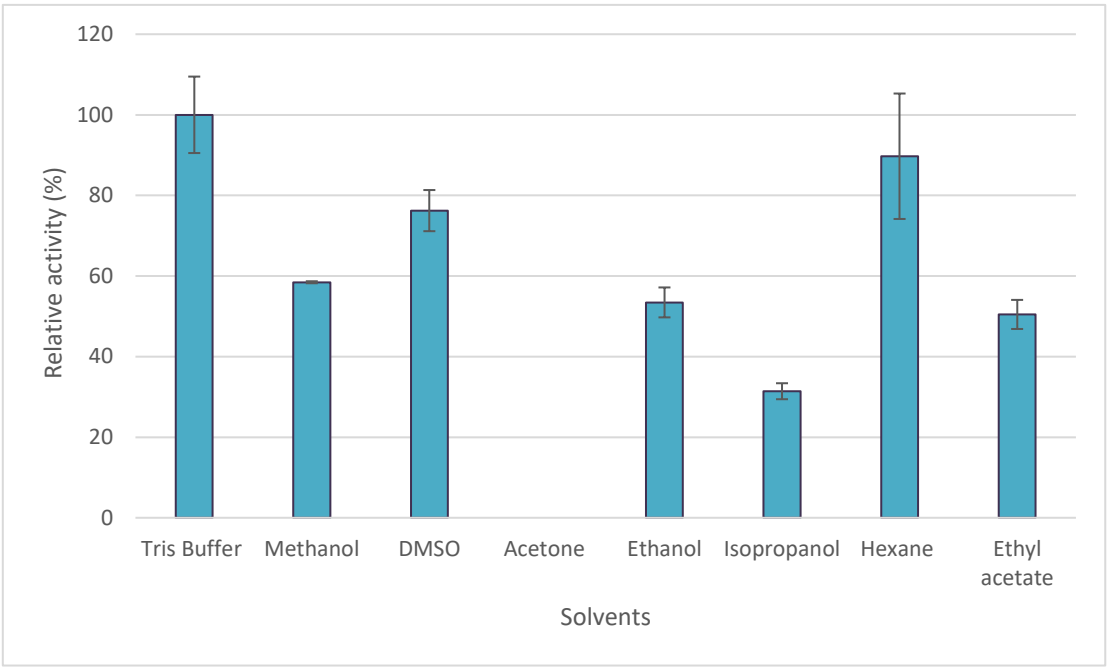

B

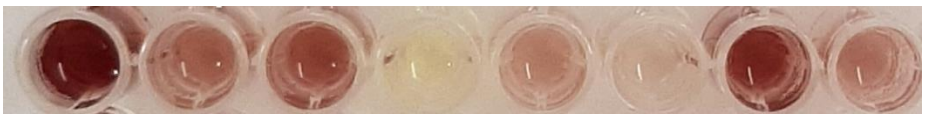

Figure 3.12: The effect of organic solvents on the assay. The acetonitrile was dissolved in each organic solvent and 5 µl of the solution was added to wells containing 1 µg/µl of NHase and 50 mM Tris-HCl (pH 7.2) so that the total volume in the well was 100 µl. The NHase reaction was followed by the amidase reaction. The reaction was terminated with the addition of 50 µl of 0.1 M $FeCl_3$ in 0.1 M hydrochloric acid and the absorbance was measured at 510 nm. (A) The relative activity (%) of the reactions were calculated in relation to the Tris buffer which was used as the standard buffer throughout the assay. The standard deviation between duplicate measurements is indicated by the error bars. (B) A visual representation of the observed effect of increasing NHase concentration on product output over time.

3.3.8 The effect of different nitrile substrates on the assay

Enzyme engineering efforts can be directed at expanding an enzymes substrate profile, as an enzymes narrow substrate specificity can greatly limit the synthesis of important chiral compounds required in industry (Nie *et al.*, 2018). As a result, a variety of substrates were chosen to verify the assay's capacity to detect enzyme activity when using diverse substrates. Since the assay involves a second enzyme, amidase, the investigation here is not uniquely focused on the NHase's ability to hydrolyse the substrates. Rather the focus is on whether the assay as a whole is able to assess a wide variety of substrates, which would also depend on the amidase's ability to transfer an acyl group from the substrates.

The substrates were chosen based on their chemical structure, steric hindrance and electronic properties, as those are the main factors influencing the NHase's ability to catalyse the substrate (Mashweu *et al.*, 2020b). Acetonitrile, acrylonitrile and butyronitrile are short, unbranched aliphatic nitriles that have shown to be efficiently catalysed in past studies (Mashweu *et al.*, 2020b; Nagasawa *et al.*, 1991b; Wieser *et al.*, 1998b). Figure 3.13 shows that all three of these compounds were catalysed successfully by NHase. In addition, the amidase from *Pseudomonas aeruginosa* has shown the ability to transfer the acyl group from short-chain amides (Brown *et al.*, 1969; Fournand and Arnaud, 2001). Acetonitrile was taken as the reference since it was used as the substrate in the standard assay procedure.

Benzonitrile, which is a small aromatic nitrile, was also effectively hydrolysed (Figure 3.13). The result is in broad agreement with Wieser (1998) and Mashweu (2020) who both reported efficient hydrolysis of benzonitrile by L-NHase. However, Nagasawa (1993) has reported on the inability of the H-NHase to hydrolyse benzonitrile. An *ortho*-substituted benzonitrile, 2-hydroxybenzonitrile, was tested and showed high activity, more than double the activity seen by acetonitrile (Figure 3.13). This was unexpected, as the study conducted by Mashweu (2020) showed that although it was hydrolysed, it took 48 hours for the conversion. 2-hydroxybenzonitrile has an electron donating group para to the amino group which changes the electronic properties of the attached nitrile. These electronic properties were thought to make the nitrile less reactive. In contrast, 2-hydroxybenzonitrile showed high response levels to acyl transfer by amidase (Vejvoda *et al.*, 2011)

4-chlorobutyronitrile was chosen since the large chlorine atom sterically hinders the hydrolysis of the nitrile (Black *et al.*, 2010). No activity was seen when 4-chlorobutyronitrile was used in this assay (Figure 3.13) in agreement with Black (2010).

A

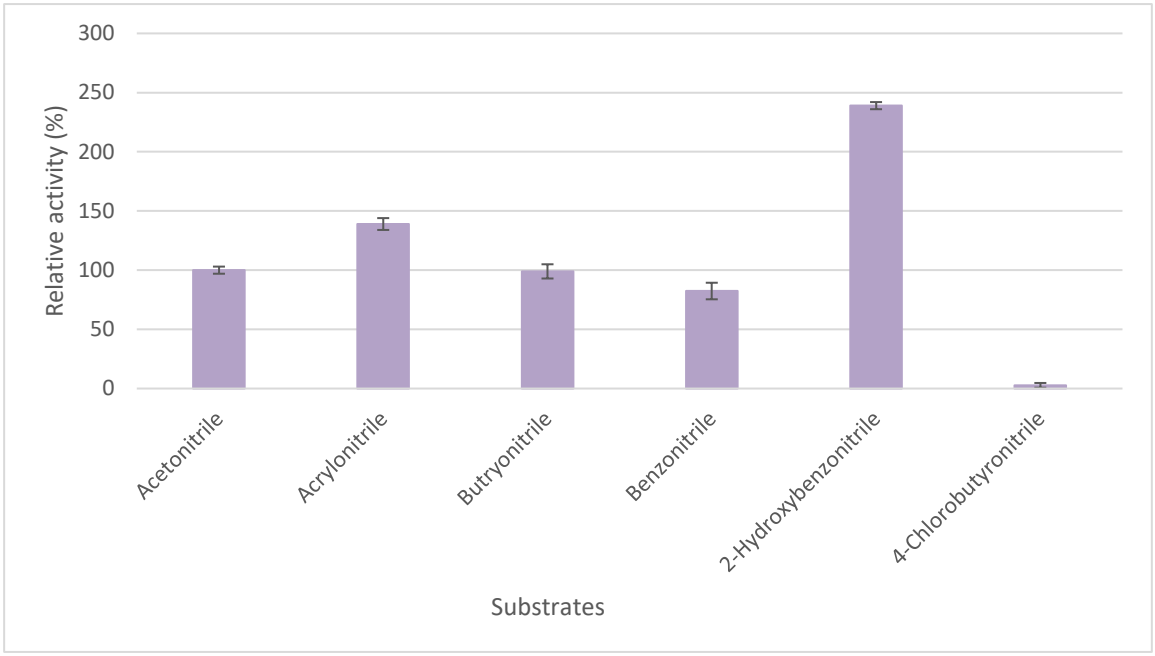

B

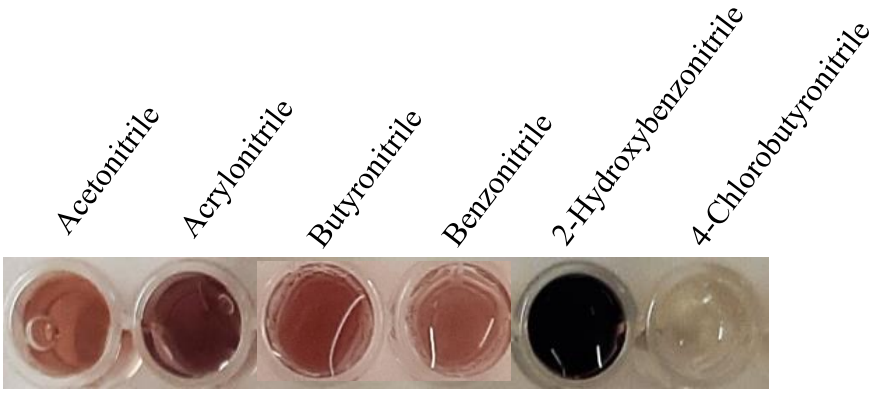

Figure 3.13: The effect of different nitrile substrates on the assay. The nitrile substrates were dissolved in DMSO and were added to wells containing 1 µg/µl of NHase and 50 mM Tris-HCl (pH 7.2). The NHase reaction was followed by the amidase reaction. The reaction was terminated with the addition of 50 µl of 0.1 M $FeCl_3$ in 0.1 M hydrochloric acid and the absorbance was measured at 510 nm. (A) The relative activity (%) of the reactions were calculated in relation to the acetonitrile which was used as the standard substrate throughout the assay. The standard deviation between duplicate measurements is indicated by the error bars. (B) A visual representation of the observed effect of increasing NHase concentration on product output over time.

3.3.9 Analysis of the kinetic parameters for NHase in this assay

The assay conditions can affect the kinetic parameters of an enzyme; therefore, kinetic parameters were determined after all the assay parameters were optimised. The kinetics are specific to this enzyme, NHase from *R. rhodochrous* ATCC BAA-870, to the substrate, acetonitrile and to the specific assay parameters.

3.3.9.1 Calculating the velocity of acetohydroxamic acid production

In order to determine the enzyme kinetic parameters, the first step is to obtain the velocity of the reaction. A time-course reaction of substrate concentrations ranging from 0 to 100 mM was performed. Using the standard curve (Figure 3.3), the absorbance values were translated to the concentration of acetohydroxamic acid produced at each time point for the different substrate concentrations. A graph of acetohydroxamic acid concentration plotted against time was generated for each substrate concentration (Figure 3.14). The gradient of each of these graphs provided the velocity of the reaction. The reaction was run for up to 10 minutes, which is within the linear range of the NHase reaction. These results could then be used to evaluate the enzyme kinetic parameters K_m and V_{max}.

The results in Figure 3.14, show that increasing concentrations of acetonitrile lead to increasing concentration of the end product, acetohydroxamic acid. These results are in line with the results seen in Figure 3.7. Most importantly the velocity of the reaction can be determined by the gradient of the graphs. The gradient values can be seen on the equation for each graph (m = gradient). Based on the gradient values, there is an increase in velocity accompanying an increase in substrate concentration before it levels off. This is in line with the Michaelis-Menten hyperbolic equation which dictates that the rate of the reaction increases with substrate concentration, but once the enzymes are saturated with substrate the rate will not be significantly affected any more. At the saturated stage, the rate of product formation depends on the activity of the enzyme itself.

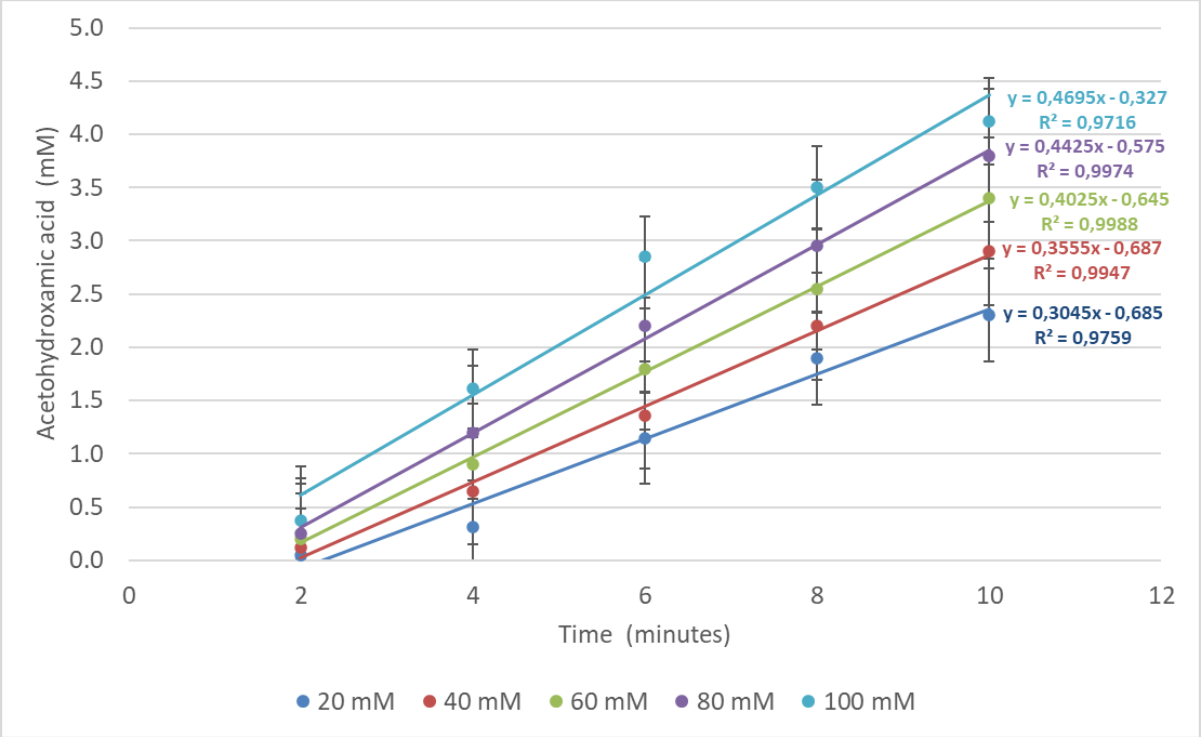

Figure 3.14: The effect of reaction time on acetohydroxamic acid produced using different concentrations of acetonitrile. Increasing concentration of acetonitrile was added to wells containing 1 µg/µl of NHase enzyme. The reaction was stopped at 2 minutes intervals for 10 minutes. The absorbance readings were extrapulated form the equation of the standard curve to give the concentration of acetohydroxamic acid produced at each time point. The standard deviation between duplicate measurements is indicated by the error bars.

3.3.9.2 Determination of kinetic parameters of NHase using Lineweaver-Burk, Hanes-Woolf and Eadie-Hofstee plots

The Lineweaver-Burk (Figure 3.15), Eadie-Hofstee (Figure 3.16) and Hanes-Woolf plots (Figure 3.17) were used to graphically depict the linearised form of the Michaelis-Menten equation. The graphs show the change in substrate concentration as a function of reaction velocity indicating first order kinetics. These three main models for linearising the Michaelis-Menten equation were employed in this study because each has distinct advantages and limitations. They were compared based on their ability to precisely fit the experimental points to produce the most precise estimation of the K_m and V_{max} parameters.

The Lineweaver-Burk plot is the most used method for data linearisation, and it provides the most accurate estimations of K_m and V_{max}. However, its disadvantage is that it places the most amount of weight on the velocity values at low substrate concentrations and at these

concentrations the precision of determining the velocity is at its lowest because small amounts of product have formed. The correlation coefficient (R^2 value) of the analysis was 0.9466 which indicates that the correlation is fairly strong regardless that there was uneven spacing of the points towards the lower concentration values.

The Eadie-Hofstee plot overcomes the uneven weighting of the low concentration values. However, its disadvantage is that the velocity, which is a dependent variable, is used on both axes, and therefore any errors made while measuring the velocity is magnified. This can lead to inaccurate estimations of K_m and V_{max} parameters. The R^2 value for this analysis was 0.8961, indicating a relatively weak correlation which could be due to errors made when measuring the velocity.

Lastly, the Hanes-Woolf plot also overcomes the uneven weighting of the low concentration values. However, its disadvantage is the use of substrate concentration on both axes. As a result, basic pipetting errors that cause uneven substrate concentrations are amplified, resulting in incorrect predictions of the K_m and V_{max} parameters. The R^2 value for this analysis was 0.9929 which is the highest correlation of all three types of plots. This indicates that the Hanes-Woolf model fits this data the best.

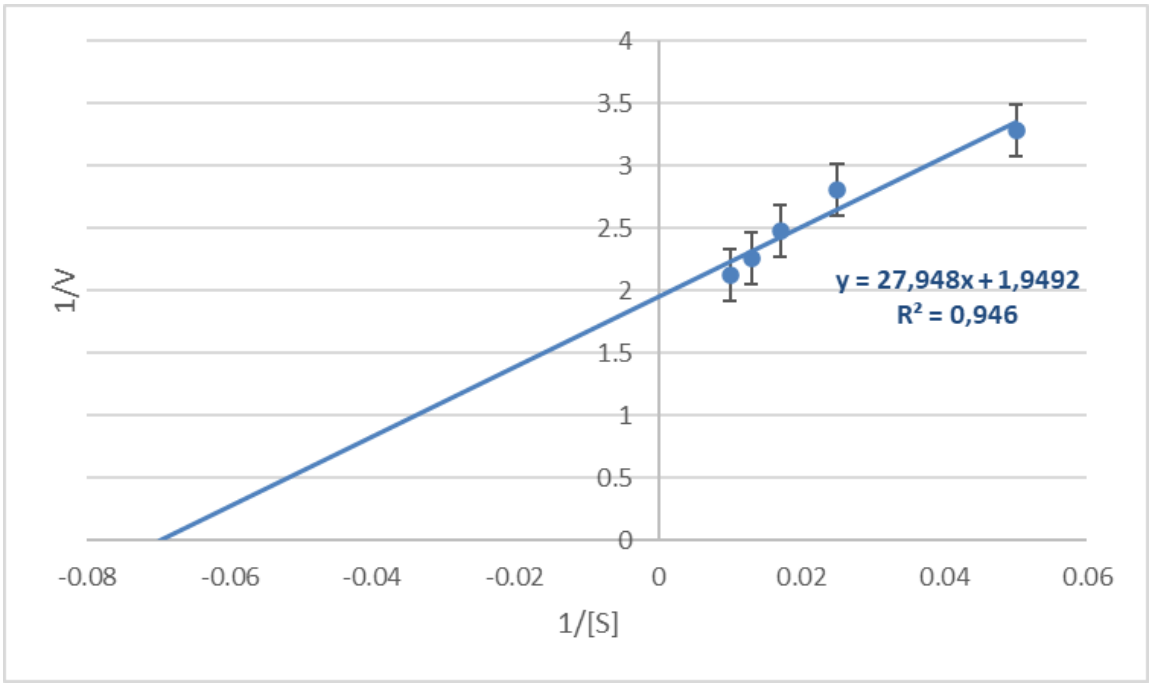

Figure 3.15: The Lineweaver-Burk plot for the NHase. The linear curve was constructed using the velocity obtained from the gradient of the curves from Figure 3.14 and the substrate concentration. The standard deviation between duplicate measurements is indicated by the error bars.

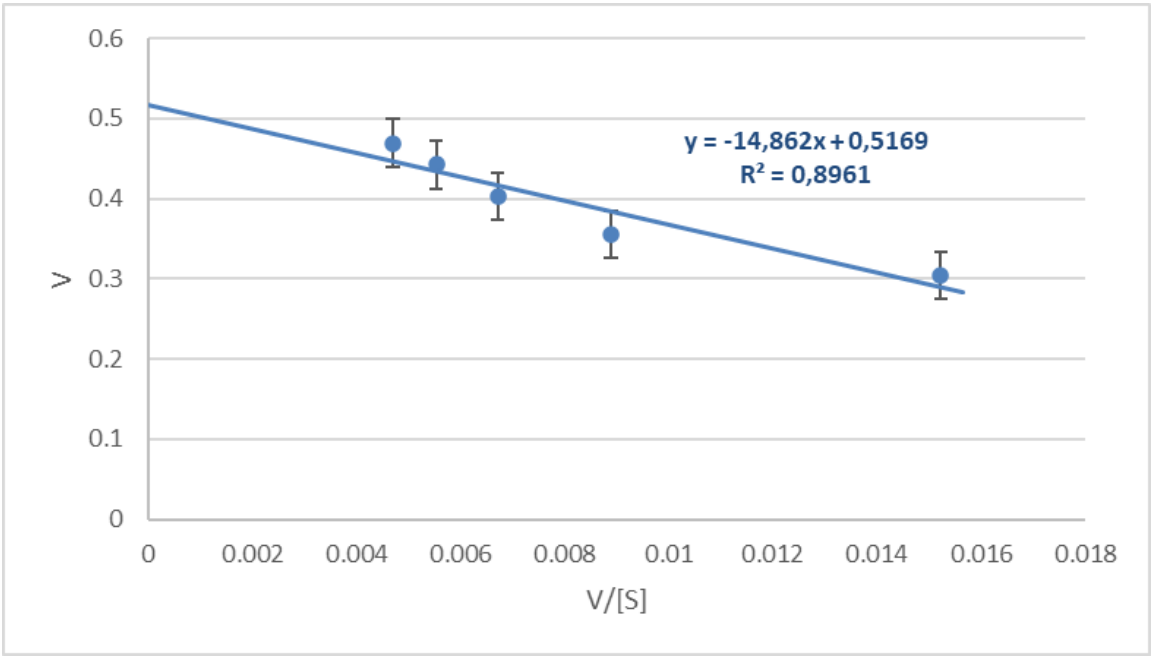

Figure 3.16: The Eadie-Hofstee plot for the NHase. The linear curve was constructed using the velocity obtained from the gradient of the curves from Figure 3.14 and the substrate concentration. The standard deviation between duplicate measurements is indicated by the error bars.

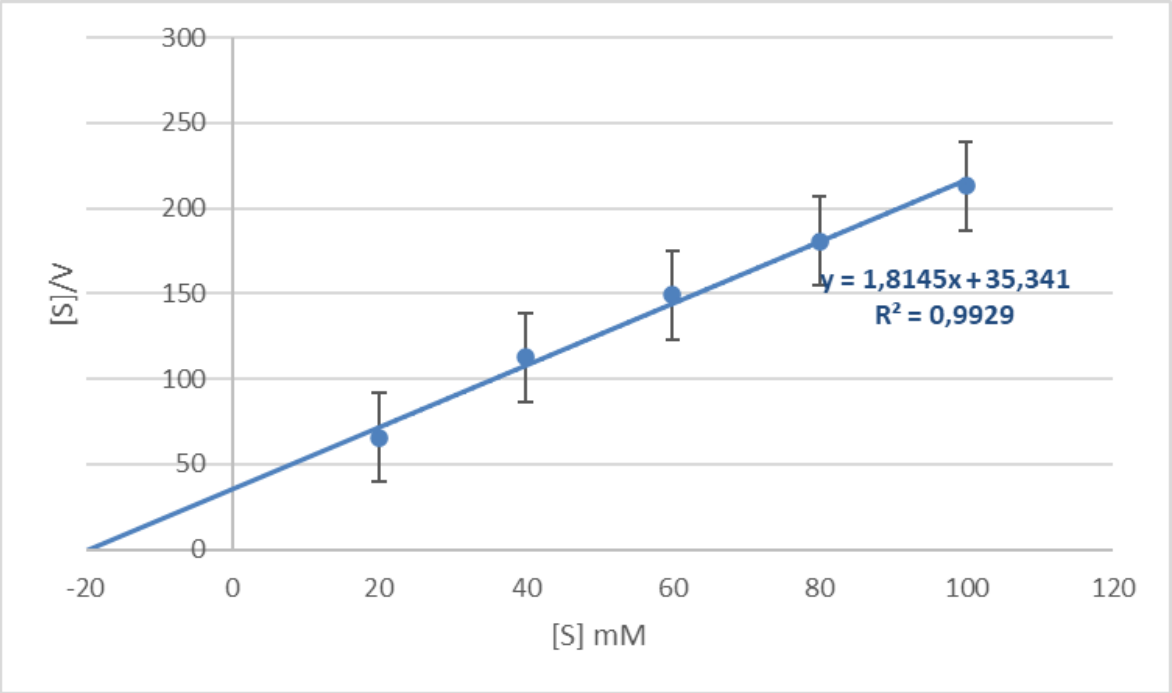

Figure 3.17: The Hanes-Woolf plot for the NHase. The linear curve was constructed using the velocity obtained from the gradient of the curves from Figure 3.14 and the substrate concentration. The standard deviation between duplicate measurements is indicated by the error bars.

3.3.9.3 V_{max} and K_m values for the NHase

The V_{max} and K_m values for the NHase in this assay using acetonitrile as a substrate are summarised in Table 3.1. Despite the fact that the Lineweaver-Burk plot and the Eadie-Hofstee plot had the lowest two R^2 values, their V_{max} and K_m values are very close to each other, this could suggest that those values are the most accurate, or that they are both affected by the same error. Nonetheless, the Hanes-Woolf plot values are not significantly different from the other two and had the highest R^2 value, indicating it was the best fit for the data. While K_m and *Vmax* values are unique to each enzyme and an assay, comparing the results to those of comparable NHases can help put the kinetic parameter values into context. No kinetic assays have been conducted on the NHase from the ATCC BAA-870 strain, therefore a homologous NHase was used for comparison of the kinetic parameters. The *Km* value of 10.2 mM obtained from a study conducted by Idan (2008), is similar to the *Km* values obtained in this assay. The low K_m values indicate that the NHase has a high affinity for acetonitrile. The *Vmax* determined by Idan (2008)

was 0.15 mM/min which is lower than the *Vmax* values obtained in this study. The high *Vmax* values indicate that the NHase form the ATCC BAA-870 strain is an important biocatalyst.

Table 3.1: A summary of kinetic parameters for the NHase.

	V_{max} (mM/min)	K_m (mM)
Lineweaver-Burk	0.51	14.34
Eadie-Hofstee	0.52	14.86
Hanes-Woolf	0.55	19.48

Chapter 4: General discussion and conclusion

NHases are important enzymes since they can transform nitriles, which are low-cost intermediates, into high-value industrial chemicals like acrylamide. The chemical method that is currently in use necessitates extreme conditions such as high temperatures, strong acids and bases, and produces toxic by-products. Enzymes, on the other hand, are evolved towards mild conditions. As a result, utilizing enzymes as a biocatalyst in industry provides a number of benefits, including the need for mild reaction conditions, efficiency, and environmental friendliness (Riva and Fessner, 2014). Furthermore, they have high selectivity which allows for the creation of novel substrates that chemical processes cannot produce (Benerjee *et al.*, 2002). In addition, NHases are being used in bioremediation to remove toxic nitrile waste that is produced in industry (Gong *et al.*, 2017).

However, despite their tremendous capabilities, enzymes have evolved to meet the needs of their natural role and host and may lack some characteristics required for an enzyme to function as an industrial catalyst. Therefore, enzyme engineering is being used to optimise enzymes so that they can have high activity and remain stable at tough manufacturing circumstances such as high temperatures, very basic or acidic pH values and high substrate/product concentration.

In this study the aim was to develop a high-throughput assay that can measure enzyme activity. This was done as a prelude to doing indirect evolution on the NHase. Indirect evolution involves adding random mutations to the DNA sequence which results in large mutant libraries. Without a sensitive, accurate high-throughput screening assay there is no way to detect the mutants with the improved capability.

Before the assay could be designed, the NHase enzyme had to be expressed. The NHase enzyme is made up of two subunits, alpha and beta, and they form a heterotetramer. Initial studies by Joni Frederick (2006) showed that co-expression of the subunits on one plasmid did not result in sufficient expression of both subunits. Therefore, the subunits were individually cloned on two separate plasmids, the pRSFDuet-1 which contained the alpha subunit and chaperone protein and pET21a(+) which contained the beta subunit. By cloning the subunits onto different vectors, it put each subunit under the control of separate promoters which helped increase the expression of each subunit. However, co-expression of the subunits in T7 Express competent *E. coli* cells still showed that the alpha subunit was under expressed when compared to the beta subunit. Furthermore, when the alpha subunit was individually expressed it showed good expression levels, therefore ruling out the possibility of it causing protein toxicity on the

host cell. This finding is intriguing because the pRSFDuet-1 plasmid (which contains the alpha subunit) is the smaller of the two plasmids and has a high copy number, implying that it should produce more protein. Although it is logical to think that a high copy number will result in a high protein yield, a high plasmid number can create metabolic stress and plasmid instability.

Increasing the pRSFDuet-1 plasmid to 4 x the amount of the pET21a(+) plasmid resulted in decreased transformation efficiency and did not increase the amount of alpha subunit expression. Nonetheless, because the alpha and beta subunits form homodimers, a functional protein can be produced as long as some alpha subunits are available. Future work for achieving equal expression includes cloning the subunits onto plasmids with different types of promoters, so that expression is controlled under two different inducers, such as IPTG.

Contrarily, the alpha subunit showed higher solubility levels compared to the beta subunit which formed aggregates. This could be related to the excessive production of beta polypeptides, which could result in aggregation. In the future, minimising aggregation may require experimenting with lower temperature conditions during expression or reducing the amount of IPTG used for expression.

Once NHase was successfully expressed it was possible to begin optimising the activity assay. A coupled enzyme assay was chosen because neither nitrile nor amides react with another molecule to form a coloured complex that can be detected. When an amidase and an NHase are coupled, the amidase can transfer the acyl group from the amide to hydroxylamine, resulting in hydroxamic acid, which can then be detected by adding Fe^{3+}.

Since hydroxylamine was added to the wells in order to ensure that the end product was produced solely as a result of its relationship with the amide and not due to a relationship with the NHase, experiments were carried out. Increasing concentrations of hydroxylamine was added to the wells during the NHase reaction as well as the amidase reaction. The results showed that low concentration of hydroxylamine inhibited NHase activity confirming that the coloured compound was not due to its interaction with the NHase. On the other hand, at high hydroxylamine concentrations amidase still had activity.

When constructing an assay, it is critical to make sure it is sensitive enough to detect modest levels of enzyme activity. As a result, it was necessary to determine how much acetohydroxamic acid was required to get an absorbance reading. The results showed that at 5 mM acetohydroxamic acid resulted in an absorbance reading of 0.5. Using an absorbance reading of 0.5 is desired as it is a good compromise between limiting the optical noise in the

spectrophotometer and having a good signal to measure. Thus, since an absorbance of 0.5 was obtained at a low concentration of 5 mM acetohydroxamic acid, the assay can be sensitive enough to detect low activity levels.

Following this, the effect of substrate concentration on the amidase was investigated. The amidase enzyme was optimised first to ensure that the amidase was the non-limiting enzyme reaction (Robinson, 2015). As a result, the signal generated by the assay will represent the NHase activity. The results showed that at 100 mM acetamide the amidase is not affected. Furthermore, the effect of different concentrations of amidase in time was determined. Amidase concentration and time have an inverse relationship. Thus, to save on expensive amidase enzyme, 0.4 units of amidase was chosen, and the reaction duration was set to 30 minutes (Table 4.1). The drawback here was that the high-throughput ability of the assay decreased due to the increased time.

Next, optimisation of the NHase reaction was conducted. The effect of acetonitrile (substrate) and acetamide (product) on the NHase activity was determined. Enzyme inhibition can be caused by excessive quantities of both substrate and product. However, the results showed that NHase activity increased with increasing concentrations of acetonitrile. Therefore, in order to maximise the sensitivity of the assay 100 mM acetonitrile could be used (Table 4.1). In addition, NHase activity was not significantly affected by high concentrations of acetamide. Lastly, the effect of NHase concentration on the rate of change of absorbance in time was determined. The goal here was to yield maximum activity in the least amount of time. Therefore, 1.0 µg/µl of NHase was chosen as the best concentration of NHase to use in the assay and the time was set to 10- minutes so that the assay remained in the linear range (Table 4.1).

After that, the influence of pH and temperature on the assay was investigated. Using a range of temperatures and pH values the optimal activity for the assay was determined. The pH and temperature graphs both displayed two peaks, which could be owing to each enzyme's ideal assay conditions being different. Based on past literature and owing to the fact that most enzymes favour mild conditions the pH optimum was determined to be pH 8 and the optimal temperature was determined to be 35˚C (Table 4.1).

Since nitrile compounds can be hydrophobic, the next step was to evaluate the impact of various organic solvents on the assay. Organic solvents can denature proteins and therefore minimal amounts should be used. The results showed that Tris-HCl buffer had the highest activity,

followed by hexane and the DMSO. However, since DMSO can dissolve both polar and non-polar substrates it should be used as the organic solvent when examining the NHase's substrate profile.

Finally, a variety of different nitrile compounds were chosen to see if this assay could be used to assess the NHase substrate profile. The nitriles were chosen based on their size and steric hindrance, two criteria that influence the NHase's ability to catalyse various substrates. The results showed that small, aliphatic nitriles namely, acetonitrile, acrylonitrile and butyronitrile were all successfully catalysed. In addition, benzonitrile an aromatic substrate was successfully catalysed. Interestingly, 2-hydroxybenzonitrile demonstrated a 2-fold higher enzyme activity than the aliphatic nitriles. This is in contrast to previous research, which found that the catalysis of this nitrile was slow and incomplete (Mashweu *et al.*, 2020).

Once the assay was fully optimised so that the measured absorbance is a true indication of NHase activity, the enzyme kinetics for the NHase was investigated. The small *Km* values indicate that the NHase has a high affinity towards acetonitrile, while the high *Vmax* values indicate that the NHase from *R. rhodochrous* ATCC BAA-870 is an important biocatalyst.

Thus, in conclusion a proof of concept for a high-throughput screening assay to measure NHase activity was developed in this study as summarised in Table 4.1. Although the assay has been optimised for quantitative usage, it could be utilised as a qualitative assay in any laboratory. Furthermore, this assay can be adapted for use in high-throughput, automated machinery.

4.1 Future work and suggestions

Although this assay was optimised using the NHase from *R. rhodochrous* ATCC BAA-870, this assay can be used for any NHase enzyme. As a result, future work could include creating an "easy-to-use" kit that can be offered commercially. To meet this goal, future research must be done to reduce the overall assay volume so that the total volume of the assay is performed at 100 µl. This would aid in increasing the throughput of the assay while lowering costs. Decreasing the volume of the assay is challenging and will require scientific research since both enzymes have shown to precipitate in smaller volumes. Developing a kit would also entail research into increasing the shelf life of the reaction components of the assay such as the enzymes, acetonitrile substrates which are light sensitive, the hydroxylamine and acidic ferric chloride solutions which are easily hydrolysed (Knight and Sylva, 1974; Monzyk and Crumbliss, 1979) as well as the Tris- HCl buffer.

This project resulted in a proof of concept for an assay that can be adapted for high throughput; the next step is to confirm its high throughput capabilities, particularly with automated equipment like Bio-Rad's ZE5 Cell Analyzer. Using the automated machinery, the assay time can be decreased, and the accuracy of the assay can be increased since there is little room for human error.

Lastly, the assay was developed for detecting activity of NHase mutants in large libraries produced by indirect evolution. As a result, the project's next step is to do indirect evolution on the wild-type NHase to see if there are any viable mutants that can be evolved to improve the industrial capabilities of the NHase.

Table 4.1: Summery of optimal parameters for performing the assay.

Parameter	Value
Acetonitrile	100 mM
Nitrile hydratase	1.0 µg/µl
Incubation time for nitrile hydratase step	10-minutes
Amidase	0.4-units
Hydroxylamine	20 mM
Incubation time for amidase step	30-minutes
pH	pH 8
Temperature	35˚C
Organic solvent	Tris-HCl (DMSO can be used when assessing multiple nitriles)
Substrates	Optimised for acetonitrile but assay can be used for small aliphatic nitriles and small aromatic nitriles.

REFERENCES

Wieser, M., Takeuchi, K., Wada, Y., Yamada, H., Nagasawa, T., 1998. Low-molecular-mass nitrile hydratase from Rhodococcus rhodochrous J1: puri¢cation, substrate speci¢city and comparison.

Acker, M.G., Auld, D.S., 2014. Considerations for the design and reporting of enzyme assays in high-throughput screening applications. Perspect. Sci., Reporting Enzymology Data – STRENDA Recommendations and Beyond 1, 56–73. https://doi.org/10.1016/j.pisc.2013.12.001

Aharoni, A., Gaidukov, L., Khersonsky, O., McQ Gould, S., Roodveldt, C., Tawfik, D.S., 2005. The "evolvability" of promiscuous protein functions. Nat. Genet. 37, 73–76. https://doi.org/10.1038/ng1482

Alam, M.T., Olin-Sandoval, V., Stincone, A., Keller, M.A., Zelezniak, A., Luisi, B.F., Ralser, M., 2017. The self-inhibitory nature of metabolic networks and its alleviation through compartmentalization. Nat. Commun. 8, 16018. https://doi.org/10.1038/ncomms16018

Andrić, P., Meyer, A.S., Jensen, P.A., Dam-Johansen, K., 2010. Reactor design for minimizing product inhibition during enzymatic lignocellulose hydrolysis: II. Quantification of inhibition and suitability of membrane reactors. Biotechnol. Adv. 28, 407–425. https://doi.org/10.1016/j.biotechadv.2010.02.005

Anton, B.P., Fomenkov, A., Raleigh, E.A., Berkmen, M., 2016. Complete Genome Sequence of the Engineered *Escherichia coli* SHuffle Strains and Their Wild-Type Parents. Genome Announc. 4. https://doi.org/10.1128/genomeA.00230-16

Armstrong, E.F., 1930. Enzymes. By J.B.S. Haldane, M.A. Monographs on Biochemistry. Edited by R.H.A. Plimmer, D.Sc., and Sir F. G. Hopkins, M.A., M.B., D.Sc., F.R.S. Pp.

vii+235. London: Longmans, Green & Co., 1930. Price 14s. J. Soc. Chem. Ind. 49, 919–920. https://doi.org/10.1002/jctb.5000494433

Asano, Y., Tani, Y., Yamada, H., 1980. A New Enzyme “Nitrile Hydratase” which Degrades Acetonitrile in Combination with Amidase. Agric. Biol. Chem. 44, 2251–2252. https://doi.org/10.1080/00021369.1980.10864311

Aslanzadeh, S., Ishola, M.M., Richards, T., Taherzadeh, M.J., 2014. Chapter 1 - An Overview of Existing Individual Unit Operations, in: Qureshi, N., Hodge, D.B., Vertès, A.A. (Eds.), Biorefineries. Elsevier, Amsterdam, pp. 3–36. https://doi.org/10.1016/B978-0-444-59498-3.00001-4

Banerjee, A., Kaul, P., Sharma, R., Banerjee, U.C., 2003. A high-throughput amenable colorimetric assay for enantioselective screening of nitrilase-producing microorganisms using pH sensitive indicators. J. Biomol. Screen. 8, 559–565. https://doi.org/10.1177/1087057103256910

Baneyx, F., 1999. Recombinant protein expression in Escherichia coli. Curr. Opin. Biotechnol. 10, 411–421. https://doi.org/10.1016/S0958-1669(99)00003-8

Bank, R.P.D., n.d. RCSB PDB - 1IRE: Crystal Structure of Co-type nitrile hydratase from Pseudonocardia thermophila [WWW Document]. URL https://www.rcsb.org/structure/1IRE (accessed 3.22.22).

Bhalla, T.C., Kumar, Vijay, Kumar, Virender, Thakur, N., Savitri, null, 2018. Nitrile Metabolizing Enzymes in Biocatalysis and Biotransformation. Appl. Biochem. Biotechnol. 185, 925–946. https://doi.org/10.1007/s12010-018-2705-7

Bhatia, R.K., Bhatia, S.K., Mehta, P.K., Bhalla, T.C., 2016. Bio-statistical enhancement of acyl transfer activity of amidase for biotransformation of N-substituted aromatic amides. J. Gen. Appl. Microbiol. 62, 90–97. https://doi.org/10.2323/jgam.62.90

Bisswanger, H., 2017. Enzyme Kinetics: Principles and Methods. John Wiley & Sons.

Bisswanger, H., 2014. Enzyme assays. Perspect. Sci., Reporting Enzymology Data – STRENDA Recommendations and Beyond 1, 41–55. https://doi.org/10.1016/j.pisc.2014.02.005

Black, G.W., Gregson, T., McPake, C.B., Perry, J.J., Zhang, M., 2010. Biotransformation of nitriles using the solvent-tolerant nitrile hydratase from Rhodopseudomonas palustris CGA009. Tetrahedron Lett. 51, 1639–1641. https://doi.org/10.1016/j.tetlet.2009.12.094

Blackmond, D.G., Hodnett, N.S., Lloyd-Jones, G.C., 2006. Mechanistic Implications of Pseudo Zero Order Kinetics in Kinetic Resolutions. J. Am. Chem. Soc. 128, 7450–7451. https://doi.org/10.1021/ja062173f

Brenner, S., Lerner, R.A., 1992. Encoded combinatorial chemistry. Proc. Natl. Acad. Sci. 89, 5381–5383. https://doi.org/10.1073/pnas.89.12.5381

Brown, j.e., Brown, p.r., Clarke, p.h.y. 1969, n.d. Butyramide-utilizing Mutants of Pseudomonas aeruginosa 8602 which Produce an Amidase with Altered Substrate Specificity. Microbiology 57, 273–285. https://doi.org/10.1099/00221287-57-2-273

Brzoska, A.J., Firth, N., 2013. Two-Plasmid Vector System for Independently Controlled Expression of Green and Red Fluorescent Fusion Proteins in Staphylococcus aureus. Appl. Environ. Microbiol. 79, 3133–3136. https://doi.org/10.1128/AEM.00144-13

Cameron, R.A., Sayed, M., Cowan, D.A., 2005. Molecular analysis of the nitrile catabolism operon of the thermophile Bacillus pallidus RAPc8. Biochim. Biophys. Acta 1725, 35–46. https://doi.org/10.1016/j.bbagen.2005.03.019

Cavicchioli, R., Charlton, T., Ertan, H., Omar, S.M., Siddiqui, K.S., Williams, T.J., 2011. Biotechnological uses of enzymes from psychrophiles. Microb. Biotechnol. 4, 449–460. https://doi.org/10.1111/j.1751-7915.2011.00258.x

Chen, Y., Jiao, S., Wang, M., Chen, J., Yu, H., 2018. A novel molecular chaperone GroEL2 from Rhodococcus ruber and its fusion chimera with nitrile hydratase for co-enhanced activity and stability. Chem. Eng. Sci. 192, 235–243. https://doi.org/10.1016/j.ces.2018.07.045

Cheng, Z., Lan, Y., Guo, J., Ma, D., Jiang, S., Lai, Q., Zhou, Z., Peplowski, L., 2020. Computational Design of Nitrile Hydratase from Pseudonocardia thermophila JCM3095 for Improved Thermostability. Molecules 25, 4806. https://doi.org/10.3390/molecules25204806

Chiyanzu, I., 2008. An investigation into the biocatalytic application of the thermostable nitrile hydratase from the thermophilic strain Geobacillus pallidus RAPc8.

Cleland, W.W., 1979. Optimizing coupled enzyme assays. Anal. Biochem. 99, 142–145. https://doi.org/10.1016/0003-2697(79)90055-1

Desai, L.V., Zimmer, M., 2004. Substrate selectivity and conformational space available to bromoxynil and acrylonitrile in iron nitrile hydratase. Dalton Trans. Camb. Engl. 2003 872–877. https://doi.org/10.1039/b313380j

Easterby, J. S., 1973. Coupled enzyme assays: a general expression for the transient. Biochim. Biophys. Acta 293, 552–558. https://doi.org/10.1016/0005-2744(73)90362-8

Easterby, John S., 1973. Coupled enzyme assays: A general expression for the transient. Biochim. Biophys. Acta BBA - Enzymol. 293, 552–558. https://doi.org/10.1016/0005-2744(73)90362-8

Eilertsen, J., Schnell, S., 2018. A kinetic analysis of coupled (or auxiliary) enzyme reactions. https://doi.org/10.26434/chemrxiv.5746065.v3

Fawcett, J.K., Scott, J.E., 1960. A Rapid And Precise Method For The Determination Of Urea. J. Clin. Pathol. 13, 156–159.

Fernandes, J.M.C., Dias, A.A., Bezerra, R.M.F., 2022. Kinetic Analysis Misinterpretations Due to the Occurrence of Enzyme Inhibition by Reaction Product: Comparison between Initial Velocities and Reaction Time Course Methodologies. Appl. Sci. 12, 102. https://doi.org/10.3390/app12010102

Fournand, D., Arnaud, A., 2001. Aliphatic and enantioselective amidases: from hydrolysis to acyl transfer activity. J. Appl. Microbiol. 91, 381–393. https://doi.org/10.1046/j.1365-2672.2001.01378.x

Fournand, D., Bigey, F., Arnaud, A., 1998. Acyl Transfer Activity of an Amidase from Rhodococcus sp. Strain R312: Formation of a Wide Range of Hydroxamic Acids. Appl. Environ. Microbiol. 64, 2844–2852.

Frederick, J., Brady, D., Dirr, H., 2006. Characterisation of the nitrile biocatalytic activity of rhodococcus rhodochrous ATCC BAA-870.

Frederick, J., Hennessy, F., Horn, U., de la Torre Cortés, P., van den Broek, M., Strych, U., Willson, R., Hefer, C.A., Daran, J.-M.G., Sewell, T., Otten, L.G., Brady, D., 2020. The

complete genome sequence of the nitrile biocatalyst Rhodococcus rhodochrous ATCC BAA-870. BMC Genomics 21, 3. https://doi.org/10.1186/s12864-019-6405-7

Gong, J.-S., Shi, J.-S., Lu, Z.-M., Li, H., Zhou, Z.-M., Xu, Z.-H., 2017. Nitrile-converting enzymes as a tool to improve biocatalysis in organic synthesis: recent insights and promises. Crit. Rev. Biotechnol. 37, 69–81. https://doi.org/10.3109/07388551.2015.1120704

Gorman, L.A.S., Dordick, J.S., 1992. Organic solvents strip water off enzymes. Biotechnol. Bioeng. 39, 392–397. https://doi.org/10.1002/bit.260390405

Gottesman, S., 1996. Proteases and their targets in escherichia coli. Annu. Rev. Genet. 30, 465–506. https://doi.org/10.1146/annurev.genet.30.1.465

Graumann, K., Premstaller, A., 2006. Manufacturing of recombinant therapeutic proteins in microbial systems. Biotechnol. J. 1, 164–186. https://doi.org/10.1002/biot.200500051

Grodberg, J., Dunn, J.J., 1988. ompT encodes the Escherichia coli outer membrane protease that cleaves T7 RNA polymerase during purification. J. Bacteriol. 170, 1245–1253. https://doi.org/10.1128/jb.170.3.1245-1253.1988

Gumataotao, N., Kuhn, M.L., Hajnas, N., Holz, R.C., 2013. Identification of an Active Site-bound Nitrile Hydratase Intermediate through Single Turnover Stopped-flow Spectroscopy. J. Biol. Chem. 288, 15532–15536. https://doi.org/10.1074/jbc.M112.398909

Halling-Sørensen, B., Nors Nielsen, S., Lanzky, P.F., Ingerslev, F., Holten Lützhøft, H.C., Jørgensen, S.E., 1998. Occurrence, fate and effects of pharmaceutical substances in the environment- A review. Chemosphere 36, 357–393. https://doi.org/10.1016/S0045-6535(97)00354-8

Hartl, F.U., Hayer-Hartl, M., 2002. Molecular Chaperones in the Cytosol: from Nascent Chain to Folded Protein. Science 295, 1852–1858. https://doi.org/10.1126/science.1068408

Hertzberg, R.P., Pope, A.J., 2000. High-throughput screening: new technology for the 21st century. Curr. Opin. Chem. Biol. 4, 445–451. https://doi.org/10.1016/s1367-5931(00)00110-1

Hopmann, K.H., 2014. Full reaction mechanism of nitrile hydratase: a cyclic intermediate and an unexpected disulfide switch. Inorg. Chem. 53, 2760–2762. https://doi.org/10.1021/ic500091k

Ido, E., Han, H.P., Kezdy, F.J., Tang, J., 1991. Kinetic studies of human immunodeficiency virus type 1 protease and its active-site hydrogen bond mutant A28S. J. Biol. Chem. 266, 24359–24366.

Kashiwagi, M., Fuhshuku, K.I., Sugai, T., 2004. Control of the nitrile-hydrolyzing enzyme activity in Rhodococcus rhodochrous IFO 15564: Preferential action of nitrile hydratase and amidase depending on the reaction condition factors and its application to the one-pot preparation of amides from aldehydes. J. Mol. Catal. B Enzym. 29, 249–258. https://doi.org/10.1016/j.molcatb.2003.12.014

Kaul, P., Banerjee, U.C., 2008. Predicting enzyme behavior in nonconventional media: correlating nitrilase function with solvent properties. J. Ind. Microbiol. Biotechnol. 35, 713–720. https://doi.org/10.1007/s10295-008-0332-y

Kita, K., Okino, N., Ito, M., 2000. Reverse hydrolysis reaction of a recombinant alkaline ceramidase of Pseudomonas aeruginosa. Biochim. Biophys. Acta 1485, 111–120. https://doi.org/10.1016/s1388-1981(00)00029-9

Knight, R.J., Sylva, R.N., 1974. Precipitation in hydrolysed iron(III) solutions. J. Inorg. Nucl. Chem. 36, 591–597. https://doi.org/10.1016/0022-1902(74)80119-3

Kobayashi, M., Komeda, H., Nagasawa, T., Yamada, H., Shimizu, S., 1993. Occurrence of Amidases in the Industrial Microbe Rhodococcus rhodochrous J1. Biosci. Biotechnol. Biochem. 57, 1949–1950. https://doi.org/10.1271/bbb.57.1949

Kobayashi, M., Nagasawa, T., Yamada, H., 1989. Nitrilase of Rhodococcus rhodochrous J1. Purification and characterization. Eur. J. Biochem. 182, 349–356. https://doi.org/10.1111/j.1432-1033.1989.tb14837.x

Kobayashi, M., Nishiyama, M., Nagasawa, T., Horinouchi, S., Beppu, T., Yamada, H., 1991. Cloning, nucleotide sequence and expression in Escherichia coli of two cobalt-containing nitrile hydratase genes from Rhodococcus rhodochrous J1. Biochim. Biophys. Acta BBA - Gene Struct. Expr. 1129, 23–33. https://doi.org/10.1016/0167-4781(91)90208-4

Kokkonen, P., Beier, A., Mazurenko, S., Damborsky, J., Bednar, D., Prokop, Z., 2021. Substrate inhibition by the blockage of product release and its control by tunnel engineering. RSC Chem. Biol. 2, 645–655. https://doi.org/10.1039/D0CB00171F

Laemmli, U.K., 1970. Cleavage of Structural Proteins during the Assembly of the Head of Bacteriophage T4. Nature 227, 680–685. https://doi.org/10.1038/227680a0

Lan, Y., Zhang, X., Liu, Z., Zhou, L., Shen, R., Zhong, X., Cui, W., Zhou, Z., 2017. Overexpression and characterization of two types of nitrile hydratases from Rhodococcus rhodochrous J1. PloS One 12, e0179833. https://doi.org/10.1371/journal.pone.0179833

Lee, S.Y., Choi, J.H., Xu, Z., 2003. Microbial cell-surface display. Trends Biotechnol. 21, 45–52. https://doi.org/10.1016/S0167-7799(02)00006-9

Lee, S.Y., Kim, H.U., Chae, T.U., Cho, J.S., Kim, J.W., Shin, J.H., Kim, D.I., Ko, Y.-S., Jang, W.D., Jang, Y.-S., 2019. A comprehensive metabolic map for production of bio-based chemicals. Nat. Catal. 2, 18–33. https://doi.org/10.1038/s41929-018-0212-4

Liu, Y., Cui, W., Xia, Y., Cui, Y., Kobayashi, M., Zhou, Z., 2012. Self-Subunit Swapping Occurs in Another Gene Type of Cobalt Nitrile Hydratase. PLOS ONE 7, e50829. https://doi.org/10.1371/journal.pone.0050829

Martínková, L., Stolz, A., Rantwijk, F. van, D'Antona, N., Brady, D., Otten, L.G., 2014. Nitrile Converting Enzymes Involved in Natural and Synthetic Cascade Reactions, in: Cascade Biocatalysis. John Wiley & Sons, Ltd, pp. 249–270. https://doi.org/10.1002/9783527682492.ch11

Martínková, L., Uhnáková, B., Pátek, M., Nešvera, J., Křen, V., 2009. Biodegradation potential of the genus Rhodococcus. Environ. Int. 35, 162–177. https://doi.org/10.1016/j.envint.2008.07.018

Mashweu, A.R., Chhiba-Govindjee, V.P., Bode, M.L., Brady, D., 2020a. Substrate Profiling of the Cobalt Nitrile Hydratase from Rhodococcus rhodochrous ATCC BAA 870. Mol. Basel Switz. 25. https://doi.org/10.3390/molecules25010238

Mashweu, A.R., Chhiba-Govindjee, V.P., Bode, M.L., Brady, D., 2020b. Substrate Profiling of the Cobalt Nitrile Hydratase from Rhodococcus rhodochrous ATCC BAA 870. Molecules 25, 238. https://doi.org/10.3390/molecules25010238

Mashweu, A.R., Chhiba-Govindjee, V.P., Bode, M.L., Brady, D., 2020c. Substrate Profiling of the Cobalt Nitrile Hydratase from Rhodococcus rhodochrous ATCC BAA 870. Molecules 25, 238. https://doi.org/10.3390/molecules25010238

Meriç, S., Tünay, O., San, H.A., 2002. A New Approach to Modelling Substrate Inhibition. Environ. Technol. 23, 163–177. https://doi.org/10.1080/09593332508618428

Michaelis, L., Menten, M.L., Johnson, K.A., Goody, R.S., 2011. The original Michaelis constant: translation of the 1913 Michaelis-Menten paper. Biochemistry 50, 8264–8269. https://doi.org/10.1021/bi201284u

Miranda, M., Murado, M.A., Sanroman, A., Lema, J.M., 1991. Mass transfer control of enzymatic hydrolysis of polysaccharides by glucoamylase. Enzyme Microb. Technol. 13, 142–147. https://doi.org/10.1016/0141-0229(91)90170-F

Mitra, S., Holz, R.C., 2007. Unraveling the catalytic mechanism of nitrile hydratases. J. Biol. Chem. 282, 7397–7404. https://doi.org/10.1074/jbc.M604117200

Miyanaga, A., Fushinobu, S., Ito, K., Wakagi, T., 2001. Crystal structure of cobalt-containing nitrile hydratase. Biochem. Biophys. Res. Commun. 288, 1169–1174. https://doi.org/10.1006/bbrc.2001.5897

Monzyk, B., Crumbliss, A.L., 1979. Mechanism of ligand substitution on high-spin iron(III) by hydroxamic acid chelators. Thermodynamic and kinetic studies on the formation and dissociation of a series of monohydroxamatoiron(III) complexes. J. Am. Chem. Soc. 101, 6203–6213. https://doi.org/10.1021/ja00515a009

Mouafo Tamnou, E.B., Tamsa Arfao, A., Nougang, M.E., Metsopkeng, C.S., Noah Ewoti, O.V., Moungang, L.M., Nana, P.A., Atem Takang-Etta, L.-R., Perrière, F., Sime-Ngando, T., Nola, M., 2021. Biodegradation of polyethylene by the bacterium Pseudomonas aeruginosa in

acidic aquatic microcosm and effect of the environmental temperature. Environ. Chall. 3, 100056. https://doi.org/10.1016/j.envc.2021.100056

Nagasawa, T., Shimizu, H., Yamada, H., 1993. The superiority of the third-generation catalyst, Rhodococcus rhodochrous J1 nitrile hydratase, for industrial production of acrylamide. Appl. Microbiol. Biotechnol. 40, 189–195. https://doi.org/10.1007/BF00170364

Nagasawa, T., Takeuchi, K., Yamada, H., 1991a. Characterization of a new cobalt-containing nitrile hydratase purified from urea-induced cells of Rhodococcus rhodochrous J1. Eur. J. Biochem. 196, 581–589. https://doi.org/10.1111/j.1432-1033.1991.tb15853.x

Nagasawa, T., Takeuchi, K., Yamada, H., 1991b. Characterization of a new cobalt-containing nitrile hydratase purified from urea-induced cells of Rhodococcus rhodochrous J1. Eur. J. Biochem. 196, 581–589. https://doi.org/10.1111/j.1432-1033.1991.tb15853.x

Nie, Y., Wang, S., Xu, Y., Luo, S., Zhao, Y.-L., Xiao, R., Montelione, G.T., Hunt, J.F., Szyperski, T., 2018. Enzyme Engineering Based on X-ray Structures and Kinetic Profiling of Substrate Libraries: Alcohol Dehydrogenases for Stereospecific Synthesis of a Broad Range of Chiral Alcohols. ACS Catal. 8, 5145–5152. https://doi.org/10.1021/acscatal.8b00364

Okamoto, S., Eltis, L.D., 2007. Purification and characterization of a novel nitrile hydratase from Rhodococcus sp. RHA1. Mol. Microbiol. 65, 828–838. https://doi.org/10.1111/j.1365-2958.2007.05834.x

Olsen, M.J., Stephens, D., Griffiths, D., Daugherty, P., Georgiou, G., Iverson, B.L., 2000. Function-based isolation of novel enzymes from a large library. Nat. Biotechnol. 18, 1071–1074. https://doi.org/10.1038/80267

Onyeogaziri, F.C., Papaneophytou, C., 2019. A General Guide for the Optimization of Enzyme Assay Conditions Using the Design of Experiments Approach. SLAS Discov. Adv. Sci. Drug Discov. 24, 587–596. https://doi.org/10.1177/2472555219830084

Owusu, R.K., Cowan, D.A., 1989. Correlation between microbial protein thermostability and resistance to denaturation in aqueous: organic solvent two-phase systems. Enzyme Microb. Technol. 11, 568–574. https://doi.org/10.1016/0141-0229(89)90084-7

Packer, M.S., Liu, D.R., 2015. Methods for the directed evolution of proteins. Nat. Rev. Genet. 16, 379–394. https://doi.org/10.1038/nrg3927

Payne, M.S., Wu, S., Fallon, R.D., Tudor, G., Stieglitz, B., Turner, I.M., Nelson, M.J., 1997. A stereoselective cobalt-containing nitrile hydratase. Biochemistry 36, 5447–5454. https://doi.org/10.1021/bi962794t

Prasad, S., Raj, J., Bhalla, T.C., 2009. Purification of a hyperactive nitrile hydratase from resting cells of Rhodococcus rhodochrous PA-34. Indian J. Microbiol. 49, 237–242. https://doi.org/10.1007/s12088-009-0033-x

Pravda, L., Berka, K., Svobodová Vařeková, R., Sehnal, D., Banáš, P., Laskowski, R.A., Koča, J., Otyepka, M., 2014. Anatomy of enzyme channels. BMC Bioinformatics 15, 379. https://doi.org/10.1186/s12859-014-0379-x

Prepechalová, I., Martínková, L., Stolz, A., Ovesná, M., Bezouska, K., Kopecký, J., Kren, V., 2001. Purification and characterization of the enantioselective nitrile hydratase from Rhodococcus equi A4. Appl. Microbiol. Biotechnol. 55, 150–156. https://doi.org/10.1007/s002530000507

Reed, M.C., Lieb, A., Nijhout, H.F., 2010. The biological significance of substrate inhibition: A mechanism with diverse functions. BioEssays 32, 422–429. https://doi.org/10.1002/bies.200900167

Riva, S., Fessner, W.-D., 2014. Cascade Biocatalysis: Integrating Stereoselective and Environmentally Friendly Reactions. John Wiley & Sons.

Robinson, P.K., 2015. Enzymes: principles and biotechnological applications. Essays Biochem. 59, 1–41. https://doi.org/10.1042/bse0590001

Rosano, G.L., Ceccarelli, E.A., 2014. Recombinant protein expression in Escherichia coli: advances and challenges. Front. Microbiol. 5, 172. https://doi.org/10.3389/fmicb.2014.00172

Roskoski, R., 2007. Enzyme Assays, in: Enna, S.J., Bylund, D.B. (Eds.), XPharm: The Comprehensive Pharmacology Reference. Elsevier, New York, pp. 1–7. https://doi.org/10.1016/B978-008055232-3.60040-6

Roughton, F.J.W., Booth, V.H., 1946. The effect of substrate concentration, pH and other factors upon the activity of carbonic anhydrase. Biochem. J. 40, 319–330.

Sahu, R., Meghavarnam, A.K., Janakiraman, S., 2019. A simple, efficient and rapid screening technique for differentiating nitrile hydratase and nitrilase producing bacteria. Biotechnol. Rep. 24, e00396. https://doi.org/10.1016/j.btre.2019.e00396

Santoro, S.W., Schultz, P.G., 2002. Directed evolution of the site specificity of Cre recombinase. Proc. Natl. Acad. Sci. 99, 4185–4190. https://doi.org/10.1073/pnas.022039799

Schmid, K., 2020. Nitrile hydratase enantioselectivity as a function of genetic diversity and directed evolution (Thesis).

Schmidt, N.D., Peschon, J.J., Segel, I.H., 1983. Kinetics of enzymes subject to very strong product inhibition: analysis using simplified integrated rate equations and average velocities. J. Theor. Biol. 100, 597–611. https://doi.org/10.1016/0022-5193(83)90325-9

Shahar, A., Melamed-Frank, M., Kashi, Y., Shimon, L., Adir, N., 2011. The Dimeric Structure of the Cpn60.2 Chaperonin of Mycobacterium tuberculosis at 2.8 Å Reveals Possible Modes of Function. J. Mol. Biol. 412, 192–203. https://doi.org/10.1016/j.jmb.2011.07.026

Sninsky, J.J., Uhlin, B.E., Gustafsson, P., Cohen, S.N., 1981. Construction and characterization of a novel two-plasmid system for accomplishing temperature-regulated, amplified expression of cloned adventitious genes in Escherichia coli. Gene 16, 275–286. https://doi.org/10.1016/0378-1119(81)90083-4

Soobben, M., 2020. Production of nitrile hydrolysing biocatalysts from Rhodococcus rhodochrous (Thesis).

Sørensen, H.P., Mortensen, K.K., 2005. Advanced genetic strategies for recombinant protein expression in Escherichia coli. J. Biotechnol. 115, 113–128. https://doi.org/10.1016/j.jbiotec.2004.08.004

Strompfová, V., Lauková, A., Simonová, M., Marciňáková, M., 2008. Occurrence of the structural enterocin A, P, B, L50B genes in enterococci of different origin. Vet. Microbiol. 132, 293–301. https://doi.org/10.1016/j.vetmic.2008.05.001

Sun, Y., Cheng, J., 2002. Hydrolysis of lignocellulosic materials for ethanol production: a review. Bioresour. Technol., Reviews Issue 83, 1–11. https://doi.org/10.1016/S0960-8524(01)00212-7

Takihara, H., Matsuura, C., Ogihara, J., Iwabuchi, N., Sunairi, M., 2014a. *Rhodococcus rhodochrous* ATCC12674 Becomes Alkane-Tolerant upon GroEL2 Overexpression and Survives in the *n*-Octane Phase in Two Phase Culture. Microbes Environ. advpub. https://doi.org/10.1264/jsme2.ME14114

Takihara, H., Ogihara, J., Yoshida, T., Okuda, S., Nakajima, M., Iwabuchi, N., Sunairi, M., 2014b. Enhanced Translocation and Growth of *Rhodococcus erythropolis* PR4 in the Alkane Phase of Aqueous-Alkane Two Phase Cultures Were Mediated by GroEL2 Overexpression. Microbes Environ. 29, 346–352. https://doi.org/10.1264/jsme2.ME13158

Uhr, M.L., 1990. Coupled enzyme systems: Exploring coupled assays with students. Biochem. Educ. 18, 48–50. https://doi.org/10.1016/0307-4412(90)90025-J

van Pelt, S., van Rantwijk, F., Sheldon, R.A., 2009. Synthesis of Aliphatic (S)-α-Hydroxycarboxylic Amides using a One-Pot Bienzymatic Cascade of Immobilised Oxynitrilase and Nitrile Hydratase. Adv. Synth. Catal. 351, 397–404. https://doi.org/10.1002/adsc.200800625

Vejvoda, V., Martínková, L., Veselá, A.B., Kaplan, O., Lutz-Wahl, S., Fischer, L., Uhnáková, B., 2011. Biotransformation of nitriles to hydroxamic acids via a nitrile hydratase–amidase cascade reaction. https://doi.org/10.1016/J.MOLCATB.2011.03.008

Vera, A., González-Montalbán, N., Arís, A., Villaverde, A., 2007. The conformational quality of insoluble recombinant proteins is enhanced at low growth temperatures. Biotechnol. Bioeng. 96, 1101–1106. https://doi.org/10.1002/bit.21218

What is the difference between T7 Express (NEB #C2566H/I) and BL21(DE3) (NEB #C2527H/I)? | NEB [WWW Document], n.d. URL

https://international.neb.com/faqs/2014/12/12/what-is-the-difference-between-t7-express-neb-c2566h-i-and-bl21-de3-neb-c2527h-i (accessed 8.23.21).

Wieser, M., Takeuchi, K., Wada, Y., Yamada, H., Nagasawa, T., 1998a. Low-molecular-mass nitrile hydratase from Rhodococcus rhodochrous J1: purification, substrate specificity and comparison with the analogous high-molecular-mass enzyme. FEMS Microbiol. Lett. 169, 17–22. https://doi.org/10.1111/j.1574-6968.1998.tb13293.x

Wieser, M., Takeuchi, K., Wada, Y., Yamada, H., Nagasawa, T., 1998b. Low-molecular-mass nitrile hydratase from Rhodococcus rhodochrous J1: purification, substrate specificity and comparison with the analogous high-molecular-mass enzyme. FEMS Microbiol. Lett. 169, 17–22. https://doi.org/10.1111/j.1574-6968.1998.tb13293.x

Wu, B., 2011. Substrate inhibition kinetics in drug metabolism reactions. Drug Metab. Rev. 43, 440–456. https://doi.org/10.3109/03602532.2011.615320

Wyatt, J.M., Knowles, C.J., 1995. Microbial degradation of acrylonitrile waste effluents: the degradation of effluents and condensates from the manufacture of acrylonitrile. Int. Biodeterior. Biodegrad., Biosorption and Bioremediation 35, 227–248. https://doi.org/10.1016/0964-8305(95)00031-Y

Wyk, V., Caroline, J., 2008. The relationship between structure and thermostability of a nitrile hydratase from Goebacillus pallidus RAPc8 (Thesis). University of the Western Cape.

Y, H., S, Sasaki, S, H., K, O., S, Shimizu, M, K., 2002. Site-directed mutagenesis for cysteine residues of cobalt-containing nitrile hydratase. J. Inorg. Biochem. 91, 70–77. https://doi.org/10.1016/s0162-0134(02)00373-2

Yamada, H., Kobayashi, M., 1996a. Nitrile hydratase and its application to industrial production of acrylamide. Biosci. Biotechnol. Biochem. 60, 1391–1400. https://doi.org/10.1271/bbb.60.1391

Yamada, H., Kobayashi, M., 1996b. Nitrile hydratase and its application to industrial production of acrylamide. Biosci. Biotechnol. Biochem. 60, 1391–1400. https://doi.org/10.1271/bbb.60.1391

Yoshino, M., Murakami, K., 2015a. Analysis of the substrate inhibition of complete and partial types. SpringerPlus 4, 292. https://doi.org/10.1186/s40064-015-1082-8

Yoshino, M., Murakami, K., 2015b. Analysis of the substrate inhibition of complete and partial types. SpringerPlus 4, 292. https://doi.org/10.1186/s40064-015-1082-8

Zeng, W., Guo, L., Xu, S., Chen, J., Zhou, J., 2020. High-Throughput Screening Technology in Industrial Biotechnology. Trends Biotechnol. 38, 888–906. https://doi.org/10.1016/j.tibtech.2020.01.001

Zhou, Z., Hashimoto, Y., Cui, T., Washizawa, Y., Mino, H., Kobayashi, M., 2010. Unique biogenesis of high-molecular mass multimeric metalloenzyme nitrile hydratase: intermediates and a proposed mechanism for self-subunit swapping maturation. Biochemistry 49, 9638–9648. https://doi.org/10.1021/bi100651v